Improvement of forecasting heavy rainfall events using Weather Research and Forecasting (WRF) model

By

Mohammad Alfi Hasan

MASTER OF SCIENCE IN WATER RESOURCES DEVELOPMENT

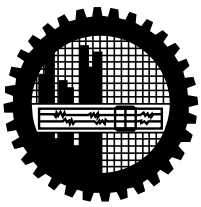

INSTITUTE OF WATER AND FLOOD MANAGEMENT

BANGLADESH UNIVERSITY OF ENGINEERING AND TECHNOLOGY

November, 2014

Improvement of forecasting heavy rainfall events using Weather Research and Forecasting (WRF) model

By

Mohammad Alfi Hasan

A thesis submitted to the Institute of Water and Flood Management (IWFM) of Bangladesh University of Engineering and Technology, Dhaka in partial fulfillment of the requirements for the degree of

MASTER OF SCIENCE IN WATER RESOURCES DEVELOPMENT

INSTITUTE OF WATER AND FLOOD MANAGEMENT

BANGLADESH UNIVERSITY OF ENGINEERING AND TECHNOLOGY

November, 2014

INSTITUTE OF WATER AND FLOOD MANAGEMENT

BANGLADESH UNIVERSITY OF ENGINEERING AND TECHNOLOGY

The thesis titled **"Improvement of forecasting heavy rainfall events using Weather Research and Forecasting (WRF) model"** submitted by Mohammad Alfi Hasan, Roll No. 0412282032, Session April 2012, has been accepted as satisfactory in partial fulfillment of the requirement for the degree of M.Sc. in Water Resources Development on November 23, 2014.

BOARD OF EXAMINERS

.....
Chairman (Supervisor)
Dr. A.K.M. Saiful Islam
Professor
Institute of Water and Flood Management
Bangladesh University of Engineering and Technology, Dhaka

.....
Dr. G.M. Tarekul Islam (Ex-officio) (Member)
Professor and Director
Institute of Water and Flood Management
Bangladesh University of Engineering and Technology, Dhaka

.....
Dr. Sujit Kumar Bala (Member)
Professor
Institute of Water and Flood Management
Bangladesh University of Engineering and Technology, Dhaka

.....
Dr. Md. Rafi Uddin (External) (Member)
Associate Professor
Department of Physics
Bangladesh University of Engineering and Technology, Dhaka

CANDIDATE'S DECLARATION

It is hereby declared that this thesis or any part of it has not been submitted elsewhere for the award of any degree or diploma.

…….

Mohammad Alfi Hasan

Dedicated to

The People of Bangladesh

ACKNOWLEDGEMENT

It is my pleasure to take the opportunity to thank those who made it possible for me to complete this thesis. First and foremost, I would like to show my deepest gratitude to Almighty Allah.

I want to thank to my supervisor, Dr. A. K. M. Saiful Islam, Professor, Institute of Water and Flood Management (IWFM), Bangladesh University of Engineering and Technology (BUET), Dhaka for his generous help and support to develop my knowledge, problem solving ability and experience in this thesis work planning, designing and execution. His comments and advices during this research work are sincerely appreciated. I also want to thank, my wife, Supria Paul for her support throughout this study.

I am grateful to Dr. Sujit Kumar Bala, Professor, IWFM, BUET, for providing me valuable advice and suggestions for the improvement of the quality of the work. I am deeply grateful to Dr. G.M. Tarekul Islam, Professor and Director, IWFM, BUET, to support and allow me to do this research and suggestions. I also thank Dr. Rafi Uddin, Associate Professor, Department of Physics, BUET; for taking time to serve as my external examiner.

Special thanks to my friends and lab partners, for their encouraging support to completion of this study.

ABSTRACT

Heavy rain events have become a major source of meteorological disasters over Bangladesh, responsible for deadly floods and landslide in recent years. Such events caused severe property damage and loss of life. Therefore, rainfall forecasting is essential for the socioeconomic development of Bangladesh. Especially, forecast of heavy rainfall is crucial for flood warning, disaster management and crop production. Forecasting heavy rainfall events are quite challenging due to low forecasting efficiency over the monsoon region including Bangladesh. Numerical Weather Prediction (NWP) models are the great tool for the rainfall forecasting which are widely used all over the globe. Weather Research and Forecasting (WRF) model is a next generation NWP model, which can be used in variety of scientific applications including operational weather forecast. There are several physical options in WRF, which are responsible for generating rainfall in the model. With a selection of suitable physical schemes, the forecast skill of heavy rainfall events can be increased effectively. Therefore, this study is conducted to evaluate the high impact rainfall events over Bangladesh using WRF model.

The rainfall event during 11th June, 2007 and 24th-27th June, 2012 are the two severest and deadliest rainfall events over Bangladesh in recent decades. In present study, these two events are selected to evaluate performance of WRF model over the country. There are twelve cumulus schemes and ten microphysics schemes in the latest version of WRF. Based on the review of previous literature, Kessler, Lin et al., WRF Single–moment 6–class and Stony–Brook University schemes are chosen as microphysics schemes and Kain-Fritsch, Betts-Miller-Janjic, New Grell 3D, Tiedtke and New Arakawa–Schubert schemes are chosen as cumulus schemes to assess the heavy rainfall events over the region. Considering these cumulus and microphysics schemes, nineteen combinations of physical schemes are simulated in the study for a heavy rainfall event using WRF model. Several evaluation indices are calculated for four days of the event which include Root Mean Square, percentage bias, and false alarm, hit score, proportion correct etc. Using these indices, accuracy of rainfall events with different thresholds are evaluated as well as false forecast ratio are also measured for each physical schemes of WRF. After verifying several aspects of

rainfall forecast for different rainfall threshold value, a suitable physical scheme is found that can produce effective forecast in heavy rainfall events over the country.

From the analysis, Stoony Brook University scheme along with Tiedtkel scheme has been found as the most suitable scheme over the eastern hilly region of the country. In generating high impact rainfall event, cumulus physical schemes play greater role than microphysics physical schemes. WRF Single–moment 6–class microphysics scheme and New Grell 3D cumulus schemes also showed reasonable performance in capturing heavy rainfall events. It is also found that, the existing default physical scheme (Kessler and Kain-Fritsch (new) scheme) that is commonly used by Bangladesh Meteorological Department (BMD) has poorly performed in capturing high impact rainfall over the Chittagong Division.

TABLE OF CONTENTS

LIST OF TABLES

LIST OF FIGURES

ABBREVIATIONS AND ACRONYMS

AR4	The Fourth Assessment Report by IPCC
AS	New Arakawa–Schubert
BBS	Bangladesh Bureau of Statistics
BJ	Betts-Miller-Janjic
BMD	Bangladesh Meteorological Department
BUET	Bangladesh University of Engineering and Technology
CRU	Climatic Research Unit
FAR	False Alarm Ratio
GCM	General Circulation Model
GR	New Grell 3D
HT	Hit rate
IWFM	Institute of Water and Flood Management
KE	Kessler
KF	Kain-Fritsch
LN	Lin et al.
MM5	Fifth-Generation Penn State Mesoscale Model
NCAR	National Center for Atmospheric Research
NMM	Non-hydrostatic Mesoscale Model
NWP	Numerical Weather Prediction
PBIAS	Percent bias
PC	Proportion Correct
RMSE	Root mean square error
SU	Stony–Brook University
TD	Tiedtke
TRMM	Tropical Rainfall Measuring Mission
TS	Threat Score
WM	WRF Single–moment 6–class
WRF	Weather Research Forecasting

CHAPTER I
INTRODUCTION

1.1 Background

Bangladesh is located in the tropical monsoon region and rainfall plays a crucial part in water resource management and agriculture of the country (Shahid, 2010). The erratic heavy rainfall events may affect ecosystems, agriculture, food security, urban drainage, water availability, water quality and health and livelihood of people of the country (Choudhury et al., 2004; Mirza, 2002; Sarker and Rashid, 2013). As, most of the natural disasters of Bangladesh have meteorological origin, heavy rainfall events associated other hydrologic phenomenon caused severe catastrophe by damaging life and properties (Ahasan et al., 2013b; Rafiuddin et al., 2010). On the monsoon of 2007, the county received unprecedented heavy rainfall together with the onset of flooding by Himalayan-fed rivers which led to severe flooding in more than half of the districts of Bangladesh. Heavy rainfall at 14 September of 2004 and 28 July of 2009 resulted in severe urban flooding and drainage congestion in the capital city of the country, Dhaka. Specially, in the eastern hilly region, heavy rainfall events caused deadly landside in recent years, which has been identified as a new natural disaster of the country. On 11 June, 2007, around 425mm rainfall was recorded at Chittagong port where at least 128 people died and more than 150 people injured (Ahasan et al., 2013a). During 25-27 June 2012, around 400mm rainfall was recorded at Chittagong port within a 12-h period where at least 90 people died and city faced sever water logging in some areas (BBC, 2012). Landside fatality also was observed during 2008 and 2010 due to heavy rainfall events over the country. Recent studies also suggest that the frequency and magnitude of heavy rainfall events have already been increased under the global warming scenario including high altitude areas of Bangladesh (Hasan et al., 2013). It is, therefore, obvious that an operational scenario to provide quantitative precipitation forecast of heavy rainfall events with greater accuracy is essentially important for the county's economy and society (Haines et al., 2006). An efficient forecast can save millions of lives and properties from the upcoming disasters. Therefore understanding high impact rainfall is a matter of necessity for the scientific community and policymakers of Bangladesh.

1.2 Rationale of the study

At present state, existing operational forecast provides low performance for the heavy rainfall events especially over the higher altitude areas of Asian region (Kumar et al., 2010). Forecasting high impact rainfall event over Bangladesh is a challenging tusk for both scientific researcher and weather forecaster. Existing skill in high impact rainfall events are not sometime sufficient for disaster management practice of Bangladesh. In this context, numerical weather prediction model (NWP) is the most widely used tool for forecasting the rainfall events all around the globe. For Bangladesh, rainfall prediction using NWP models like Fifth-Generation Mesoscale Model (MM5) or Weather Research and Forecast model (WRF) have been introduced in recent years. The recently developed NCAR mesoscale model Weather Research Forecasting (WRF) system has improved model physics, cumulus parameterization schemes, planetary boundary layer physics. It is a widely used forecasting model all around the globe. There are several physical schemes that needs to be defined for simulating WRF model for a particular event. Cumulus and microphysics schemes play primary role in rainfall physics of the model. There are many options of cumulus and microphysics schemes, but to accurately predict heavy rainfall events the most appropriate combination of these schemes are required. Selection of right combination of the physical schemes, especially cumulus and microphysics schemes is essential for better performance of the model, which eventually improves the forecast skill of the model. In this context, a few studies have been conducted so far in Bangladesh using WRF model (Ahasan and Debsarma, 2014; Das et al., 2011; Mannan et al., 2013). Mannan et al. (2013) considered six different micro-physic schemes with Kain-Fritsch (KF) cumulus scheme to simulate rainfall over Bangladesh by WRF model. Ahasan et al. (2013b) simulated WRF using KF as cumulus and YSU as PBL scheme in understand heavy rainfall over the country. However, most of these studies either focused on PBL or radiation physical schemes or considered only one combination of cumulus and microphysics scheme to evaluate rainfall events. No robust evaluation of existing cumulus and microphysics physical schemes of the model has been done yet over Bangladesh, which is highly important for rainfall generation within the model. Hence, this study has been carried out to find the most suitable combination of physical scheme of WRF model over the country. By doing so, it will eventually improve the capability to forecast high intensive rainfall over the region.

1.3 Objectives of the study and possible outcomes

The main objectives of the project are as follows-

i. Setting up and evaluation (calibration and validation) of WRF model with observed BMD and TRMM (v3B42) satellite data.

ii. To identify an optimized physical scheme for forecasting high altitude extreme rainfall using the model.

This study is expected to provide an optimized physical scheme for better forecast of heavy extreme rainfall over Bangladesh which will eventually help flood forecasting, food security and future climate prediction.

1.4 Limitations of the study

The main limitations of the study are

- Two heavy rainfall events are selected for the study, one is for domain configuration and another is for the sensitivity test. Due to the limitation of time, and computational resources, sensitivity test cannot be done for more than one high intensive rainfall event.
- Though initial domain has been selected trough calibration process, more experiment requires to understand the effect of domain size for each physical scheme. Due to the limitation in computational facility, and time, it could not be possible to consider in the study.
- The forecast validation has been conducted over the eastern region of Bangladesh as more intense rainfall occurs in that region. However, best physical schemes needs to be validated for other areas of Bangladesh considering different rainfall events.
- The whole evaluation process has been carried out using TRMM(3B42V6) real time grid data with a 25 km resolution. But, observed point data is more accurate than TRMM(3B42V6) data. However, due to lack of enough spatial coverage of observed BMD data, TRMM product has been used. The study result could be more accurate, if grid points were taken with higher resolution.

1.5 Organization of the Chapters

The thesis contains eight chapters. The organization of the chapters is as follows:

Chapter one provides the background of the study and present state of the problems. It also draws attention to the objectives of the study with limitations and organization of the chapters. Chapter two examines state of rainfall over Bangladesh, cause of high intensive rainfall and detail of rainfall patterns over the country. It also contains previous progress in rainfall forecasting and application of numerical weather model over Indian regions. The chapter also reviewed the rainfall induced hazard over Bangladesh and present practice of heavy rainfall forecast using WRF model. Detail overview of WRF model and its physical assumptions are also provided in this chapter. Chapter three have discussed the methodology of the study in detail. Description of domain size experiment and evaluation of different physical schemes experiment are indicated in this chapter. The chapter also discusses the methodology of calibration of model domain. Chapter four describes the performance of different physical scheme in forecasting high impact rainfall events. Finally, chapter five concludes the results of the study and provides recommendations for further study.

CHAPTER II
LITERATURE REVIEW

2.1 Introduction

This chapter provides a description of rainfall characteristics of Bangladesh. Heavy rainfall is usually occurs during monsoon season. Previous heavy rainfall events which had significantly impact over the country are also reviewed in this chapter. The current state of high intensive rainfall forecast is also presented.

2.2 Rainfall over Bangladesh

According to AMS (2014), all solid or liquid aqueous particles that originate in the atmosphere and fall into the earth surface are precipitation. Rainfall, hail, snow, drizzle or sheets are the main form of precipitation. Rainfall can be considered as the amount of liquid precipitation that reach earth surface and collected by rain gauge.

Rainfall is the most dominant element of the climate in Bangladesh. The country has a tropical monsoon climate with high amount of rainfall. Distinctive seasonal pattern exists in annual rainfall cycle which is more prominent than temperature cycle.

2.3 Historical rainfall events

Rainfall is considered as both curse and blessing for the people of Bangladesh. Due to agricultural economy, rainfall plays an essential role in living and livelihood of country's population. In contrary, the excessive rainfall in the Ganges, Brahmaputra and Meghna basin during monsoon and pre-monsoon seasons, was primary responsible for monsoon flooding in previous decades. Frequent monsoon flood over the region caused tremendous damage in the agricultural production, infrastructure and livelihood and exerted a great loss in the country's economy.

In the 20th century, eighteen major floods were recorded among those of 1987, 1988 and 1998 were of catastrophic consequence (Ali, 1999). In recent years, three major floods occurred during 2004, 2005 and 2010. The flood of 1988 occurred throughout August and September, inundated about 82000 km^2 of land (about 60% of the area).

Rainfall together with synchronization of very high flows of all the three major rivers of the country in only three days aggravated the flood (Mirza, 2002).

In 1998, over 75% of the total area of the country was flooded. A combination of heavy rainfall within and outside the country and synchronization of peak flows of the major rivers contributed to the river cause this catastrophic disaster (Shahid, 2011). The 2004 flood was very similar to the 1988 and 1998 floods with two thirds of the country under water due to heavy rainfall (Brammer, 1990; Cannon, 2002).

Other than flood, disasters like water logging and land side were happened due to the high intensive local rainfall events in recent years. Due to the heavy rainfall during 10 -11 June 2007, landslides and collapsed walls caused widespread damages in six areas of Chittagong city and in different Upazilas of the District. The landslide event killed 124 people and destroyed houses, roads and embankments, as well as disrupted electricity, gas lines and communication facilities. According to the Bangladesh weather office, rainfall measured on 11 June (until 9 pm) was 408 mm, the heaviest in 25 years. A number of areas were under water as a result of incessant rainfall over the four days prior to the date of reporting. On 11 June, it was reported that 41 wards (consisting of 1.5 million people) were waterlogged. On Tuesday, 12 June, the number of people in the waterlogged areas decreased to 500,000, as the water level receded. The maritime ports of Chittagong, Cox's Bazar and Mongla hoisted cautionary signal No-3, as advised by the government's meteorological department. Four reasons were identified for the landslide: indiscriminate cutting of hill forest cover for setting up slum dwellings, abnormal rise in the level of high tide, high tide combined with concurrent heavy rainfall, and the poor drainage system.

In subsequent years, like 2008 and 2010, 11 and 96 people died in landside due to heavy rainfall in Chittagong division. Most recently, in 2012, heavy rainfall following landside was responsible for death of 122 people in Chittagong, Cox's Bazar and Bandarban district. Death toll in these three districts stood at 122 from 26th June to 5th July. According to the Meteorological Department this was the worst flood and landslide in the Chittagong region in the last 60 years, and in terms of rainfall in short span of time. The immediate impact of the hazards was initial displacement of the population who moved to temporary makeshift shelters, host families and

community shelters. While, majority of families have returned to their dwellings, long term effect of the hazard has impacted the residences' livelihoods, water and sanitation facilities, and has damaged or destroyed their houses. About 6.5 lakh of people inundated and thousands acres of cropland ruined away as different districts were flooded following access rainfall all over the country (Shelter and Cluster, 2012).

Other than landslide, major cities of country faced serious water logging problem during the heavy rainfall events.

In this context, the catastrophe of these rainfall events can be reduced by disaster management. Hence, efficient and accurate rainfall forecast, especially for the high intensive events is crucial for the pre-disaster management approach. By improving operational forecast more effective and reliable, the extent of damage from the heavy rainfall events can easily be reduced. Therefore, in current assessment, an attempt has been made to improve the high intensity rainfall forecast over Bangladesh.

2.4 Rainfall prediction

Prediction of high intensive rainfall is always challenging to the scientific community. To forecast monsoon rainfall, many studies has been done so far over the South Asian region. Dhar and Nandargi (1995) have found that severe rainstorms i.e., heavy rainfall over Indian region do not occur uniformly. They have found that all the rain storms, which have occurred over this region, have taken place during monsoon and pre-monsoon season only. Also the breakup of meteorological disturbances causing the rainstorms indicates that most of the rainstorms are caused due to Low Pressure Systems (LPS) which include low, depression, deep depression and cyclonic storm. Orography plays a significant role on intensity and distribution of heavy rainfall ((Desai et al., 1996; Ganesan et al., 2001; Mannan et al., 2013; Rakhecha and Pisharoty, 1996). Therefore, forecasting heavy rainfall events is a challenging job for scientist of theses region including Bangladesh.

There are several methods available to forecast rainfall events. Rahman et al. (2013) used simple regression model to forecast summer monsoon rainfall over Bangladesh.

However, most efficient and advance way of rainfall forecasting is using the numerical weather models. Numerical Weather Prediction (NWP) models are the mathematical models of the atmosphere and oceans to predict the weather based on current weather conditions. NWP becoming an important tool in research and operation weather forecasting in recent years. With the growing skill of NWPs, and the availability of cheap computing power, a variety of new applications has emerged for specialized and standard versions of the models. Now a day, almost every countries of the world use NWPs to forecast weather parameters in different time scales.

Many regional and event based study has been done so far using NWP models to improve the high intensive rainfall forecast. Kumar et al. (2008) conducted a study to evaluate heavy rainfall event during 26th July, 2005 over the Mumbai, India. They used WRF model, a next generation meso-scale weather forecasting model to examine the performance of rainfall forecast. They identified the effect of topography in generation of heavy rainfall over the city. A meso-scale vortex was captured in the simulations which appeared to enhance the localized, heavy rainfall events over the Mumbai.

To understand and predict severe local storms of India, Litta and Mohanty (2008) simulated Non-hydrostatic Mesoscale Model (NMM) for a thunderstorm event that occurred on 20 May 2006 at Kolkata. The model performed well in capturing stability indices, which act as indicators of severe convective activity along with the thunderstorm-affected parameters as in the observations. The results of these analyses showed that the 3 km WRF–NMM has better capability when it comes to thunderstorm simulation.

Kumar et al. (2010) performed a simulation of high impact rainfall events over the whole Indian subcontinent to analyze the performance of physical options of WRF model. Presence of monsoon depression over the Indian monsoon region was investigated with different physical options of WRF. A number of experiments for forecasts up to 72 hours were performed with two nested domains at the resolution of 45 km and 15 km respectively. Three monsoon depressions were selected for the study; 2-4th July; 2-4th August and 29th August to 1st September, 2004. The model was

capable of capturing the movement of the monsoon depression with a lead time of 72 hours. It was found that the model can be very useful for forecasting of rainfall and depression tracks in short range time scales over Indian monsoon region. However, the study did not showed spatial analysis over Bangladesh.

Three heavy rainfall events (25–28 June 2005, 29–31 July 2004, and 7–9 August 2002) over the Indian monsoon region are simulated by Routray et al. (2010). In this study, WRF-3DVAR was used as NWP model. The study found that, the assimilation of Indian conventional and non-conventional observation datasets into numerical weather forecast models can help improve the simulation accuracy of meso-convective activities over the Indian monsoon region.

Deb et al. (2008) conducted an experiment over the summer monsoon of 2006, over the central and western parts of the India. Due to meteorological complexities involved in replicating the rainfall occurrences over a region, the Weather Research and Forecast (WRF–ARW version) modeling system with two different cumulus schemes in a nested configuration was chosen in the study. The analysis found that, the spatial distributions of large-scale circulation and moisture fields have been simulated reasonably well in this model, though there are some spatial biases in the simulated rainfall pattern.

Das et al. (2008) conducted a performance study of four NWP models namely, the MM5, ETA, RSM and WRF. The study examined the whole monsoon period of 2006. In the analysis, it was found that, WRF was able to produce best 1-day forecast and MM5 was able to produce best 3-day forecast.

Considering tropical cyclone, ‘Mala’, WRF model was simulated during 26-29 April 2006, by Pattanayak and Mohanty (2008). In this study, two state-of the-art mesoscale models; MM5 and WRF were used to evaluate the performances of both the modeling the simulation of the above-mentioned tropical cyclones. The results indicated that the WRF model had better performance in respect of track and intensity prediction than the MM5 model.

Shah et al. (2010) performed an experiment to understand early summer monsoon prediction by numerical weather model. They simulated WRF for the summer monsoon of 2009 to evaluate the performance of forecast with INSAT observation data over western India. The study was undertaken to comprehensively assess the cloudiness prediction performance of WRF model. Their analysis revealed that that the probability of detection (POD) of cloud by WRF model is 84% and the false alarm rate (FAR) is around 18%.

A study was made to understand atmospheric chemistry using WRF-CHEM model, over the Indian sub-continent. However, the study did not focus water components and their density(Kumar et al., 2012).

To predict cyclonic track, very severe cyclonic storm 'Nargis' was simulated using WRF by Pattanaik and Rao (2009). Though the model was simulated over the South Asian region, the model evaluation has limited to pressure bar and wind speed determination. Assessment for rainfall was not made in the study.

A number of studies have been conducted to predict high intensive rainfall over Bangladesh. Ahasan et al. (2014) used MM5 model to predict high impact rainfall over the country. The study evaluated the sensitivity of MM5 model over the region to predict high intensive rainfall. Six events are considered in the study. Events are 21st June, 11th July and 14th September of 2004 and 11th June, 21st July and 7th September of 2007. TRMM and BMD data has been used as observed data in the study. Evaluating MM5, they found that model rainfall underestimate observed rainfall in most the physical schemes. Three best schemes are suggested in their study further evaluation of WRF model. Moreover, Model did not do well in capturing spatial patterns of rainfall over the country.

Das et al. (2011) has carried out a research work several unusual tornadic storms cases during Aug-Sep 2008 which caused loss of lives and properties of Bangladesh. They studied the synoptic features responsible for occurring such unusual storms during monsoon season by using Radar data and WRF mesoscale model.

Ahasan et al. (2014) made an attempt to predict monsoon rainfall events of Bangladesh using NCAR Mesoscale Model (MM5) conducting two historical rainfall events on 11 June 2007 and 14 September 2004 . The model was simulated considered, Anthes-Kuo cumulus parameterization scheme with MRF PBL scheme. The predictions were made for Day-1 (24-h), Day-2 (48-h) and Day-3 (72-h) in advance. The predictions were more accurate for Day-1 (24-h) and Day-2 (48-h). The prediction deteriorated as the prediction time increases.

To predict heavy rainfall events, recent study have used extensively a meso-scale NMM model called Weather research and forecasting (WRF) model. During recent years the WRF model has become very popular for studying meso-scale weather systems. It is mainly because of three reasons: (a) The model is very user friendly to select various physics options, (b) The model can be operated on a personal computer and (c) Freely availability of NCEP GFS outputs in the Internet to use as initial and boundary conditions. Therefore, to evaluate heavy rainfall events over Bangladesh, WRF model can be an effective tool for operational forecast. Bangladesh Metrological Department (BMD) also uses Weather Research and Forecasting (WRF) model alongside other NWP models to forecast various weather events up to seven days over the country. BMD forecast 24H, 48H and 72H rainfall using this model after every 6 hour time cycle. This model can be applied for different purpose like operational weather forecast, climate change study, atmospheric feedback study and various other atmospheric researches. However, before the model is used for operational applications, it is necessary to identify the best physics option applicable for the specific region, depending on the geographical, topographical and seasonal characteristics of synoptic and thermo-dynamical features. Therefore, a comprehensive physical sensitivity study is required for the better evolution of the model.

Many studies have been made around the world to evaluate physical schemes of WRF model. WRF sensitivity in rainfall prediction were observed over Europe, USA, China, Sri lanka, Korea, Malaysia, Taiwan, New Zealand etc. (Bukovsky and Karoly, 2009; De Silva et al., 2010; Im et al., 2013; Maussion et al., 2011; Mooney et al., 2013; Sohrabinia et al., 2012; Wardah et al., 2009; Yeh and Chen, 2004).

To evaluate the performance of WRF in forecasting high intensive rainfall over Indian subcontinent, Kumar et al. (2010) made a study considering three rainfall depression of 2004. They used a combination of three cumulus schemes to simulate the model. The schemes are KF scheme, Grell and Devenyi scheme and Betts-Miller-Janjic (BMJ) scheme. Among these schemes, the BMJ scheme produced better results compared to other cumulus schemes for the Indian monsoon. They used micro physics scheme of Lin et al. (1983), long wave radiation scheme of RRTM, Short wave radiation scheme of Dudhia, surface layer physics based on Monin-Obukhov with Carslon-Boland viscous sub layer and land surface of Noah Land surface model (LSM). Two PBL schemes were also tested in the study where Mellor-Yamada-Janjic (MYJ) produced better rainfall forecast as compared to the Yonsei University (YSU) scheme.

Kumar et al. (2008) has use WRF model to evaluate high intensive rainfall over Mumbai, India. They have used the WRF –Single Momentum 6-class grapple scheme and The Grell–Devenyi (GD) ensemble scheme as microphysics and cumulus scheme respectively. The Rapid Radiative Transfer Model (RRTM) (Mlawer et al., 1997) scheme was chosen for long-wave radiation with the Dudhia (1989) scheme for short-wave radiation in the study.

To simulate severe thunderstorm over Gadanki (India) on 21May 2008, a study was done using high resolution WRF model with 2 km grid spacing(Rajeevan et al., 2010). The study examined the sensitivity of four different cloud microphysical schemes (Thompson, WSM6, Lin and Morrison). It was found that Thompson scheme simulations were closer to observation over Gadanki (India).

Ratnam and Cox (2006) also performed a sensitivity test of cumulus scheme of MM5 model for simulating monsoon rainfall. Among the selected two cumulus scheme, Grell (GR) and Kain-Fritsch (KF); KF showed smaller root mean square (RMS) error against ERA40 quasi-observe data.

For Bangladesh region, some studies have also been conducted using WRF model. Ahasan et al. (2013b) carried out an analysis on rainfall events of 7 September, 2011 using WRF model. The model was simulated using KF as cumulus and YSU as PBL

scheme. The rainfall was validated with TRMM 3B42RT and observed rainfall data. The results indicate that the WRF model was able to simulate the heavy rainfall event, and associated synoptic features reasonably well, though there are some biases in the rainfall pattern. However, such study did not conduct a sensitivity study for the physical schemes.

A heavy rainfall event occurred over Bangladesh during 8th to 9th August, 2011. Considering this rainfall event, Mannan et al. (2013) performed an analysis to identify the fundamental dynamic process with aim of accurate the forecast and early warning. The study considered six different micro-physic schemes with Kain-Fritsch (KF) cumulus scheme to simulate the event by WRF model. According to the analysis, Kain-Fritsch scheme along with Lin-et al. scheme performed well in capturing heavy rainfall over the country.

Other than these two study, there are no study found that used WRF model over Bangladesh to simulate heavy rainfall events. Though, Mannan et al. (2013) considered six micro-physic scheme to analyze heavy rainfall, Ahasan et al. (2013) and Mannan et al. (2013) both used only one cumulus scheme to evaluate the model performance. However, model used both cumulus and microphysic scheme to produce rainfall over a perticular area. To improve model performcance in forcasting heavy rainfall event over Bangladesh, a comprehensive study is required by testing sensitivity of both set of cumulus and microphysic schemes. Hence, in the present study, an attempt has been made to identify the best possible combination of cumulus and microphysic scheme of WRF in analyzing heavy rainfall events over the country.

In this context, heavy rainfall events needs to be seleceted according to their importance. Therefore, the damage and fatality rate due to the direct impact of heavy rainfall events can be considered as appropiate indicators. During June 2007 and June 2012, two most severe disasters of the recent decades happened over south-eastern hilly region of Bangladesh, where 127 and 122 people died respectively due to heavy rainfall and its resulting landslide. Therefore, in this study 11th June, 2007 rainfall event has been used for WRF domain configuration experiment and 27th June, 2012 event has been selected for the sensitivity analysis of physical schemes. It should be noted that, though Ahasan et al. (2014) simulated 11th June, 2007 event using MM5

model considering only one physical scheme, they did not used latest WRF NWP model with other combination. Again, for 27th June, 2012 rainfall event, no study has been made so far using any kind of numerical weather model. Hence, 27th June, 2012 rainfall event has been selected for the evolution of the physical schemes of WRF.

2.5 Model descriptions of WRF

The Weather Research and Forecasting (WRF) Model is a non-hydrostatic, mesoscale numerical weather prediction system designed to serve both atmospheric research and operational forecasting needs. It was developed by the joint effort of the National Center for Atmospheric Research (NCAR), the National Oceanic and Atmospheric Administration (represented by the National Centers for Environmental Prediction (NCEP) and the (then) Forecast Systems Laboratory (FSL)), the Air Force Weather Agency (AFWA), the Naval Research Laboratory, the University of Oklahoma, and the Federal Aviation Administration (FAA). WRF-ARW is one of the major components of WRF modeling system which is currently in operational use at NCEP, AFWA, and other centers. The WRF-ARW dynamical core is primarily design for calculating advection, pressure-gradients, Coriolis, buoyancy, filters, diffusion, and time differentiation. It is portable and efficient on available parallel computing platforms. WRF-ARW allows users to generate atmospheric simulations based on real data (observations, analyses) or idealized conditions. The model has various lateral boundary conditions with a full set of physical parameterization data. It can also be set as either a one-way, two way nesting or moving nest model. WRF-ARW provides advances in physics, numerics, and data assimilation contributed by developers in the broader research community (Janjic et al., 2010; Skamarock et al., 2008).

The working mechanism of WRF system is showed in Figure 2.2. Observational data in a specified format is providing into the model as an External Data sources. These data are formatted by OBSGRID and WPS system as a preprocessing mechanism. Generated results from WPS system are then provided into the model processing system. Finally analyzed model outputs are represented by different post-processing tools which are provided with the model installation.

Simulation of ARW-WRF requires different variables like topographic information, weather data, terrain data etc. Using these variables, the model can conduct numerical analysis using some fundamental fluid equations. Some core features of the model are described in following sections.

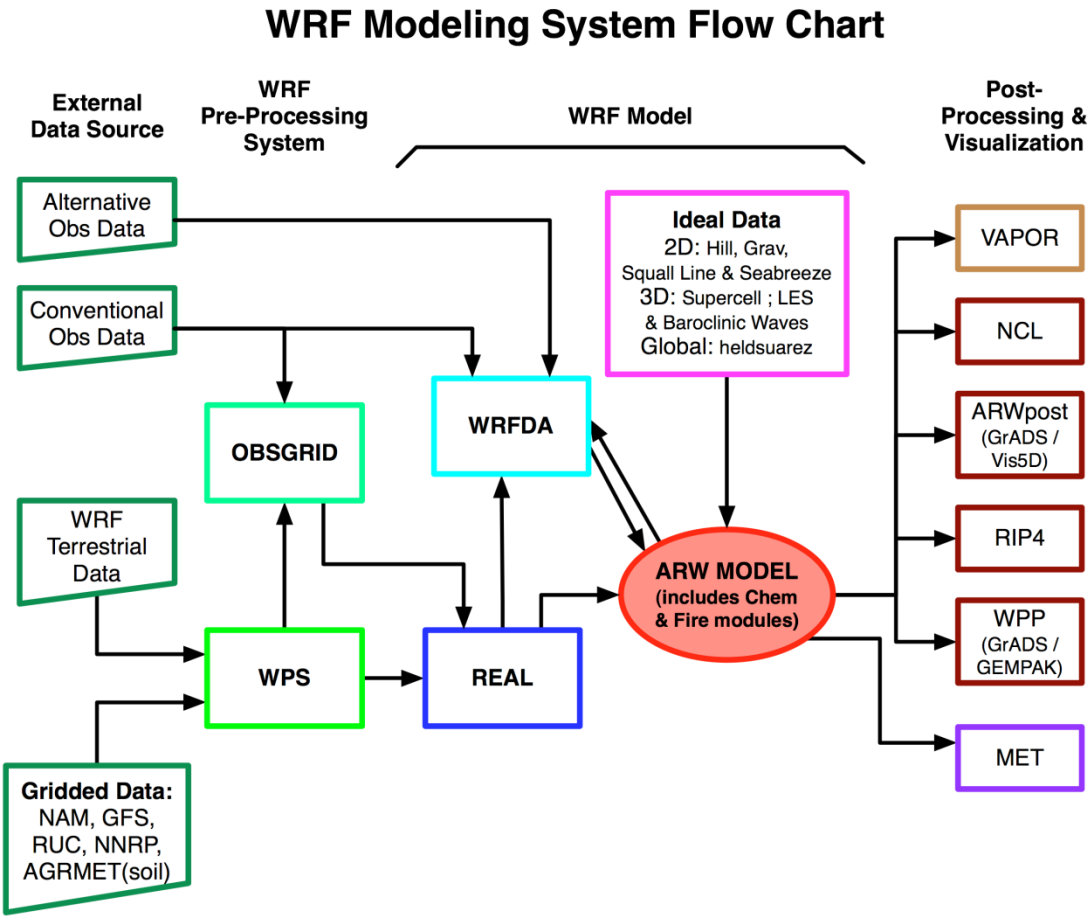

Figure 2.2: WRF Modeling System Flow Chart (Skamarock et al., 2008).

2.5.1 Governing Equations of WRF

Like other mesoscale numerical models, the basic mathematical equations of WRF are a set of conservation principles. According to Pielke Sr (2013), these are conservation of mass, heat, motion, water, and gaseous materials. In order to complete a successful simulation, these equations must be solved simultaneously. To resolve atmospheric dynamic, WRF uses non-hydrostatic Euler equation. Using method prescribed by Ooyama (1990), flux-form Euler equations can be described as follow:

$$\partial_t U + (\nabla \cdot \mathrm{V}_u) - \partial_x(p\phi_\eta) + \partial_\eta(p\phi_x) = F_U \qquad (1)$$

$$\partial_t V + (\nabla \cdot \mathrm{V}_v) - \partial_y(p\phi_\eta) + \partial_\eta(p\phi_y) = F_y \quad (2)$$

$$\partial_t w + (\nabla \cdot \mathrm{V}_w) - g(\partial_\eta p - \mu) = F_w \quad (3)$$

$$\partial_t \theta + (\nabla \cdot \mathrm{V}\theta) = F_\theta \quad (4)$$

$$\partial_t \mu + (\nabla \cdot \mathrm{V}) = 0 \quad (5)$$

$$\partial_t \emptyset + \mu^{-1}[(\nabla \cdot \mathrm{V}\varphi) - gW] = 0 \quad (6)$$

$$\partial_\eta \emptyset = -\alpha\mu \quad (7)$$

$$p = p_0 \left(R_d\theta / p_0\,\alpha\right)^{\Upsilon} \quad (8)$$

$$\nabla \cdot \mathrm{V_a} = \partial_x(U_a) + \partial_y(V_a) + \partial_\eta(\Omega_a) \quad (9)$$

$$\mathrm{V} \cdot \nabla_\mathrm{a} = U\partial_x a + V\partial_y a + \Omega\partial_\eta a \quad (10)$$

$$\Upsilon = {}^{\mathrm{c_p}}/_{\mathrm{c_v}} = 1.4 \quad (11)$$

where, U, V and W are the covariant velocities in the two horizontal and vertical directions; ω is the contra variant 'vertical' velocity; θ is the potential temperature; R_d is the gas constant for dry air; p is pressure; p_0 is the reference pressure (typically 10^5Pascals); μ is the mass per unit area; ϕ is the geo-potential height; γ is the ratio of the heat capacities for dry air and 'a' is a generic variable. Theses equations are formulated using a terrain-following hydrostatic-pressure vertical coordinate (Laprise, 1992). This hydrostatic-pressure vertical coordinate is calculated according to following equation:

$$\eta = (p_h - p_{ht})/(p_{hs} - p_{ht}) \quad (14)$$

Where, η is hydrostatic-pressure coordinate, p_h the hydrostatic component of the pressure and p_{hs} and, p_{ht} refer to values along the surface and top boundaries, respectively. An illustration of vertical coordinate system of the model is showed in Figure 2.3.

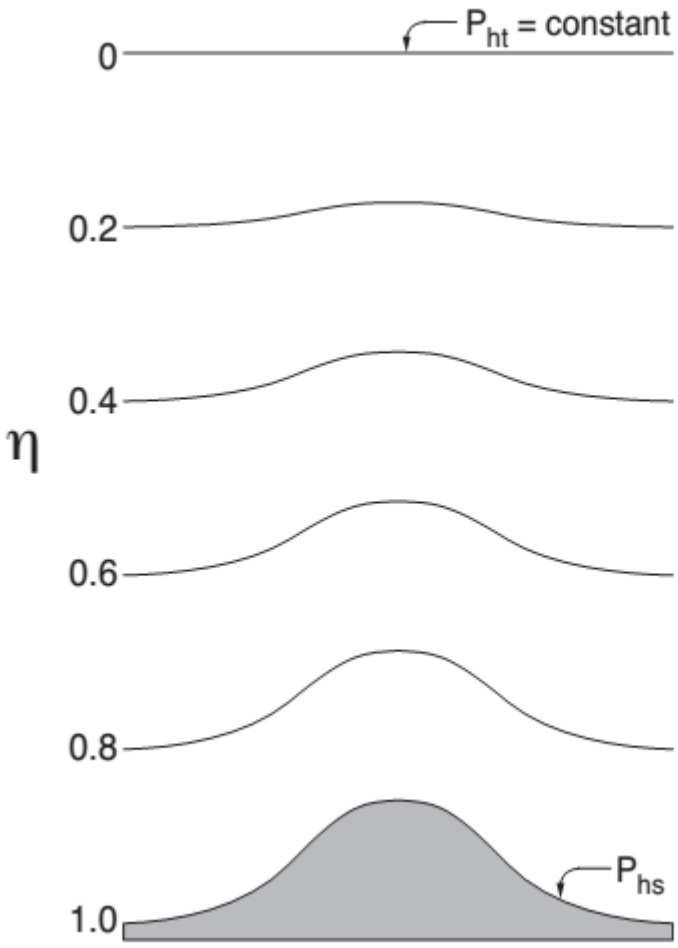

Figure 2.3: WRF vertical pressure co-ordinate (collected from (Skamarock et al., 2008))

Using Euler equations, the model calculate atmospheric process in a selected projection system.

2.5.2 Projection System

Present version of WRF-ARW use four types of geo-graphic projections to solve different variables of atmosphere. The projections are as follow:

- Lambert conformal
- Polar stereographic
- Mercator
- Latitude-longitude.

A schematic of the projection are provide in Figure 2.4. Among these four projection system, three projections requires a constant equal grid size both in horizontal and vertical directions (Haltiner and Williams, 1980). In the latest version of ARW-WRF, regular lat-long projection system also has been introduced.

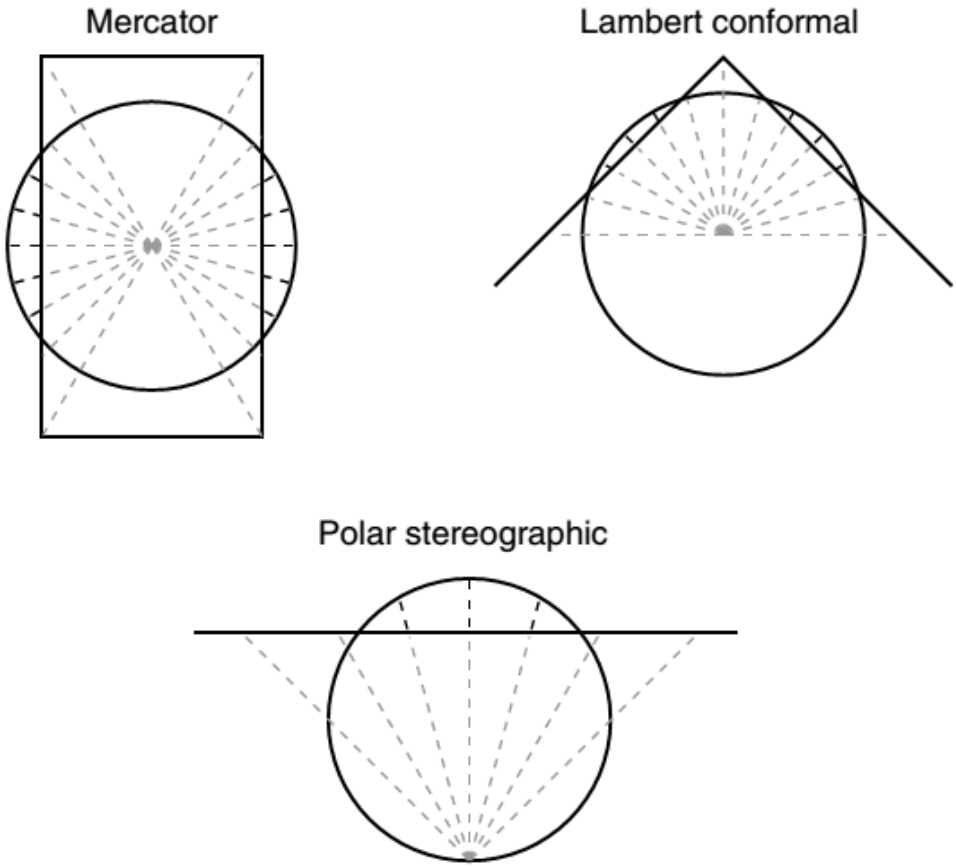

Figure 2.4: Projections that can be used in ARW-WRF model (regular long -lat projection is not shown in the figure). The radial lines connect points on the sphere and points on the projection surface. The axes of the cylinder and the cone, and the perpendicular to the plane, are parallel to Earth's axis of rotation. (Adopted from Warner (2011)).

For the computation of governing equations, the ratios of the distance in computational space to the corresponding distance on the earth's surface are computed for different projections. The equation that estimates the variable is as follow:

$$(m_x, m_y) = \frac{(\Delta x, \Delta y)}{distance\ on\ the\ earth} \quad (14)$$

Where, m_x and m_x are the map scale factor in horizontal and vertical direction respectively. Based on this map scale factors, an appropriate projection system is selected for a particular place of the earth. A selection diagram for different projection systems are provided in Figure 2.5.

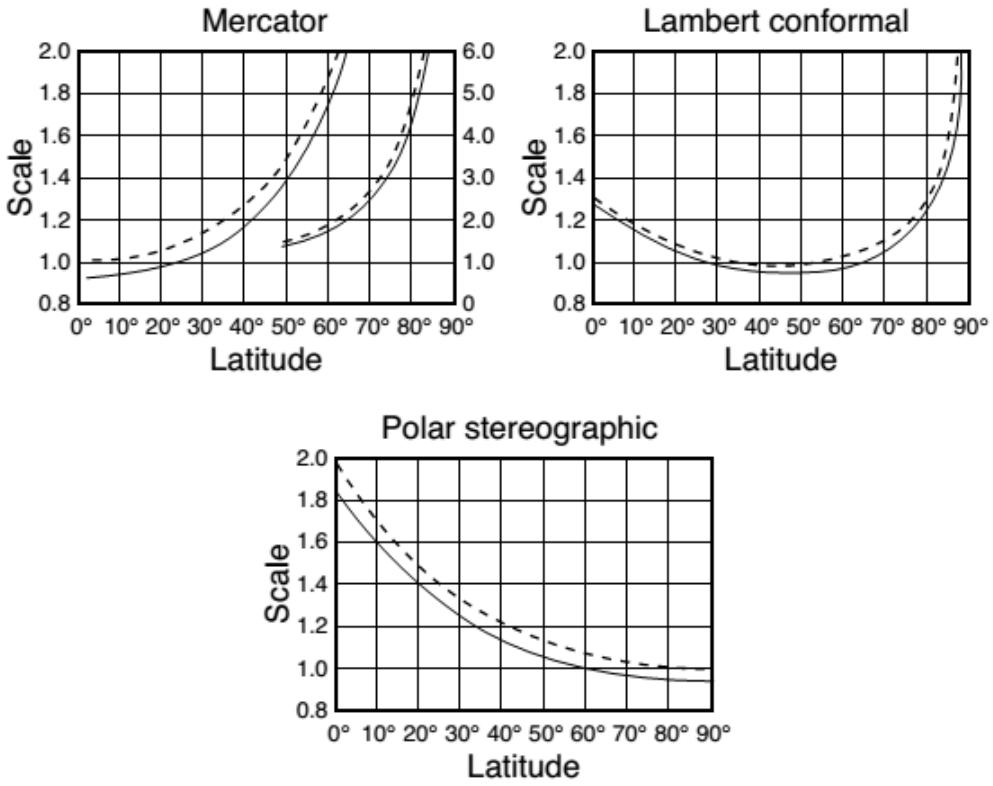

Figure 2.5: Map-scale factors for different tangent (dashed lines) and secant (solid lines) projections as a function of latitude. For the secant projections, the conical surface intersects the sphere at 30°and 60°(north or south) latitude, the plane intersects at 60°(north or south) latitude, and the cylinder intersects at 20°(north and south) latitudes(Saucier, 1989).

When map scale factor of a particular place is near one within a specific projection, the projection can be considered as the most appropriate projection for the parameterization of WRF (Saucier, 1989). For domains lying across the mid-latitudes, the Lambert projection best preserves lines of latitude and longitude. The Mercator projection best conserves the size of landmasses in the tropics, while the polar stereographic projection does the same for the polar latitudes. Lastly, for global domains, the cylindrical equidistant projection performs the best for land preservation.

2.5.3 Temporal Schemes of WRF

For the temporal analysis, WRF solve third order Range-Kutta time integration scheme (Klemp et al., 2007; Wicker and Skamarock, 2002). The scheme uses the prognostic variables of the model to solve the model equations for each simulation time step and advances into next time step. This scheme has the benefit of being a stable time differencing scheme when the CFL criteria is maintained. Time steps are outlined according to available computational facility, model capacity and domain size of experiment. For faster and high frequency analysis, the model use a similar scheme with smaller time step in an effort to maintain the Courant-Fredrichs-Lewy (CFL) criteria (Shamarock et al., 2008; Wang et al., 2009).

2.5.4 Domain configuration

To simulate WRF, a model domain needs to be fixed depending on the purpose, timeframe and location. Model domain is fixed with GEOGRID component of WRF. A simulation can be conducted in multiple resolutions. In that case, "domain nesting" option should be used. When a single, or several, higher resolution model domains (nests) are located within a more coarse, parent domain the technique is known as domain nesting. Using the technique, WRF can downscale data with very large grid spacing, such as, mesoscale model data, all the way to the turbulent scales (Moeng et al. 2007). The downscaled data provided to the parent is often beneficial as it provides the course domain with information about small-scale processes that it wouldn't be able to capture. The relationship between the parent and nest horizontal grid spacing is referred to as the spatial refinement ratio, or grid ratio, and is the ratio of nest horizontal grid spacing to parent horizontal grid spacing. Only the horizontal aspect is considered because within WRF the nest and parent share the same vertical levels. A typical grid ratio in WRF is 3:1, or any odd integer ratio (Skamarock et al., 2008). Two types of nesting are available in WRF model, 1-way nesting and 2-way nesting. In 1-way nesting, the process repeats for every parent time step. On the other hand, 2-way nesting has the additional step of feeding back information from the fine grid onto the coarse grid. Mechanism of a two way nesting of WRF is illustrated in figure X. Within a fixed domain, the spatial discretization of ARW is made by a C grid staggering method. The process is shown in Figure 4.5. In the figure, (i,j,k) indicates the location and u, v indicate the prognostic variables in each grid cell. θ is denoted as

mass point of the cell. The diagnostic variables used in the model, the pressure, p and inverse density, α, are computed at mass points.

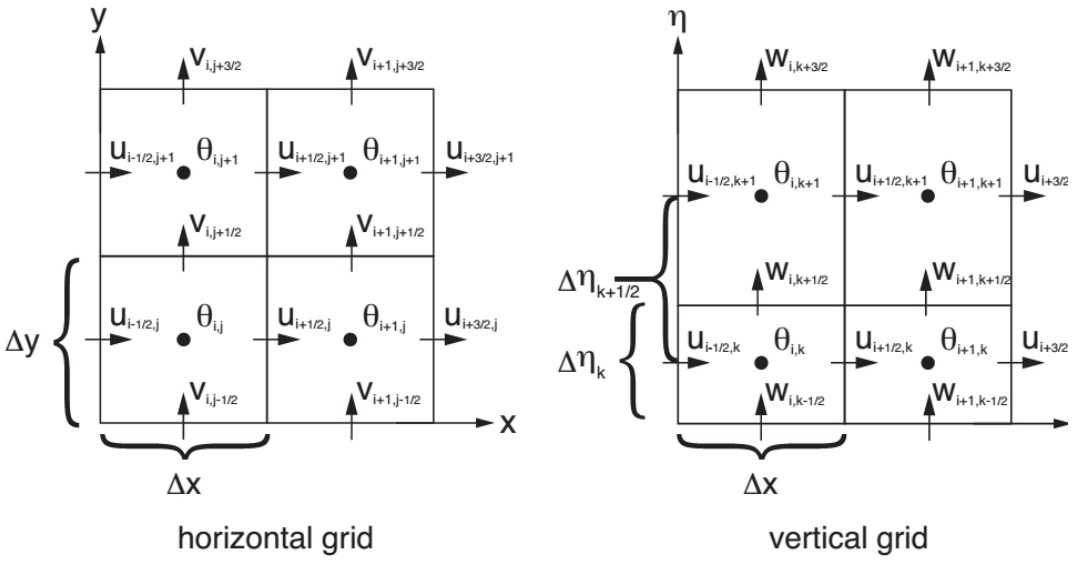

Figure 2.6: Horizontal and vertical grids of ARW.

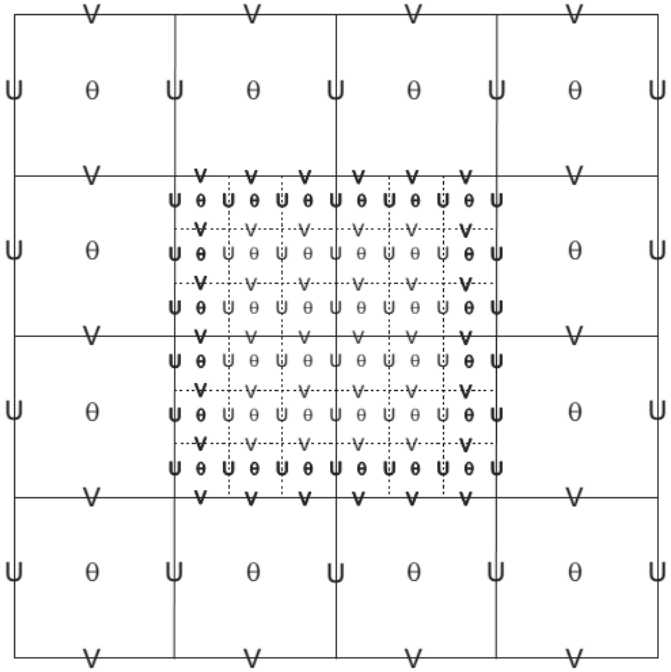

Figure 2.7 Arakawa-C grid staggering with a nested domain embedded within the parent domain using a 3:1 grid size ratio. The black solid lines denote the grid boundaries, U and V are defined as the horizontal velocity components, and θ represents scalar quantities. Obtained from Shamarock et al. (2008).

This grid configuration was chosen for the WRF-ARW model for several reasons. First, divergence modes are well represented in this setup, which allows the model to better handle mesoscale and microscale features such as clouds, convection, and small-scale circulations. Secondly, it best handles the frequencies of gravity-inertia waves (Winninghoff 1968; Arakawa and Lamb 1977).

2.5.5 Lateral boundary condition

For real-data cases, WRF simulations were initialized from a global model. There are two lateral boundary regions in the coarse grid; the specified region and the relaxation region. The relaxation region is the columns and rows adjacent to the specified region, and penetrates a certain amount of user-set grid columns/rows into the outer domain. The relaxation region is where WRF is relaxed towards the global model, with certain weighing values (Skamarock et al. 2008). This is performed every time the boundary conditions are updated, and produces a smooth mixture between the freshly updated boundary condition and the simulation.

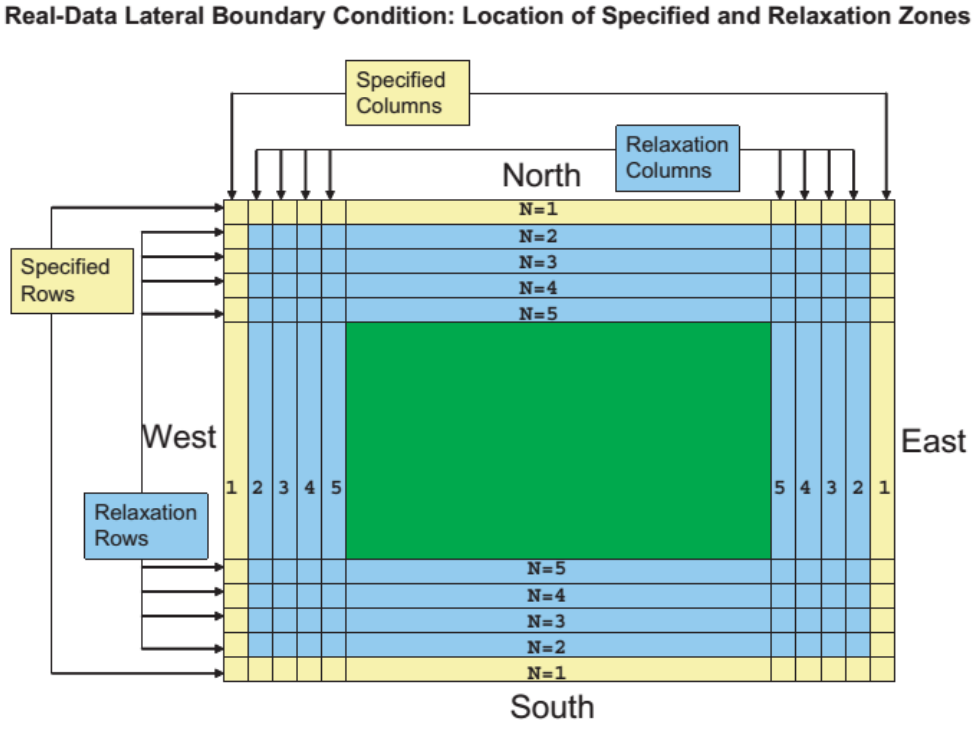

Figure 2.8: Location of Specified and relaxation zones of the real data lateral boundary condition

2.5.6 Model dynamics

Within a specific domain, WRF model solve the governing equations depending on different physical schemes. The physical schemes play an important role in WRF simulations. Selection of physical schemes is conducted based on purpose and location of a study. Depending on physical scheme, WRF model initiate variable calculation by a process called 'parameterization'. To parameterize means to define or measure a numerical factor or factors from a set parameters. In the atmospheric science, a parameterized equation is an equation which represents and parameterizes a physical process from at least two other parameters. For example, temperature-air density equation is a parameterized equation which relates pressure (one parameter) to temperature and air density (two other parameters)(Jacobson, 2005). In numerical model, like WRF, the physical schemes dictate the different process of parameterization. There are five categories of parameterization schemes available in WRF solver. They are micro-physics, cumulus parameterization, planetary boundary layers (PBL), land surface model and radiation. With these schemes WRF dynamic solver computes physical drivers in each time step using Runge-Kutta method.

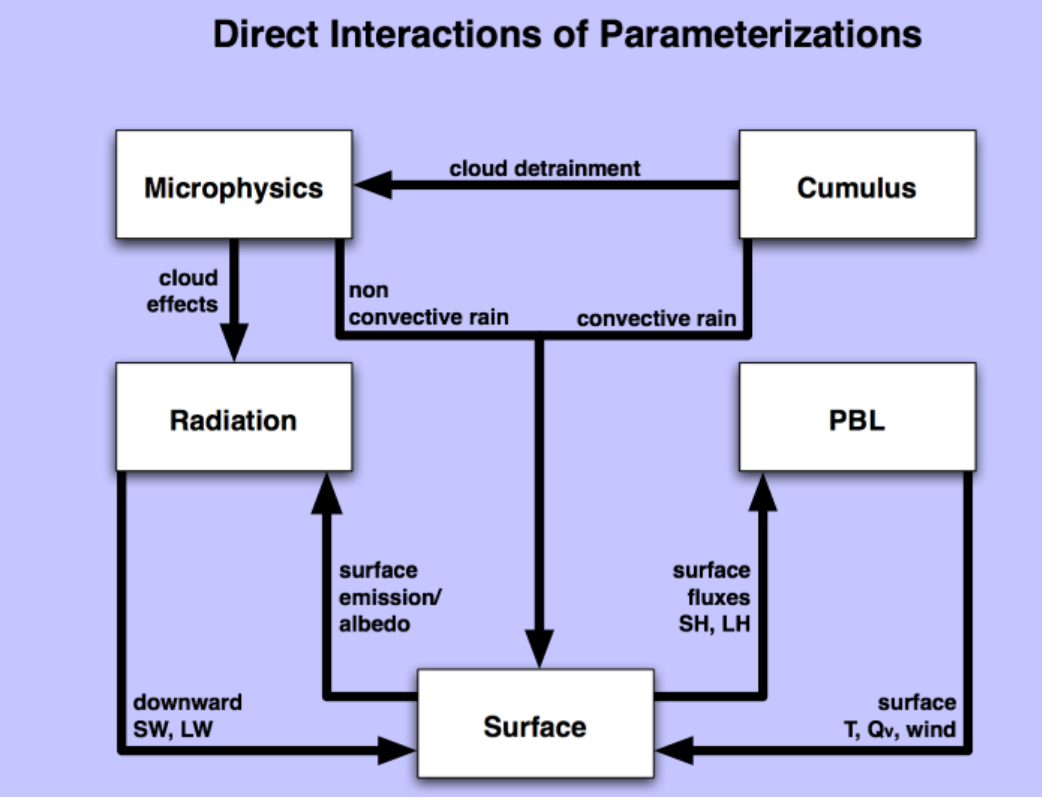

Figure 2.9: Interactions between parameterizations schemes

2.5.6.1 Microphysics Schemes

Microphysics scheme of WRF primarily deals with water vapor, cloud and precipitation process. It parameterizes small heat fluxes of atmosphere, moisture tendencies and rate of surface rainfall. The current version of WRF 3.3 supports 12 options of microphysics schemes. The schemes are responsible for determining precipitation type, size, and distribution. Complexity and variety of theses schemes relies on type of water state that are considered within the schemes. Table X1 shows type of water state variables that considered in different microphysics schemes of WRF. The basic microphysical schemes such as the WRF Single-Moment 3-class scheme has considered three state of water in cloud formation; cloud water, rain water and ice (Dudhia, 1989; Hong et al., 2004). On the other hand, advance schemes has considered up to six water state which include cloud water, water vapor, rain, ice, snow and graupel. Usually, advance schemes require more computational resources thus increase the run time of WRF simulations. After determining the state of water within a cloud the microphysical schemes can calculate the fall rates of the water with the exception of cloud water, which remains suspended in the atmosphere. For longer time-steps that are used in mesoscale applications, the precipitation may fall more than one grid level. To resolve this issue, most microphysical schemes either implements a time-splitting or a Lagrangian numerical method that helps maintain numerical stability within the model. To determine the physical traits of the precipitation within the cloud, the microphysical parameterization schemes use either single or double-moment schemes. Single-moment schemes use a single prediction equation for mass per precipitation type. Single-moment schemes also include a diagnostic scheme, which is used to determine the particle size distribution. Double-moment schemes add a prediction equation that is used to determine the number concentration per double-moment precipitation type. This allows for additional processes to be depicted such as size sorting during fall-out and even aerosol effects on clouds (Shamarock et al., 2008). A short description of each microphysics schemes are provided in the Appendix.

Kessler scheme

Kessler scheme is a simple warm cloud scheme that includes water vapor, cloud water, and rain. It follows the mechanism of Marhsall-Palmer distribution for rain (Figure 2.10). It is idealized microphysics and can do time split rainfall calculation.

The microphysical processes included are: the production, fall, and evaporation of rain; the accretion and autoconversion of cloud water; and the production of cloud water from condensation (Wicker and Wilhelmson, 1995).

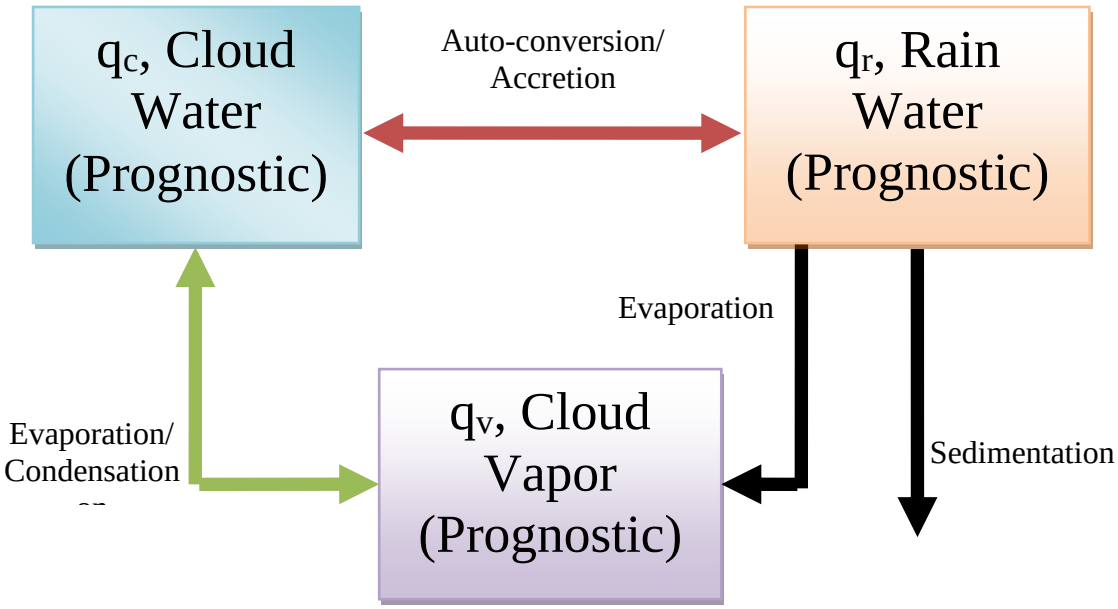

Figure 2.10: Rainfall distribution in Kessler scheme.

Purdue Lin scheme

Purdue Lin et al. scheme is a 5-class microphysics schemes which includes water vapor, cloud water, rain, cloud ice, snow, and graupel. It was first proposed by Lin et al. (1983) and later updated by Rutledge and Hobbs (1983); Tao et al. (1989). This is a relatively sophisticated microphysics scheme in WRF, and is most suitable for use in research studies. It is developed based on Purdue Cloud scheme. It can calculate ice sedimentation process.

WRF Single-Moment 3-class (WSM3) scheme

The WRF single-moment microphysics scheme follows Hong et al.(2004) including ice sedimentation and other new ice-phase parameterizations. A major difference from other approaches is that a diagnostic relation is used for ice number concentration that is based on ice mass content rather than temperature. The computational procedures are described in Hong and Lim(2006). As with WSM5 and WSM6, the freezing/melting processes are computed during the fall-term sub-steps to increase accuracy in the vertical heating profile of these processes. The order of the

processes is also optimized to decrease the sensitivity of the scheme to the time step of the model. The WSM3 scheme predicts three categories of hydrometers: vapor, cloud water/ice, and rain/snow, which is a so-called simple-ice scheme. It follows Dudhia(1989) in assuming cloud water and rain for temperatures above freezing, and cloud ice and snow for temperatures below freezing. This scheme is computationally efficient for the inclusion of ice processes, but lacks super cooled water and gradual melting rates.

WRF Single-Moment 5-class (WSM5) scheme

This scheme is similar to the WSM3 simple ice scheme. However, vapor, rain, snow, cloud ice, and cloud water are held in five different arrays. Thus, it allows supercooled water to exist, and a gradual melting of snow falling below the melting layer. Details can be found in Hong et al. (2004), and Hong and Lim(2006). As with WSM6, the saturation adjustment follows Dudhia (1989) and Hong et al.(1998) in separately treating ice and water saturation processes, rather than a combined saturation such as the Purdue Lin (above) and Goddard (Tao et al., 1989) schemes. This scheme is efficient in intermediate grids between the mesoscale and cloud-resolving grids.

WRF Single-Moment 6-class (WSM6) scheme

The six-class scheme extends the WSM5 scheme to include graupel and its associated processes. Some of the graupel-related terms followLin et al.(1983), but its ice-phase behavior is much different due to the changes ofHong et al.(2004). A new method for representing mixed-phaseparticle fall speeds for the snow and graupel particles by assigning a single fall speed to both that is weighted by the mixing ratios, and applying that fall speed to both sedimentation and accretion processes is introduced (Dudhia et al., 2008). Of the three WSM schemes, the WSM6 scheme is the most suitable for cloud-resolving grids, considering the efficiency and theoretical backgrounds.

Eta Grid-scale Cloud and Precipitation scheme

This is also known as EGCP01 or the Eta Ferrier scheme. The scheme predicts changes in water vapor and condensate in the forms of cloud water, rain, cloud ice, and precipitation ice (snow/graupel/sleet). The individual hydrometeor fields are combined into total condensate, and it is the water vapor and total condensate that are

advected in the model. Local storage arrays retain first-guess information that extract contributions of cloud water, rain, cloud ice, and precipitation ice of variable density in the form of snow, graupel, or sleet. The density of precipitation ice is estimated from a local array that stores information on the total growth of ice by vapor deposition and accretion of liquid water. Sedimentation is treated by partitioning the timeaveraged flux of precipitation into a grid box between local storage in the box and fall out through the bottom of the box. This approach, together with modifications in the treatment of rapid microphysical processes, permits large time steps to be used with stable results.

Thompson et al. scheme

A new bulk microphysical parameterization (BMP) has been developed for use with WRF or other mesoscale models. Compared to earlier single-moment BMPs, the new scheme incorporates a large number of improvements to both physical processes and computer coding plus employs many techniques found in far more sophisticated spectral/bin schemes using look-up tables. Unlike any other BMP, the assumed snow size distribution depends on both ice water content and temperature and is represented as a sum of exponential and gamma distributions. Furthermore, snow assumes a non-spherical shape with a bulk density that varies inversely with diameter as found in observations and in contrast to nearly all other BMPs that assume spherical snow with constant density.

Goddard Cumulus Ensemble Model scheme

The Goddard Cumulus Ensemble (GCE) models (Tao and Simpson, 1993) one-moment bulk microphysical schemes are mainly based onLin et al.(1983) with additional processes from Rutledge and Hobbs(1984). However, the Goddard microphysics schemes have several modifications. First, there is an option to choose either graupel or hail as the third class of ice (McCumber et al., 1991). Graupel has a relatively low density and a high intercept value (i.e., more numerous small particles). In contrast, hail has a relative high density and a low intercept value (i.e., more numerous large particles). These differences can affect not only the description of the hydrometeor population and formation of the anvil-stratiform region but also the relative importance of the microphysical-dynamical-radiative processes. Second, new saturation techniques (Tao et al., 1989, 2003) were added. These saturation techniques

are basically designed to ensure that super saturation (sub-saturation) cannot exist at a grid point that is clear (cloudy). Third, all microphysical processes that do not involve melting, evaporation or sublimation (i.e., transfer rates from one type of hydrometeor to another) are calculated based on one thermodynamic state. This ensures that all of these processes are treated equally. Fourth, the sum of all sink processes associated with one species will not exceed its mass. This ensures that the water budget will be balanced in the microphysical calculations.

Morrison et al. 2-Moment scheme

The Morrison et al.(2008) scheme is based on the two-moment bulk microphysics scheme of Morrison et al.(2005) and Morrison and Pinto(2006). Six species of water are included: vapor, cloud droplets, cloud ice, rain, snow, and graupel/hail. The code has a user-specified switch to include either graupel or hail. Prognostic variables include number concentrations and mixing ratios of cloud ice, rain, snow, and graupel/hail, and mixing ratios of cloud droplets and water vapor (total of 10 variables). The prediction of two-moments (i.e., both number concentration and mixing ratio) allows for a more robust treatment of the particle size distributions, which are a key for calculating the microphysical process rates and cloud/precipitation evolution. Several liquid, ice, and mixed-phase processes are included.

Table 2.1: Microphysics schemes of WRF model

Model ID	**Scheme**	**Reference**	**Mass Variables**
1	Kessler	Kessler (1969)	Qc Qr
2	Lin (Purdue)	Lin et al. (1983)	Qc Qr Qi Qs Qg
3	WSM3	Hong et al. (2004)	Qc Qr
4	WSM5	Hong et al. (2004)	Qc Qr Qi Qs
5	Eta (Ferrier)	Rogers et al. (2001)	Qc Qr Qs (Qt*)
6	WSM6	Hong and Lim (2006)	Qc Qr Qi Qs Qg
7	Goddard	Tao et al. (1989)	Qc Qr Qi Qs Qg
8	Thompson	Thompson et al. (2004)	Qc Qr Qi Qs Qg
9	Milbrandt	Milbrandt and Yau (2005)	Qc Qr Qi Qs Qg Q_h
10	Morrison	Morrison et al. (2009)	Qc Qr Qi Qs Qg
13	SUNY	Lin and Colle (2011)	Qc Qr Qi Qs Qg
14	WDM5	Lim and Hong (2010)	Qc Qr Qi Qs
16	WDM6	Lim and Hong (2010)	Qc Qr Qi Qs Qg

* Advects only total condensate

2.5.6.2 Cumulus Parameterization Schemes

Convection of cloud is the collective movement or aggregation of the water particles (in any state) either through advection or diffusion or both of them. This process plays a significant role in atmospheric circulation especially in precipitation amount of any particular area. Convention is widely varies in size, shape and duration. It can be happened in isolated area or organized in group or cells. It is responsible for rainfall and snowfall, cloud, vertical stability, flood, ice storms and blizzard. Convection produces feedbacks that influence large scale flow patterns. However, the process is quite complex and physical uncertainties still exist to understand the process. Thus, cumulus parameterization schemes are developed in WRF to address this issue. These schemes mainly conceptualize the convection process of atmosphere. The model use convective parameterization to predict the collective effects of convective clouds that may exists in a single grid (Arakawa and Lamb, 1977). Some available schemes of WRF are listed below:

1. Kain–Fritsch Scheme (Kain, 2004)
2. Betts–Miller–Janjic Scheme (Janjic, 1994)
3. Grell–Freitas Ensemble Scheme (Grell and Freitas, 2013)
4. Old Simplified Arakawa–Schubert Scheme (Pan and Wu, 1995)
5. Grell 3D Ensemble Scheme (Grell and Dévényi, 2002)
6. Tiedtke Scheme (Zhang et al., 2011)
7. New Simplified Arakawa–Schubert Scheme (Han and Pan, 2011)
8. Grell–Devenyi (GD) Ensemble Scheme (Grell and Dévényi, 2002)

Short descriptions of each cumulus parameterization schemes are provide in following section.

Kain-Fritsch scheme

The modified version of the Kain-Fritsch scheme (Kain,2004) is based on Kain and Fritsch(1990) and Kain and Fritsch(1993), but has been modified based on testing within the Eta model. As with the original KF scheme, it utilizes a simple cloud model with moist updrafts and downdrafts, including the effects of detrainment, entrainment, and relatively simple microphysics.

Betts-Miller-Janjic scheme

The Betts-Miller-Janjic (BMJ) scheme (Janjic, 1994, 2000) was derived from the Betts-Miller (BM) convective adjustment scheme (Betts, 1986; Betts and Miller, 1986). However, the BMJ scheme differs from the Betts-Miller scheme in several important aspects. The deep convection profiles and the relaxation time are variable and depend on the cloud efficiency, a non dimensional parameter that characterizes the convective regime (Janjic, 1994). The cloud efficiency depends on the entropy change, precipitation, and mean temperature of the cloud. The shallow convection moisture profile is derived from the requirement that the entropy change be small and nonnegative (Janjic, 1994). The BMJ scheme has been optimized over years of operational application at NCEP, so that, in addition to the described conceptual differences, many details and/or parameter values differ from those recommended inBetts(1986) andBetts and Miller(1986). Recently, attempts have been made to refine the scheme for higher horizontal resolutions, primarily through modifications of the triggering mechanism.

Grell-Devenyi ensemble scheme

Grell and Devenyi(2002) introduced an ensemble cumulus scheme in which effectively multiple cumulus schemes and variants are run within each grid box and then the results are averaged to give the feedback to the model. In principle, the averaging can be weighted to optimize the scheme, but the default is an equal weight. The schemes are all mass-flux type schemes, but with differing updraft and downdraft entrainment and detrainment parameters, and precipitation efficiencies. These differences in static control are combined with differences in dynamic control, which is the method of determining cloud mass flux. The dynamic control closures are based on convective available potential energy (CAPE or cloud work function), low-level vertical velocity, or moisture convergence. Those based on CAPE either balance the rate of change of CAPE or relax the CAPE to a climatological value, or remove the CAPE in a convective time scale.

Grell-3 scheme

The Grell-3 scheme was first introduced in Version 3.0, and so is new, and not yet well tested in many situations. It shares a lot in common with the Grell-Devenyi in scheme, being based on an ensemble mean approach, but the quasi-equilibrium

approach is no longer included among the ensemble members. The scheme is distinguished from other cumulus schemes by allowing subsidence effects to be spread to neighboring grid columns, making the method more suitable to grid sizes less than 10 km, while it can also be used at larger grid sizes where subsidence occurs within the same grid column as the updraft.

2.5.6.3 PBL Schemes

The planetary boundary layer plays a critical role in lower tropospheric processes such as vertical heat, moisture, and momentum fluxes caused by eddy transport in an atmospheric column. Since most of these processes are sub-grid-scale sized, parameterization schemes are needed to resolve in numerical models. The planetary boundary layer schemes are used to determine the horizontal and vertical diffusion processes and also the flux profile within the boundary layer. For horizontal diffusion, the horizontal deformation term or a constant eddy viscosity value is used when these terms are treated independently from vertical mixing. Diffusion rates are determined from moisture, wind, and temperature at the top and bottom of model level. For this reason, diffusion rates are considered to be local to each layer. Hence, diffusion has to be calculated specifically for each model layer. The scheme initially calculates planetary boundary effects starting from the surface model layer and ends at the free atmosphere model layer (Skamarock et al., 2008).

2.5.6.4 Land surface schemes:

The purpose of land surface models is to use atmospheric information from the surface layer scheme, radiative forcing from the radiation schemes, and precipitation forcing from the microphysical and cumulus parameterization schemes, and combined them with static data of earth surface. This combination of data provides information on the heat and moisture fluxes over land and water points on the model's grid. The heat and moisture fluxes obtained from this data are then implemented as a lower boundary layer condition, which can be used in the planetary boundary schemes. While land-surface models don't provide tendencies, it does update land-surface variables that include ground skin temperature, soil temperature profiles, soil moisture profiles, snow cover and canopy properties. One of the notable land-surface schemes is the Noah land surface scheme which is developed jointly by NCAR and NCEP to serve both operational and research applications. This scheme resolves vegetation

effects, soil temperature, soil moisture, snow cover, canopy moisture, and frozen soil. For soil moisture and temperature, this scheme contains four levels that include thickness layers of 10, 30, 60, and 100 cm. The Noah land-surface scheme provides sensible and latent heat fluxes to the planetary boundary layer schemes. Additionally, this scheme also predicts soil ice, fractional snow cover effects, urban effects, and surface emissivity properties (Dudhia et al. 2011).

2.5.6.5 Radiation schemes:

The radiation plays an important in atmospheric process as it is affect temperature, pollution concentration, visibility and color. Therefore, WRF model can parameterize longwave and shortwave radiations using some define schemes. The longwave radiation schemes account for either thermal or infrared radiation that is absorbed and emitted by atmospheric gases and land surfaces. Upward radiation flux from the surface is determined by emissivity at the ground, which is dependent on the landtype and the ground skin temperature. Visible and surrounding wavelengths that make up the solar spectrum are included in shortwave radiation schemes. While the only source of shortwave radiation is from the sun, these schemes also include absorption, reflection, and scattering by atmospheric gases and the surface. The upward heat flux from shortwave radiation is determined from the surface's albedo index. Since the radiation schemes are one dimensional in a column of atmosphere, the heat fluxes in each column is treated independently from each other (Skamarock et al. 2008).

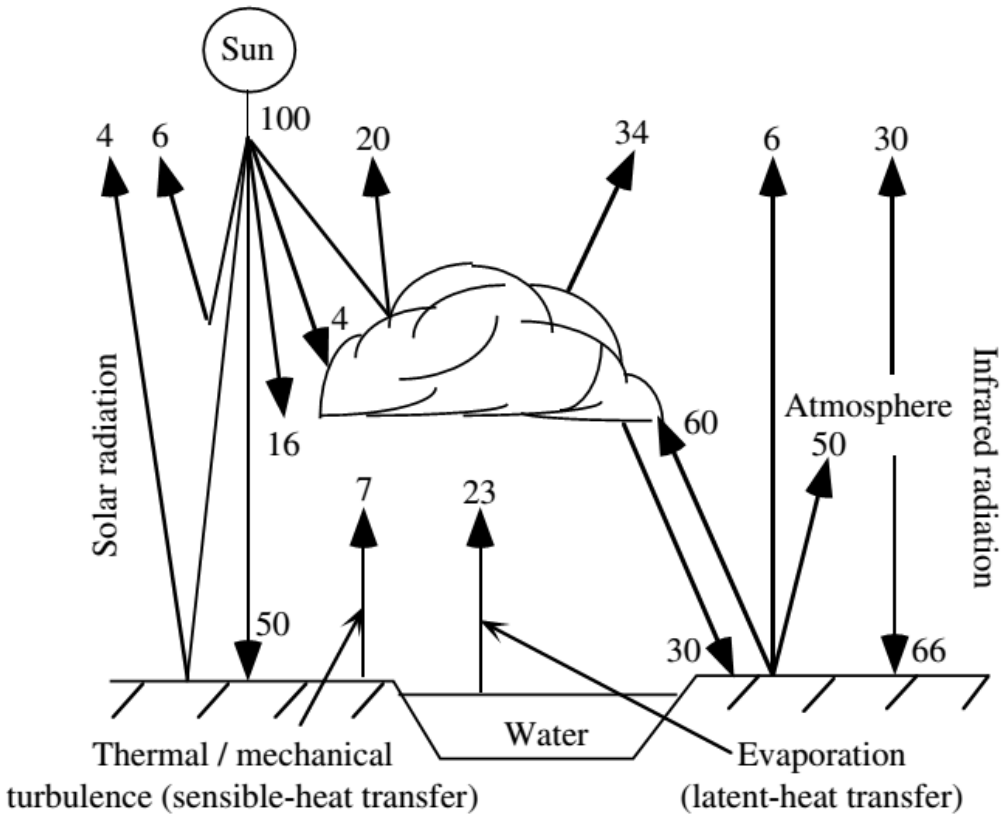

Figure 2.11: Energy balance for Earth–atmosphere system. Values are dimensionless relative quantities of energy. The sum of sources minus sinks for clouds, the atmosphere, or the Earth equals zero. For example, clouds are in radiative balance, since they absorb and emit 64 units of radiation. adopted from Jacobson (2005).

For the horizontal grid plane, the WRF-ARW uses Arakawa-C grid staggering (Fig. 2.12). For this configuration, the U component of the wind is averaged on the left and right side while the V component is averaged on the top and bottom of each cell (Fig. 10). All scalar quantities such a temperature, density and vapor mixing ratios are interpolated 10 to the center of each cell (Dudhia et al. 2011).

2.5.7 Configuration of WRF

Advanced Research WRF (ARW) is a next generation meso-scale numerical model which is widely used in different meteorological organizations of around the world. The model has several components that need to be configured in a consecutive manner in simulating a weather phenomenon. The WRF-modeling system consist three components:

a. WRF Pre-processing (WPS)
b. ARW solver (WRF core)
c. Post Processing and visualization tools

WPS or pre-processing system initialize boundary data, convert global data as model readable format, collect topographic information, process Metrologic data from global simulation, integrate topography, sea-surface temperature and meteorological variables and fixed the model domain. ARW solver get information from the WPS system and solve the model according to define physical schemes. Lastly, results from ARW needs to processed for analysis and visualization purpose by Post processing utilities. Therefore, to run a successful simulation, each steps of these components need to be configured with care.

Figure 2.12: Main components of WRF

2.5.7.1 WPS (WRF pre-processing system)

The WRF Preprocessing System (WPS) is a set of three programs whose function is to prepare input to the real program for real-data simulations. The components of WPS system is shown in Figure 2.13. Each of the programs performs one stage of the preparation:

- 'geogrid' defines model domains and interpolates static geographical data to the grids.
- 'ungrib' extracts meteorological fields from GRIB formatted files.
- 'metgrid' horizontally interpolates the meteorological fields extracted by 'ungrib' to the model grids defined by 'geogrid'.
- 'real.exe' performs vertical interpolation of meteorological fields to WRF eta levels.

There are essentially three main steps to running the WRF Preprocessing System:

1. Defining a model coarse domain and any nested domains with 'geogrid' program.

2. Extracting meteorological fields from GRIB data sets for the simulation period with

'ungrib' program.

3. Horizontally interpolating meteorological fields to the model domains with 'metgrid' program.

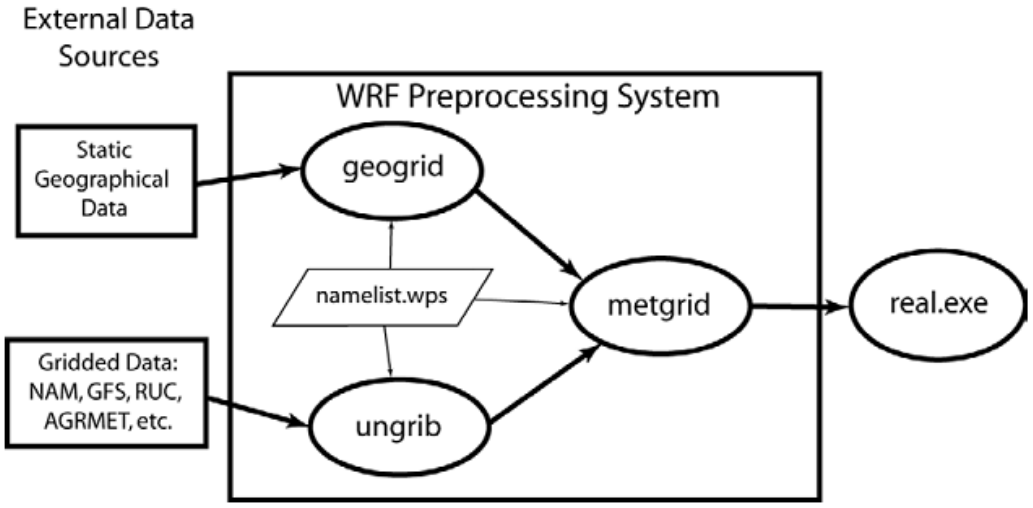

Figure 2.13: Components of WPS system. Source: Wang et al. (2009)

To configure the WPS system, one needs configure a file called 'namelist.wps'. This file is the main input module for WPS system. For initial step, the model domains need to be defined using 'geogrid' program. In the 'namelist.wps' file, there are two section which need to be modified according to simulation domain requirement. '&shrare' section take the input of model simulation runtime, model core information, simulation time interval and number of nested domain. In the '&geogrib' section of 'namelist.wps' file, one needs to provide model projection type, grid number of domain, nested domain location and grid size, resolution of both parent and nested domain, map scale ratio and location of global boundary file. After provided these information in the 'namelist.wps' the model, 'geogrid' program required to run to finalize model domain. There are several utilities like 'plotgrid.ncl' or 'grid1.exe' that allow to visualize the domain size of the intended simulation. Running 'geogrid' some '.nc' file will be created with domain information. Having downloaded meteorological data in GRIB format, next step is to extract fields to the intermediate

format using ‘ungrib.exe’. To simulate the program, editing of the “share” and “ungrib” section of the namelist.wps file is required. After modifying meteorological information of global data, ‘ungrib.exe’ is run which will produce some intermediate meteorological files. A static geo-information table name ‘Vtable’ is provided to proceed into next step. ‘metgrib.exe’ has to be simulated using ‘Vtable’ and intermediate file generated by ungrib.exe. Finally, initial phase of WPS will be completed after linking output data with ARW solver. (Wang et al., 2009).

2.5.7.2 ARW solver

After linking the WPS outputted data, the ‘real.exe’ program should be used for the initialization of that data. The ‘wrf.exe’ program is responsible for running the WRF model, which generates gridded forecasts. Before the model is initialized by the real.exe and processed by wrf.exe programs, the ‘namelist.input’ file within the WRFV3/run directory has to be edited. The namelist file contains over one hundred of options thus for simulating a forecast. Time steps, model physics, soil layer, length of simulation all parameters need to be described in this file. A description of ‘namelist.input’ variables is provided in the appendix section.

.

With the namelist properly configured, the real.exe program is used to initialize the data within the met_em* files. After the data initialization, the wrf.exe program will generate the forecasts with the initialized met_em* files. The output files will be available in .netcdf format.

CHAPTER III
DATA AND METHODOLOGY

3.1 Introduction

In the following chapters heavy rainfall events are defined and spatial distribution of heavy rainfall events are identified over Bangladesh. To identify best physical schemes, two severe events are selected and rational are described. One rainfall events is required for selecting model domain of WRF and another for evaluating different physical schemes. For the both experiments observed data sets are also required to compare the model results. Detail of these two experiments with description of observed data sets are presented in this chapter.

3.2 Heavy rainfall events

Bangladesh, formed by a delta plain at the confluences of the Ganges, Brahmaputra and Meghna river and tributaries, has a tropical monsoon climate characterized by heavy seasonal rainfall, high temperature and high humidity. Four climate seasons are characterized throughout the year, namely, pre-monsoon, monsoon, post-monsoon and winter seasons. Pre-monsoon season (from March to May) can be classified by high temperature and the occurrence of thunderstorms. Monsoon starts from month of June and end in the month of September. About 75% total rainfall happen during this time period of the year. October and November months are characterized as post-monsoon season with some amount of rainfall that occurs during this period. Driest and coolest winter season starts from the month of December and end in February (Das, 1988; Islam and Uyeda, 2007; Jacobson, 2005). The country has land an area of 147570 square kilometer, bordered by a 4,095 kilometer land frontier with Indian and a 193km frontier with Myanmar. It is straddling on the tropic of cancer, surrounded by the Asssam Hills in the east, the Meghalaya Plateau in the north, the Himalayas lying farther to the north. To its south lies the Bay of Bengal and to the west lie the plain land of West Bengal and vast track of Ganges Plain. This geographical setting acts as a catalyst for the heavy rainfall over the region.

A wind circulation system that seasonally reverses it direction is known as monsoon (Webster et al., 1998). Several places of the earth experience such circulation system

and South Asian monsoon system is one of the prominent among them. In South Asia, it is considered as one of primary process for regional heavy rainfall, which blows from the northeast during cooler months and reverses direction to blow from the southwest during the warmest months of the year. This circulation system has tremendous impact over South Asian country like Bangladesh where about 62.5% of the annual rainfall occurs during the monsoon season(Chang and Krishnamurti, 1987). Therefore, to understand the functionality of the heavy rainfall events, it is require understanding the causes of the monsoon phenomenon.

Though the monsoon phenomenon is regional in character, it is affected by the global movement of air known as the general circulation and it also affects the latter. In the north-eastern hemisphere of the globe where monsoon is predominant, land area is about 60% whereas in the rest of the world, this is about 20%. Difference in the quantity of the heat received from the sun by the land surface is the primary mechanism behind the monsoon circulation including the Indian system. As the summer in Northern Hemisphere moves northward during May, the land areas in Indian subcontinent becomes particularly prone to rapid heating because the highlands to the north protect it from any incursions of cold air. During the season, most of the solar radiation received by the areas is used up in heating the air rather than the soil as heat conductivity of soil is low. In contrast, solar radiation penetrates to greater depths in the ocean, because there can be up and down movement in water. Hence in the ocean, large part of the solar radiation is used up by water and air is heated less there. The land areas where the solar radiation falls perpendicularly are heated more than the ocean areas and the temperature difference could be as large as 10^{o}C. As a result, winds at the surface blow from low temperature zone to higher temperature zone and formulate the monsoon circulation. During winter, the sun stays in the southern hemisphere where the solar radiation falls perpendicularly and which is largely over the ocean. Because of the greater heat storage capacity of water, the ocean is heated more than the land in the season. Hence, similar kind wind circulation occurs during winter but in opposite direction. Such differential heating in summer and winter seasons is the primary reason for the generation of monsoon circulation over Bangladesh. The vast Eurasian land mass dominated by the Himalays and the Tibetan Plateau and surrounded by the Indian and Pacific oceans contributes largely to this system(Chang and Krishnamurti, 1987; Das, 1988; Raghavan, 1973; Thapliyal, 1997).

During the early part of the pre-monsoon season, a narrow zone of air mass discontinuity lies across the country that extends from the southwestern part to the northeastern part. This narrow zone of the discontinuity lies between the hot dry air coming from the upper Gangetic plain and the warm moist air coming from the Bay of Bengal. As this season progresses, this discontinuity weakens and retreats toward northwest and finally disappears by the end of the season, making room for the onset of the monsoon. The country's monsoon systems are large and stationary or slow moving. In contrast, pre-monsoon systems are small and fast moving. Pre-monsoon systems propagate southeastward whereas monsoon systems propagate to the northeast, northwest, or southeast (Rafiuddin et al., 2010). The monsoon season is highly humid and characterized by southwesterly winds with heavy rainfall. Rainfall in this season is caused by the tropical depressions that enter the country from the Bay of Bengal (Banglapedia, 2014; Krishnamurthy and Kinter III, 2003). Due to the monsoon depression, heavy rainfall events occur over Bangladesh.

High impact rainfall events become significant in human affairs when they are combined with other hydrological elements. Bangladesh is a country with high amount of rainfall event. July is the wettest month of the year. Total monthly rainfall during this month, exceeds 500 mm in almost all part of the country (Figure 3.1). Rainfall during monsoon season is caused by the tropical depressions that enter the country from the Bay of Bengal. These account for 70% of the annual total in the eastern part, 80% in the southwest, and slightly over 85% in the northwestern part of Bangladesh. The amount of rainfall in this season varies from 100 cm in the west central part to over 200 cm in the south and northeast. Average rainy days during the season vary from 60 in the west-central part to 95 days in the southeastern and over 100 days in the northeastern part. Only 2% to 4% of total annual rainfall occurs in winter season especially in the month of December.

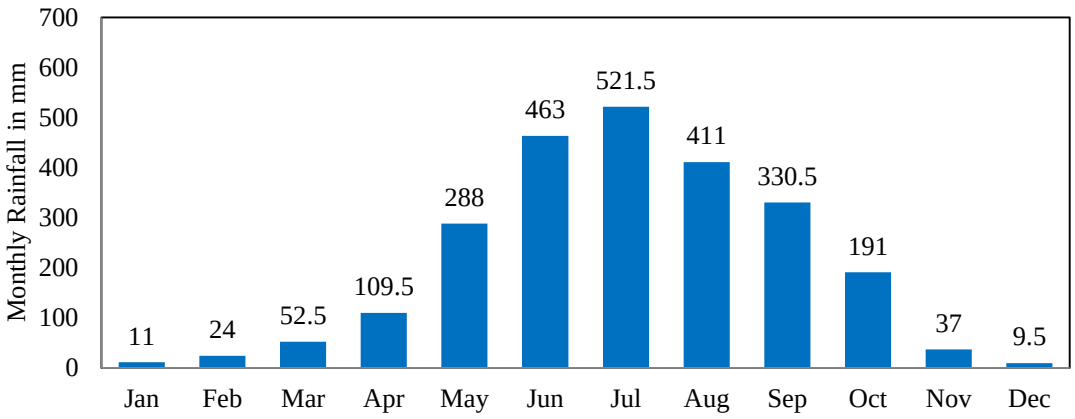

Figure 3.1: Mean monthly rainfall over Bangladesh.

Annual rainfall pattern of the country is shown in Figure 3.2. Geographic distribution of annual rainfall shows a variation from 150 cm in the west-central part of the country to more than 400 cm in the northeastern and southeastern parts. Due to geographic location and elevated terrain, north-eastern and south-eastern hilly region of the country experiences high intensive rainfall each year. Annual rainfall in both locations exceeds 3000mm, which relatively higher than the western part of the country.

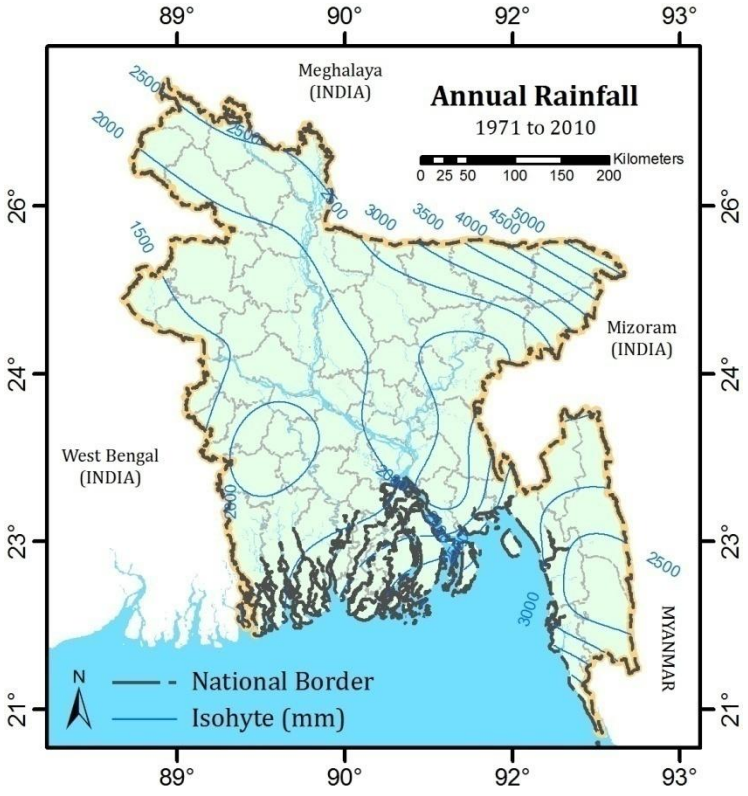

Figure 3.2: Annual rainfall pattern over Bangladesh (considering climate period of 1971 to 2010)

From the daily rainfall distribution, high intensity rainfall can be classified. When a rainfall exceeds 99 percentile of daily rainfall for a long climatic period, it can be considered as High intensity rainfall. In case of Bangladesh, considering 1961-2010 as the climate period, 99 percentile of rainfall data that are collected from thirty five stations, is plotted in Figure 3.3. From the figure, it has found that 100mm daily rainfall is the average 99th percentile rainfall of the country. Hence, in this study, rainfall events that exceed 100mm per day considered as high impact rainfall events over Bangladesh.

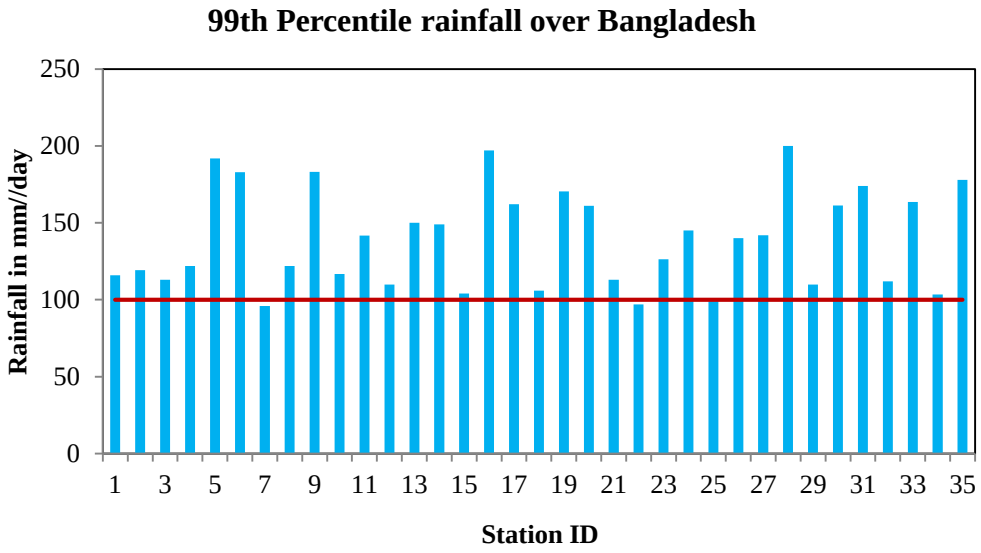

Figure 3.3: 99th Percentile rainfall over Bangladesh (red line represent threshold of high intensity rainfall)

On average, 100mm rainfall is considered to be 99% percentile rainfall of the country.

Rainfall events of 11th June, 2007 and 26th June, 2012 are the two most devastating heavy rainfall events over Bangladesh. Both of these events occurred over the south-eastern hilly region and had rainfall intensity exceeding 100mm threshold. Therefore, they are the rainfall events over the second wettest area of Bangladesh and can be considered as heavy rainfall events. Hence, these two events are selected in the present study to evaluate WRF physical schemes. A short description of the two selected rainfall events are provide in following section.

3.2.1 Rainfall event during 11th June, 2007

Heavy rainfall resulted in a landslide in Chittagong district in Bangladesh on Monday, 11 June 2007, killing 124 people so far and destroying houses, roads and embankments, as well as disrupting electricity, gas lines and communication facilities. According to the Bangladesh weather office, rainfall measured on 11 June (until 9 pm) was 408 mm, the heaviest in 25 years. A number of areas were under water as a result of incessant rainfall over the four days prior to the date of reporting. On 11 June, it was reported that 41 wards (consisting of 1.5 million people) were waterlogged. On Tuesday, 12 June, the number of people in the waterlogged areas decreased to 500,000, as the water level receded. The maritime ports ofChittagong, Cox's Bazar and Mongla hoisted cautionary signal No-3, as advised by the government's meteorological department. Four reasons were identified for the landslide: indiscriminate cutting of hill forest cover for setting up slum dwellings, abnormal rise in the level of high tide, high tide combined with concurrent heavy rainfall, and the poor drainage system.

3.2.2 Rainfall event during 27th June, 2007

The southeast region, Chittagong, Bandarban, and Cox's Bazaar, was greatly affected by the rains experiencing severe flooding, water logging, landslides and in some instances flash flooding. Death toll in the three districts of Chittagong, Bandarban and Cox's Bazar stood at 122 from 26th June to 5th July. According to the Meteorological Department this was the worst flood and landslide in the Chittagong region in the last 60 years, and in terms of rainfall in short span of time. The immediate impact of the hazards was initial displacement of the population who moved to temporary makeshift shelters, host families and community shelters. While, majority of families have returned to their dwellings, long term effect of the hazard has impacted the residences' livelihoods, water and sanitation facilities, and has damaged or destroyed their houses. About 6.5 lakh of people inundated and thousands acres of cropland ruined away as different districts were flooded following access rainfall all over the country (Shelter and Cluster, 2012).

Considering these two rainfall, WRF model has been simulated by two parts in this study. Methodology of study has been illustrated though a flow chart in Figure 3.4. After selecting two severest rainfall events, a suitable domain needs to be established for efficient forecast. Due to the reason, WRF domain size experiment has been made using 11th June, 2007 rainfall event. During the 9-10th June 2007, annual monsoon of the country started with unusually heavy rain, intensified by a storm from the Bay of Bangle. This results urban flooding and landside in the north-eastern cities of the country during 11th June, 2007. Therefore, in this study, rainfalls from 9th June to 11th June have been assessed for selecting the model domain.

3.3 Selection of model Domain

In the domain selection experiment, WRF is simulated from 2nd June to 14th June, 2012. Due to model stability, seven-day prior rainfall has also included in the simulation run.

3.3.1 Data Used

There are several historical rainfall data sets available around the world. The rainfall data sets are:

1. Global Precipitation Climatology Project (**GPCP**) (Gruber and Levizzani, 2008)
2. Tropical Rainfall Measuring Mission (**TRMM**) (Huffman et al., 2010)
3. Asian Precipitation Highly-Resolved Observational Data Integration Towards Evaluation (**APHRODITE**) (Yatagai et al., 2012)
4. Bangladesh Meteorological Department **(BMD)**
5. Climatic Research Unit **(CRU)** (Unit et al., 1997)
6. Global Precipitation Climatology Centre **(GPCC)** (Schneider et al., 2008)

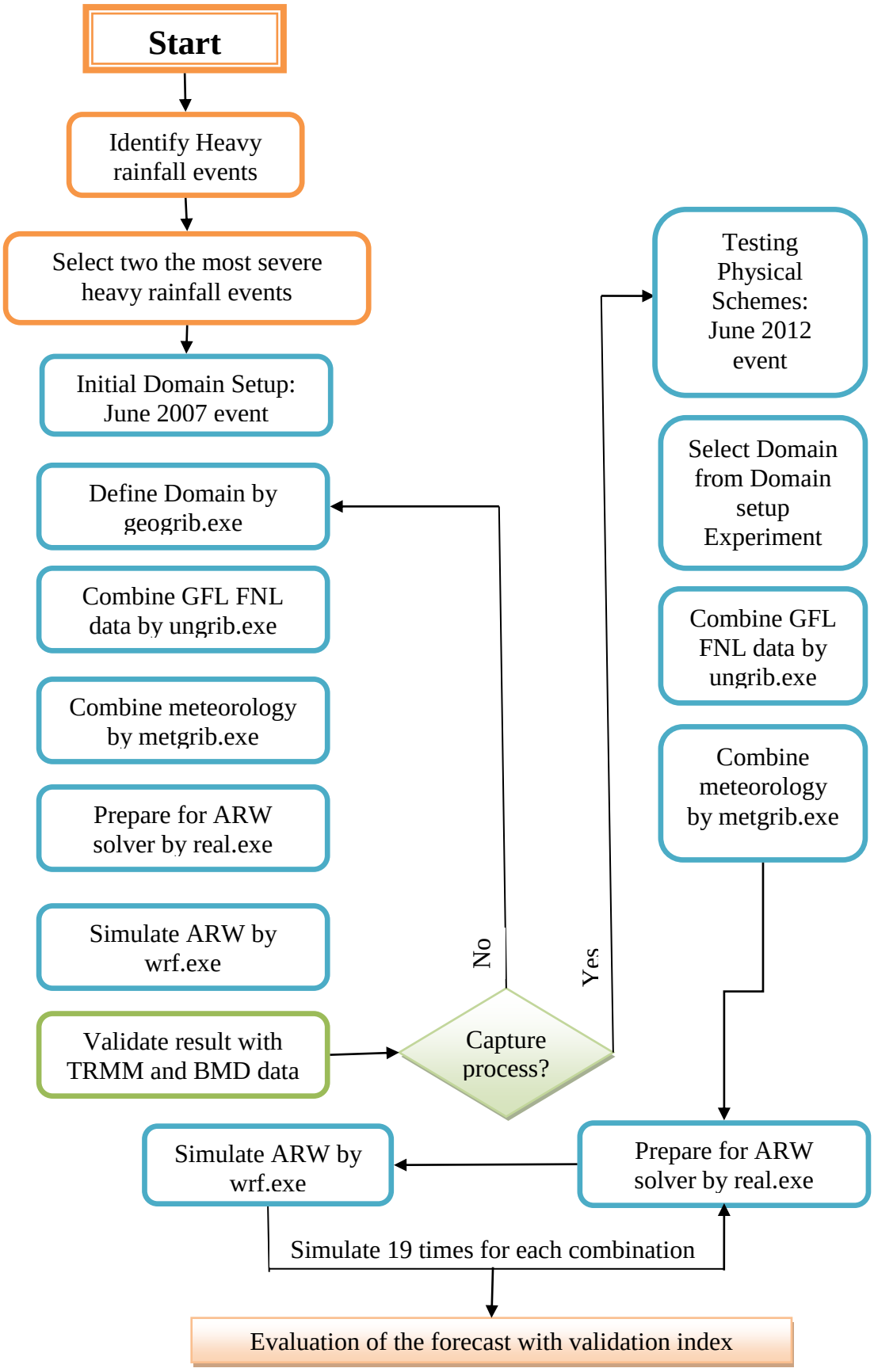

Figure 3.4: Flow chart of the methodology of the present study

Among these data sets, three data sets are selected for the 9th-11th June rainfall event; namely GPCP, TRMM and APHRODITE data sets. As, CRU and GPCC data are in monthly scale, they are avoided. For model domain selection, spatial rainfall data are required. Therefore, BMD rainfall data is not considered in the 9th-11th June rainfall analysis due to point observation. The descriptions of three selected data sets are provided in Table 3.1.

Table 3.1: Observed data that are used in domain selection experiment.

Name of Data	**Spatial Resolution**	**Time frequency**	**Extent**	**Temporal Coverage**
Global Precipitation Climatology Project (**GPCP**)	50km	day	Global	1981-2010
Tropical Rainfall Measuring Mission (**TRMM**)	25km	3 hour	Global	1998-present
Asian Precipitation Highly-Resolved Observational Data Integration Towards Evaluation (**APHRODITE**)	25km	daily	Asia	1981-2007

*3.3.1.1 Global Precipitation Climatology Project (**GPCP**)*

The Global Precipitation Climatology Project (GPCP) was established by the World Climate Research Programme to quantify the distribution of precipitation around the globe over many years. In support of this work an international group of precipitation experts developed and produces the GPCP Version 2 monthly Satellite-Gauge (SG), Pentad, and One-Degree Daily (1DD) combined precipitation data sets. The primary web site for these products is the World Meteorological Organization's World Data Center at NOAA's National Climatic Data Center. The precipitation gauge analysis used in the GPCP satellite-gauge is created by the Global Precipitation Climatology Centre. The Surface Reference Data Center (SRDC) was established in 1987 to support GPCP. Since satellites estimate rainfall through a transform of received radiance, the estimates must be verified using samples of accurate surface rainfall measurements. The SRDC, through worldwide web access, provides researchers with samples of gridded, time-space rain gauge measurements over various regions of the

globe (Adler et al., 2003). In this study, daily data of 9th-10th June rainfall event has been used for domain selection.

*3.3.1.2 Tropical Rainfall Measuring Mission (**TRMM**)*

The accurate measurement of the spatial and temporal variation of tropical rainfall around the globe remains one of the critical unsolved problems of meteorology. TRMM, during its mission and broad sampling footprint between 35°N and 35°S, is providing some of the first detailed and comprehensive dataset on the four dimensional distribution of rainfall and latent heating over vastly under sampled oceanic and tropical continental regimes. Combined with concurrent measurement of the atmosphere's radiation budget, estimates of the total diabatic heating are being realized for the first time ever on a global scale.

In this study, TRMM Product of 3B42 (V7) has been used. The purpose of the 3B42 algorithm is to produce TRMM-adjusted merged-infrared (IR) precipitation and root-mean-square (RMS) precipitation-error estimates. The algorithm consists of two separate steps. The first step uses the TRMM VIRS and TMI orbit data (TRMM products 1B01 and 2A12) and the monthly TMI/TRMM Combined Instrument (TCI) calibration parameters (from TRMM product 3B31) to produce monthly IR calibration parameters. The second step uses these derived monthly IR calibration parameters to adjust the merged-IR precipitation data, which consists of GMS, GOES-E, GOES-W, Meteosat-7, Meteosat-5, and NOAA-12 data. The final gridded, adjusted merged-IR precipitation (mm/hr) and RMS precipitation-error estimates have a daily temporal resolution and a 0.25-degree by 0.25-degree spatial resolution. Spatial coverage extends from 50 degrees south to 50 degrees north latitude.

*3.3.1.3 Asian Precipitation Highly-Resolved Observational Data Integration Towards Evaluation (**APHRODITE**)*

The APHRODITE project develops state-of-the-art daily precipitation datasets with high-resolution grids for Asia. The datasets are created primarily with data obtained from a rain-gauge-observation network. APHRODITE's daily gridded precipitation is the only long-term (1951 onward) continental-scale daily product that contains a dense network of daily rain-gauge data for Asia including the Himalayas, South and Southeast Asia and mountainous areas in the Middle East. The data are available free

of charge and are easy for GrADS and netCDF users to handle. Spatial data from these data sets has been used for observed even comparison.

3.3.2 Model Domain and pre-processing

Bangladesh Meteorological department (BMD) uses WRF model to forecast rainfall over Bangladesh. Their model domain is shown in Figure 3.5. In the study, a domain has been considered which covers complete extent of WRF domain used by BMD.

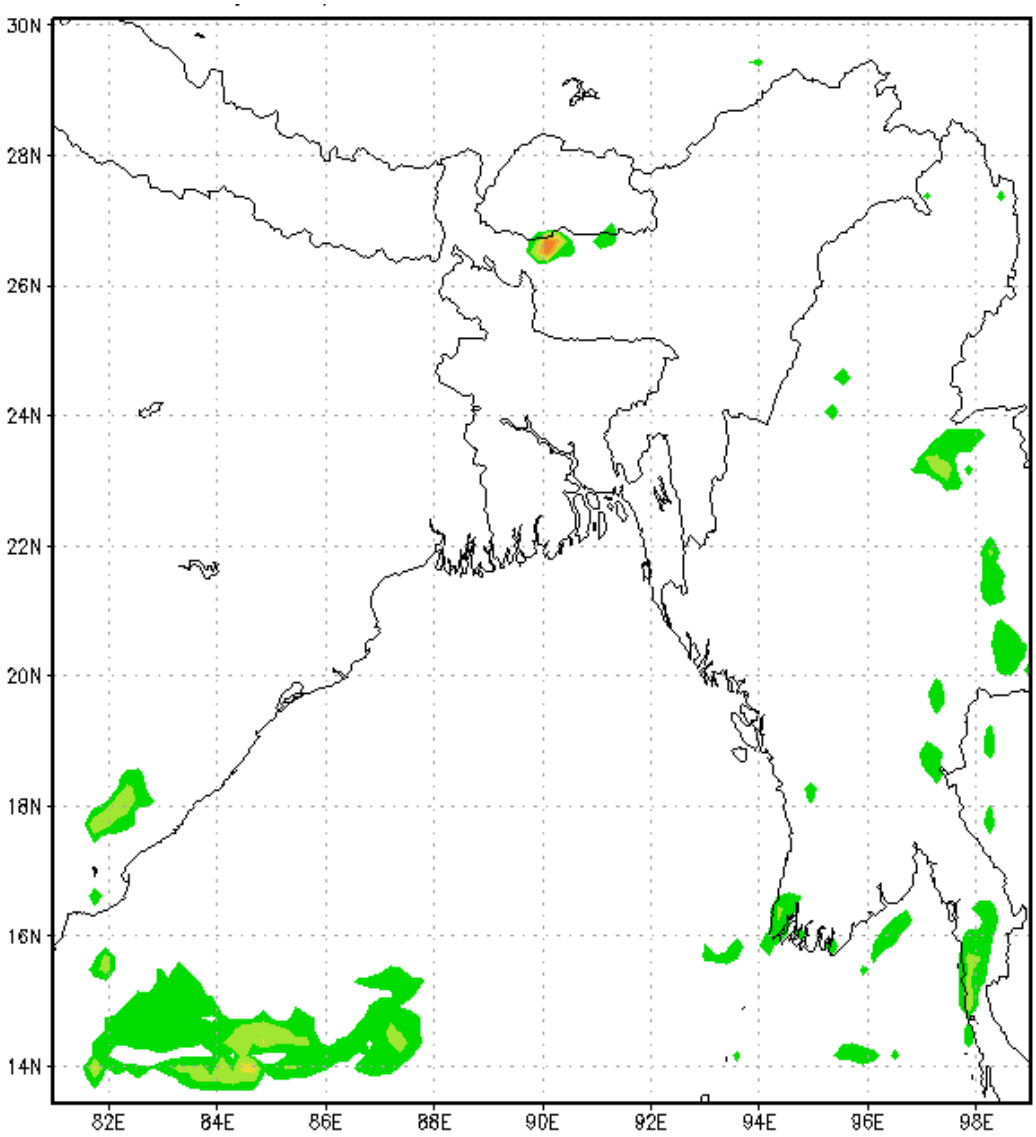

Figure 3.5: Existing Model domain of WRF used by BMD in operational weather forecast.

For the present study, a double-nested domain at 30 and 10 km resolutions has been selected. The double nested domains configured in WRF model for the study are showed in Figure 3.6. Domain 1(D1) is the coarse mesh and has 120×105 grid point in the north-south and east-west directions respectively with a horizontal grid spacing of 30km. Within the domain D1, domain 2(D2) is nested with 100×94 grid points at 10km grid spacing. These two domains are covered over whole India and Himalyan mountains to represent the regional-scale circulations and to extract the complex meteorological features in the synoptic and subsynoptic scales.

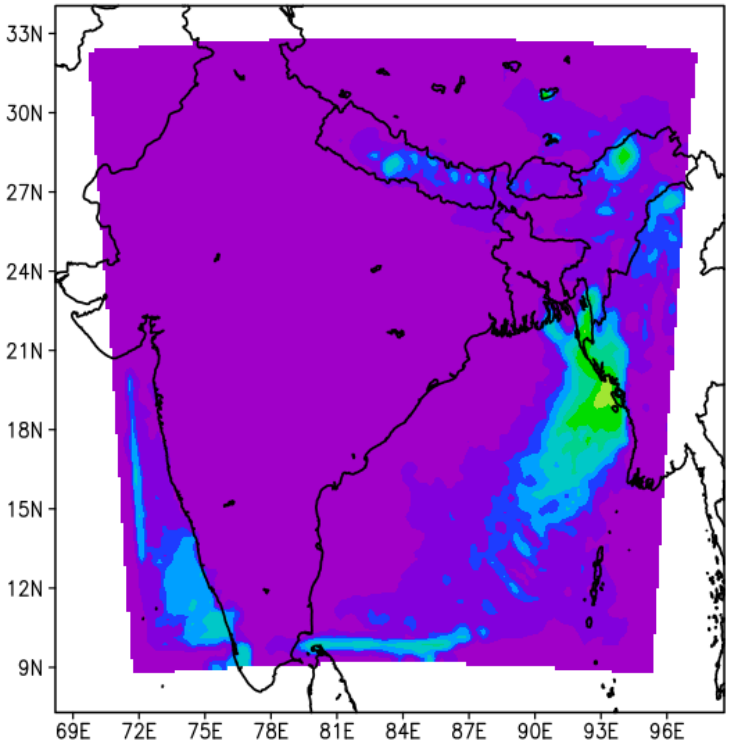

Figure 3.6: Selected domain of WRF

Domain projection system needs to be selected based on map scale factor. Figure 3.7 shows the map-scale factor for different projection system with respect to latitude. To select a particular projections system, map-scale factor of location of interest should be near one (Warner, 2011). Mid latitude over Bangladesh is around 25N. In that case, Lambert conformal projection shows map-scale factor nearest to unity for 25N latitude. Therefore, Lambert conformal projection system is used.

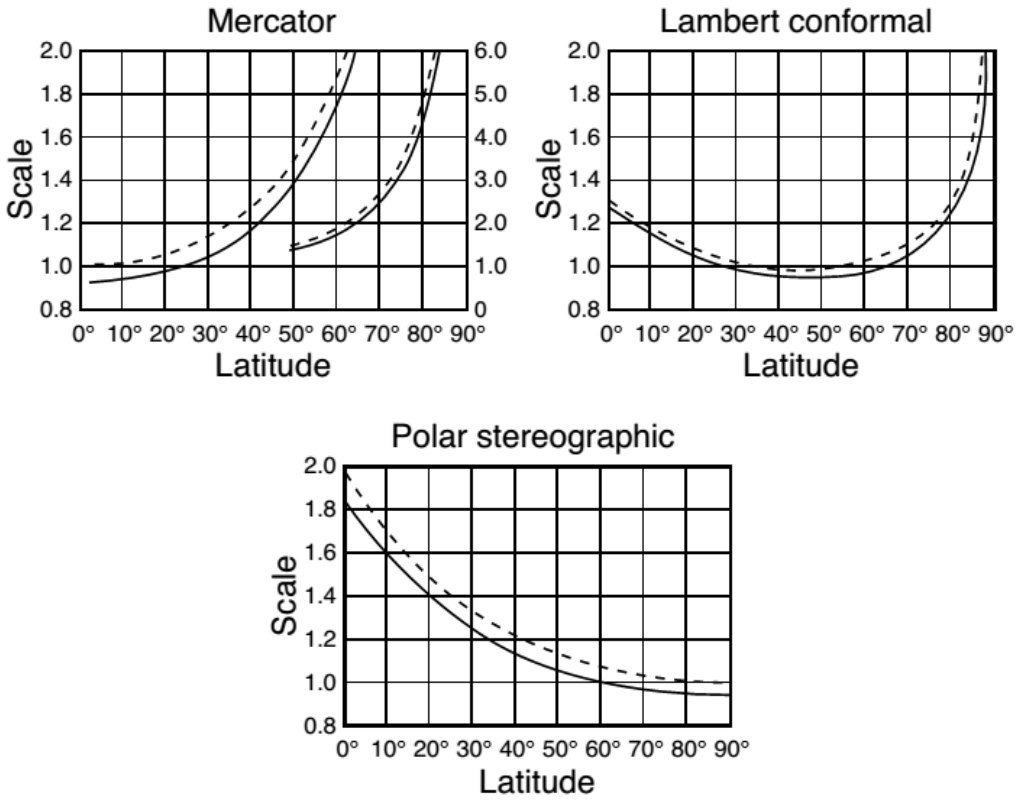

Figure 3.7: Map-scale factors for different tangent (dashed lines) and secant (solid lines) projections as a function of latitude. Adopted from Saucier (1989).

For domain nesting, 3:1 domain ratio must be maintain to preserve model stability. Hence, 30km and 10km resolution has been selected for model simulation.

All these domain information are provided in '&geogrib' section of 'namelist.wps' file.

WRF required two kinds of data for model initialization; meteorological data from global model and static topographic data.

Meteorological data are assigned as lateral boundary data in domain setup. Here, the NCEP high-resolution global final (FNL) analysis data is employed as lateral boundary data. These NCEP FNL (Final) Operational Global Analysis data has 1.0°××1.0° grid resolution grids covering the entire globe in every six hours. The product is from the Global Data Assimilation System (GDAS), which continuously collects observational data from the Global Telecommunications System (GTS), and

other sources, for many analyses. The FNLs are made with the same model which NCEP uses in the Global Forecast System (GFS), but the FNLs are prepared about an hour or so after the GFS is initialized. The FNLs are delayed so that more observational data can be used. The GFS is run earlier in support of time critical forecast needs, and uses the FNL from the previous 6 hour cycle as part of its initialization. Parameters of the data include surface pressure, sea level pressure, geopotential height, temperature, sea surface temperature, soil values, ice cover, relative humidity, u- and v- winds, vertical motion, vorticity and ozone. The data are in GRIB1 and GRIB2 format and can be downloaded freely. This data is easily useable by the WRF model. In present study, FNL data has been downloaded for 4th - 11th June, 2007 and for 19th to 28th June, 2012. Downloaded data of 4th to 11th June, 2007 are used as lateral boundary condition of domain experiment.

Static topographic information is also requisite for the configuration of model domain. There are two source of land-use classification available for WRF simulation; USGE and MODIS. USGS land use data has 24 land-use classifications where MODIS data contain only 20 categories of land use. However, both data sets are useable at 10minute, 2minute and 30second resolution. In current study, the highest resolution (30 second) of USGE data has been utilized.

Within the 'namplist.wps' file, the static and metrological data information are given. After that, the 'geogrib.exe' has been simulated to produce static domain information of the model.

After suitably modifying the namelist.wps file, a Vtable must be supplied, and the GRIB files must be linked (or copied) to the filenames that are expected by 'ungrib' program. The WPS is supplied with Vtable files for many sources of meteorological data, and the appropriate Vtable may simply be symbolically linked to the file Vtable, which is the Vtable name expected by 'ungrib' program. In the present study, Vtable.GFS has been used which is the standard Vtable of FNL meteorological data sets.

The detail of nametlist.wps file used in domain configuration is provided in APPENDIX section.

After editing the namelist.wps file and linking the appropriate Vtable and GRIB files, the ungrib.exe executable has been be run to produce files of meteorological data in the intermediate format. The final step for the model configuration is running metgrib.exe. The program has executed to horizontally interpolate meteorological data extracted by ungrib to the simulation grids defined by geogrid. Now initialization of model domain is completed and ready for input of core ARW solver.

3.3.3 Simulation of 11th June event with standard model physic

After simulating metgrib.exe, model is configured based on 0000 UTC of 04-11th June, 2007 rainfall events. For model stability, a spin up period of 5 days has been considered in the study.

To setup model physics, WRF configuration from previous literature has been used in the study. Ahasan et al. (2012) previously conducted an experiment on the south eastern region of Bangladesh with the same events but with MM5 model. In that study Anthes-Kuo cumulus parameterization schemes (CPS) with MRF planetary boundary layer (PBL) has been used. Similarly, studies also carried out over the region with different rainfall events (i.e. 21 June, 2004; 11 July, 2004) (Ahasan et al., 2013b). In these studies, different cumulus schemes were used for simulating numerical weather models. With WRF model, Ahasan et al. (2013b) conducted a research with rainfall events of 7 September, 2011. In the study, they considered Kain-Fritsch (new Era) scheme as cumulus and WSM-3 class scheme as microphysics scheme to simulate the event. As the study focused on Bangladesh and used WRF, for configuring the model domain of present analysis, Kain-Fritsch (new Era) cumulus scheme and WSM-3 class microphysics scheme have been used. These information are included in WRF by editing the 'namelist.input' file. Sample of 'namelist.input' file is provided in APPENDIX section.

Several other options need to be defined in the namelist.input file. The start and end date variables have to be set for both the parent and nested domain. An earlier starting time is chosen for the parent domain so that it could spin up precipitation for its nested domain. Since the WPS data (met_em* files) providing the boundary

conditions is 3-hourly, the input data interval or interval_seconds variable is set to 10800 seconds. Setting the history interval variable to 60 has allowed the model to produce analyses every hour. Because the WRF ran the same domain as the WPS generated initialization files, the domain variables within the domain field are copied from the WPS namelist with the exception of a few variables. The vertical dimension variable (e_vert) is responsible for setting the number of model levels within the WRF-ARW. The number of vertical levels chosen for WRF-ARW is 35. Since the input met_em.* files contains 27 meteorological levels and 4 soil levels the num_metgrid_levels and num_metgrid_soil_levels variables are set to these values, respectively. Selected physical schemes are provide in Table 3.2.

Table 3.2: Selected physical schemes in domain size experiment

Type of the schemes	**Selected scheme**
Micro-physics (mp_physics)	Kessler scheme (1)
Long wave radiation (ra_lw_physics)	RRTM scheme (1)
Shortwave radiation (ra_sw_physics)	Dudhia scheme (1)
Minutes between radiation physics calls. (radt)	30, 10 (1 minute per km of dx)
Surface-layer (sf_sfclay_physics)	MM5 Monin-Obukhov (1)
Land-surface (sf_surface_physics)	Unified Noah land-surface model (2)
Boundary-layer (bl_pbl_physics)	YSU scheme (1)
Cumulus (cu_physics)	Kain-Fritsch (new Eta) scheme (1)
Number of soil layers in land surface (num_soil_layers)	Noah land-surface model (4)
Urban physics (sf_urban_physics)	No urban physics (0)
Eddy coefficient (km_opt)	Horizontal Smagorinsky first order closure (4)

After the data was initialized, the wrf.exe program has generated the WRF-ARW forecasts with the initialized met_em* files. The wrf program has generated 3-hourly forecast output up to 12 hours for both the nested and parent domain.

3.3.4 Model result from after simulation

Results from WRF, are now converted for further analysis using ARWpost processing utility. Spatial patterns obtained from WRF simulation during 9th, 10th and 11th June, 2007 are compared with three selected historical data. After that, an appropriate adjustment has been made to fixing the model domain. With a trial and error process final domain size is finalized to simulate sensitivity test.

Final Configuration of the domain of the study is as follow:

- Domain Extant: 71°East to 97° East; 9°North to 32°North
- Spatial Resolution: 30 km by 30km (domain 1) and 10km by 10km (domain 2)
- Static data resolution: 30second (~900m resolution)
- Parent grid ration 1:3
- Grid size: 91 by 91 (D1); 115 by 115 (D2).
- Map Projection: Lambert Conformal Projection
- Reference Latitude: 21N
- Reference Longitude: 83.5E
- True Median Latitude: 21N

3.4 Simulation of sensitivity test

To understand the model performance of WRF model sensitivity test have carried out in this study. For the configuration of WRF, all the process of the domain setup experiment are followed except there are changes in input meteorological variables for different date and changes in physical schemes. Rainfall during 24th to 27th June, 2012 is selected for this sensitivity test. The events were one of the deadliest high intensive rainfall events in Bangladesh history. During the 26th June, around 323mm rainfall was recorded at Chittagong within 24h time interval, which was responsible for extended water logging and disastrous landslide in Chittagong city. Thus, if we can understand the skill of different physical schemes in such high intensive rainfall event, eventually it will help us to improve a better early warning system for such event. Therefore, sensitivity tests are carried out using this rainfall event.

There are several physical schemes available in WRF model. However, the cumulus and microphysics scheme of WRF mainly responsible for rainfall generation. There are 15 microphysics schemes and 10 cumulus scheme for WRF simulation. There will 150 combination of run that's needs to be simulated to cover all available physical schemes for the sensitivity test. To conduct a simulation using a single scheme, it requires 18 hours and 24 minutes to complete a run of 7days using a normal desktop computer (Intel Core duo processor). Therefore, it would require around 150 days just completing whole sets of analysis. Moreover, all the microphysics and cumulus schemes are not suitable for tropical climate like Bangladesh. Some of them are suitable for Antarctic regions; some are good for simulating ice and snow, some

others are suitable for theoretical assumptions. Therefore, a set of microphysics and cumulus parameterization schemes have been selected in the study considering the monsoon climatology of Indian region for the assessment of high intensive rainfall over Bangladesh. Rational behind the physical schemes are stated as follow:

3.4.1 Selection of Cumulus schemes

3.4.1.1 Kain–Fritsch Scheme

Kain–Fritsch Scheme is one of the widely used convective schemes of Numerical Weather models. Originally, Kain-Fritsch scheme was developed in 1990 (Kain and Fritsch, 1990). However, due to its effectiveness, the scheme has been modified later years and new Kain-Fritsch scheme has been incorporated in the latest version of WRF model. It can be used in NWP with moisture trigger and radiation dependent trigger. The scheme is selected for this study.

3.4.1.2 Betts–Miller–Janjic Scheme

Betts–Miller–Janjic scheme is adjustment type scheme which has both deep and shallow convection profile. Thus, the scheme is selected for the study.

3.4.1.3 Grell 3D Scheme

Grell 3D scheme has explicit updrafts and downdrafts mechanism of convection. The scheme has smaller ensemble than Grell-Dudhia scheme and has similar mechanism. It has subsidence spreading to neighboring columns which make it more suitable for <10km grid size. Therefore, this scheme has been selected in the study.

3.4.1.4 Tiedtke Scheme

Tiedtke scheme is another widely used cumulus scheme. It is quite good in capturing low cloud layers. Thus the scheme has been selected in the study.

3.4.1.5 New Simplified Arakawa–Schubert Scheme

It is another widely used vertical diffusion scheme in ARW model. This scheme is also selected in present study.

3.4.1.6 Other cumulus schemes

Zhang–McFarlane cumulus schemes developed focusing climate study over north American region. Therefore, it is considered in current study. There are some older schemes in WRF, which had replaced by newer scheme such as old Kain–Fritsch scheme, Old Simplified Arakawa–Schubert Scheme and Grell–Freitas Ensemble Scheme. Therefore they are avoided in the study.

3.4.2 Selection of Microphysics schemes

3.4.2.1 Kessler Scheme

Kessler Scheme is one of the basic microphysical schemes of WRF. It use three variables for its calculation; vapor water (Qv), cloud water (Qc) and rain water (Qr). It is selected for this study.

3.4.2.2 Lin et al. Scheme

Purdu university line et al. scheme one of the widely used scheme of WRF. Several study over Indian region used this microphysics scheme to simulate WRF(Mannan et al., 2013; Routray et al., 2010). Therefore the scheme has been selected for the study. It has 5-class microphysics including graupel.

3.4.2.3 WRF Single–moment 6–class Scheme

This scheme is the most up to date WRF single moment microphysics scheme (WRFMPs). In addition to simple 3-class Microphysics schemes (WSMP3) and mixed phase schemes (WSMP5), it has more complex of graupel. The scheme is selected for the study.

3.4.2.4 Stony–Brook University Scheme

Stony Brook University developed an advanced temperature dependent scheme which is known as Stony Brook University scheme. The scheme is a bulk microphysical parameterization (BMP) and includes a diagnosed riming intensity. It also reduces the number of parameterized microphysical processes by ∼50% as compared to conventional six-category BMPs and thus it is more computationally efficient (Lin and Colle, 2011). Thus, the scheme is selected for the study.

3.4.2.5 Other Microphysics scheme

Other microphysics schemes are not selected for the high intensive rainfall study. Eta (Ferrier) scheme has six variables of cloud microphysics with emphasize on the three state of ice; ice, snow and graupel. As monsoon climate, do not produce snow in the surface, the scheme has avoided from the study. As we consider the most complex of WRF single moment microphysics scheme (WRFMPs) scheme which is WRF Single–moment 6–class Scheme, we did not selected other two relatively simple WRFMPs scheme; WRF Single–moment 3–class and 5–class Schemes(Hong et al., 2004). The Goddard Scheme and Thompson Scheme are more focused on winter precipitation forecast which are not appropriate for the monsoon rainfall simulation (Tao et al., 1989; Thompson et al., 2008). Milbrandt–Yau, Morrison 2 and Cam V2 are the moment scheme like WRFMP6, therefore any more moment schemes are not selected(Milbrandt and Yau, 2005; Morrison et al., 2009).

3.4.3 Simulation of nineteen combination of physical scheme

Finally, five cumulus parameterization schemes and four microphysical schemes have been selected for evaluating the forecast of the high intensive rainfall event over the eastern hilly regions of Bangladesh. Thus, a set of nineteen simulation are selected which are described in Table 4.2. Simulations have been done using these schemes combination for the rainfall events of 24th June to 27th June, 2012. To stabilize the model simulation and giving a spin-up period, all the simulations have been made from 19th June to 29th June, 2012 using Global FNL data set. All the model set kept same as domain size experiment. Only physical options are changed for each experiment run. After obtaining model result for each physical scheme set, some evaluation parameter has been calculated to check performance of the forecast of different physical schemes.

Table 3.3: List of selected simulations with their respective micro-physics and cumulus scheme (model option is provided in the bracket)

ID	Name	Micro-physics scheme	Cumulus schemes
01	KEKF	Kessler (1)	Kain-Fritsch (new) (1)
02	KEBJ	Kessler (1)	Betts-Miller-Janjic (2)
03	KEGR	Kessler (1)	New Grell 3D (5)
04	KETD	Kessler (1)	Tiedtke (6)
05	LNKF	Lin et al. (2)	Kain-Fritsch (Eta) (1)

06	LNBJ	Lin et al. (2)	Betts-Miller-Janjic (2)
07	LNGR	Lin et al. (2)	New Grell 3D (5)
08	LNTD	Lin et al. (2)	Tiedtke (6)
09	WMKF	WRF Single–moment 6–class (6)	Kain-Fritsch (Eta) (1)
10	WMBJ	WRF Single–moment 6–class (6)	Betts-Miller-Janjic (2)
11	WMGR	WRF Single–moment 6–class (6)	New Grell 3D (5)
12	WMAS	WRF Single–moment 6–class (6)	New Arakawa–Schubert (14)
13	SUKF	Stony–Brook University (13)	Kain-Fritsch (Eta) (1)
14	SUBJ	Stony–Brook University (13)	Betts-Miller-Janjic (2)
15	SUGR	Stony–Brook University (13)	New Grell 3D (5)
16	SUAS	Stony–Brook University (13)	New Arakawa–Schubert (14)
17	SUTD	Stony–Brook University (13)	Tiedtke (6)
18	WMTD	WRF Single–moment 6–class (6)	Tiedtke (6)
19	LNAS	Lin et al. (2)	New Arakawa–Schubert (14)

3.4.4 Evaluation of simulated results

Both statistical and graphical model evaluation techniques were reviewed in this study. Graphical spatial pattern of each experiment has been compared with observed TRMM spatial pattern for the selected time period. Point wise evaluations also have been made with BMD and TRMM observed data for each four days of the rainfall event. As 26th June, 2012 rainfall occurred mostly over the eastern hilly region of Bangladesh, the comparison of rainfall magnitude is made over the three observed station; Chittagong, Cox's Bazar and Teknaf station using BMD and TRMM data.

Area wise model evaluation has been done in this study. During 24th to 27th June, rainfall occurs mostly in the Chittagong hilly region and cause severe damages. There to avoid false bias, an area ranging from 20.5N to 24N and 91E to 93E has been chosen in calculating error indices. The selected area is shown in Figure 3.8. In point based comparisons between two observed data, south eastern region agree more than south-western region of the country. To avoid ambiguity, spatial TRMM data of south-eastern region are selected in the forecast index analysis.

Several error indices are commonly used in numerical model evaluation. These include root mean square error (RMSE) and Percentage Bias (PBIAS). These two indices are analyzed over the chosen area.

3.4.4.1 Root mean square error (RMSE)

RMSE is one of the commonly used error index statistics(Ahasan et al., 2013a; Das et al., 2008). This index is valuable because it indicate error in the units (or squared

units) of the constituent of interest, which aids in analysis of the results. Here, RMSE of rainfall in mm is calculated for each experiment with respect to TRMM data. RMSE can be calculated with following equation:

$$RMSE = \sqrt{\frac{1}{n}\sum_{i=1}^{n}(P_i - O_i)^2}$$

Where, n is number of sample point, P is the forecast value and O is the observed value of same location.

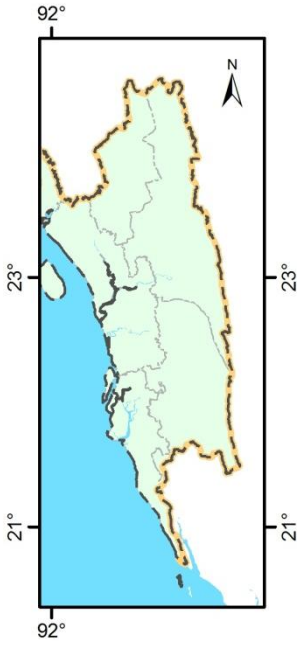

Figure 3.8: Selected area that used in area wise model evolution.

3.4.4.2 Percent bias (PBIAS)

Percent bias (PBIAS) measures the average tendency of the simulated data to be larger or smaller than their observed counterparts(Gupta et al., 1999). The optimal value of PBIAS is 0.0, with low-magnitude values indicating accurate model simulation. Positive values indicate model overestimation bias, and negative values indicate model underestimation bias. PBIAS is calculated with following equation:

$$PBIAS = \frac{\sum_{i=1}^{n}(P_i - O_i)}{\sum_{i=1}^{n} O_i} * 100$$

Where, PBIAS is the deviation of data being evaluated, expressed as a percentage. PBIAS of each point over selected area has been calculated and average of them is determined for individual experiment. Analysis has been done for each day of the rainfall events.

In this study, some forecast verification index are also used to assess the performance of WRF physical schemes. These indices can be calculated using a 2 × 2 contingency table. Two by two contingency table is wide used in non probabilistic forecast study (Doswell III, 2004; Ebert and McBride, 2000; Gilbert, 1884). Figure 3.9 shows the attributes of a 2 × 2 contingency table. Here, 'a' represent number of particular rainfall event which happened and forecasted successfully; 'b' represents the number of particular rainfall event which did not happened but forecasted by the model; 'c' represents the number of event which did happened but the model failed to forecast and 'd' represents the number of rainfall event which did not happened and model also did not forecasted them. In this study, area based contingency tables have been developed depending on four threshold of rainfall forecast. The rainfall thresholds are 1mm, 20mm, 50mm and 100mm. Four contingency tables have been made for each rainfall threshold. In the selected area, there are 120 location points which values are used in the formulation of the contingency tables. Therefore, a + b + c + d is equals to 120. Using this contingency table several forecast verification indices can be calculated which are explained as follow:

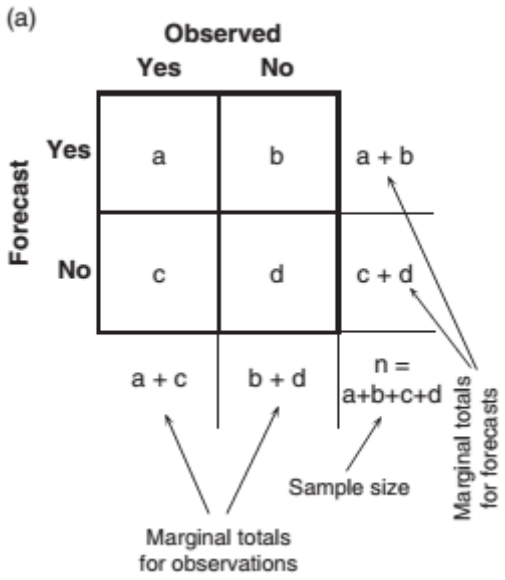

Figure 3.9: A 2 × 2 contingency table for a particular threshold of rainfall.

3.4.4.3 Proportion correct (PC)

The most direct and intuitive measure of the accuracy of non probabilistic forecasts for discrete events is the *proportion correct (PC)* proposed by Finley (1884). This is simply the fraction of the n forecast occasions for which the non probabilistic forecast correctly anticipated the subsequent event or nonevent. In terms of counts Figure 4.5, PC is give by

$$PC = \frac{a+d}{n}$$

This is an effective indicator for predicting the accuracy of a model. The indicator represents correct "yes" and "no" forecasts equally. The proportion of correct penalizes both kinds of errors (false alarms and misses) equally. The worst possible PC is zero; the best possible PC is one. However, PC does not distinguish between correct forecasts of the event, a, and correct forecasts of the nonevent, d.

3.4.4.4 Threat Score (TS)

Another alternative indicator to evaluate accuracy of rainfall event is Threat Score (TS) (Gilbert, 1884). The indicator often is used to assess simultaneously issued spatial forecasts, for example, severe weather warnings. The threat score is the number of correct "yes" forecasts divided by the total number of occasions on which that event was forecast and/or observed. In terms of Figure 4.5, it can be expressed as follow,

$$TS = \frac{a}{a+b+c}$$

It can be viewed as a proportion correct for the quantity being forecast, after removing correct "no" forecasts from consideration. The worst possible TS is zero, and the best possible TS is one.

3.4.4.5 Bias (B)

The bias (B) is the comparison of the average forecast with the average observation. It is usually represented as a ratio for verification of contingency tables. In terms of Figure 4.5, it can be written as follow,

$$B = \frac{a+b}{a+c}$$

The bias is simply the ratio of the number of "yes" forecasts to the number of "yes" observations. Unbiased forecasts exhibit B=1, indicating that the event was forecast the same number of times that it was observed. Note that bias provides no information about the correspondence between the individual forecasts and observations of the event on particular occasions, so that B is not an accuracy measure. Bias greater than one indicates that the event was forecast more often than observed, which is called over-forecasting. Conversely, bias less than one indicates that the event was forecast less often than observed, or was under-forecast.

3.4.4.6 False alarm ratio (FAR)

The false alarm ratio (FAR) is useful to understand the false forecast of a model. FAR is the fraction of "yes" forecasts that turn out to be wrong, or that proportion of the forecast events that fail to materialize. In terms of the 2×2 table in Figure 4.5, the false alarm ratio is,

$$FAR = \frac{b}{a+b}$$

The FAR has a negative orientation, so that smaller values of FAR are to be preferred. The best possible FAR is zero, and the worst possible FAR is one.

3.4.4.7 The false alarm rate (F)

The false alarm rate is the ratio of false alarms to the total number of non occurrences of the event, or the conditional relative frequency of a wrong forecast given that the event does not occur. In terms of Figure 4.5, the false alarm rate can be computed as follow,

$$F = \frac{b}{b+d}$$

3.4.4.8 Hit rate (H)

The hit rate (H) is the ratio of correct forecasts to the number of times this event occurred. In terms of Figure 4.5, it can be described,

$$H = \frac{b}{b+d}$$

This can be regarded as the fraction of those occasions when the forecast event occurred on which it was also forecast. Jointly, the hit rate and false alarm rate provide both the conceptual and geometrical basis for the signal detection approach for verifying probabilistic forecasts.

In this study, all of the forecast verification indices are calculated for each experiment and are ranked according to the performance of the model. Combined ranking using all the indices has been done for each category of rainfall threshold. Finally, the best performed physical schemes are suggested depending on threshold of rainfall event over the eastern hilly region of Bangladesh.

CHAPTER IV
RESULTS AND DISCUSSION

4.1 Introduction

After conducting domain size experiment and nineteen sensitivity test, some results can be from output of WRF model. In following section, the results of these experiments are explained in detail.

4.2 Domain Setup

Weather Research forecasting is a numerical model which has various customization options to calibrate an atmospheric phenomenon. To simulate a high intensive rainfall event, several configuration of the model needs to fix including domain size. To capture whole monsoon process, model area can be fixed but center and grid point of the domain area needs to be change, to capture reasonable well phenomenon. For domain size experiment, 9^{th}-11^{th} June event was selected. As it is mentioned earlier, the physical and parameterization information are provided according to previous high intensive rainfall study conducted by Ahasan et al. (2013b). The detail of the 'input.wps' is provided into APPENDIX section. The model simulation results are compared with TRMM, Aphrodite and GPCP data for 2 days of the event; 9^{th} June and 10^{th} June where rainfall are formed. Comparison of the model rainfall vs observed rainfall is shown in Figure 4.1 and Figure 4.2. From the figure, it has found that, with existing scheme model could not resolve magnitude and scheme of the data but atmospheric processes are captured in model domain. The primary objective of model domain experiment is to capture all existing process over Indian region but not making accuracy of magnitude and pattern of an event. Therefore, according to model simulation during 9^{th} and 10^{th} June, model captures Meghan basin rainfall circulation, rainfall pattern over Nepal Himalayan region and rainfall pattern of west coast of India. For Meghna Basin, rainfall is slightly shitted but has similar magnitude during 10^{th} June, 2007. This domain has been achieved by nudging the center of the domain and by adjusting the grid size and resolution. Considering this domain, rest of the experiment is done.

Final Configuration of the domain of the study is as follow:

- Domain Extant: 71°East to 97° East; 9°North to 32°North
- Spatial Resolution: 30 km by 30km (domain 1) and 10km by 10km (domain 2)
- Static data resolution: 30second (~900m resolution)
- Parent grid ration 1:3
- Grid size: 91 by 91 (D1); 115 by 115 (D2).
- Map Projection: Lambert Conformal Projection
- Reference Latitude: 21N
- Reference Longitude: 83.5E
- True Median Latitude: 21N

Extent of the selected domain is shown in Figure 4.3.

4.3 Simulation during 24th to 27th June, 2012

Using the domain, 18 simulations have been conducted using different physical schemes. The simulation time period is selected 20th June to 28th June due to model stability and spin-up period.

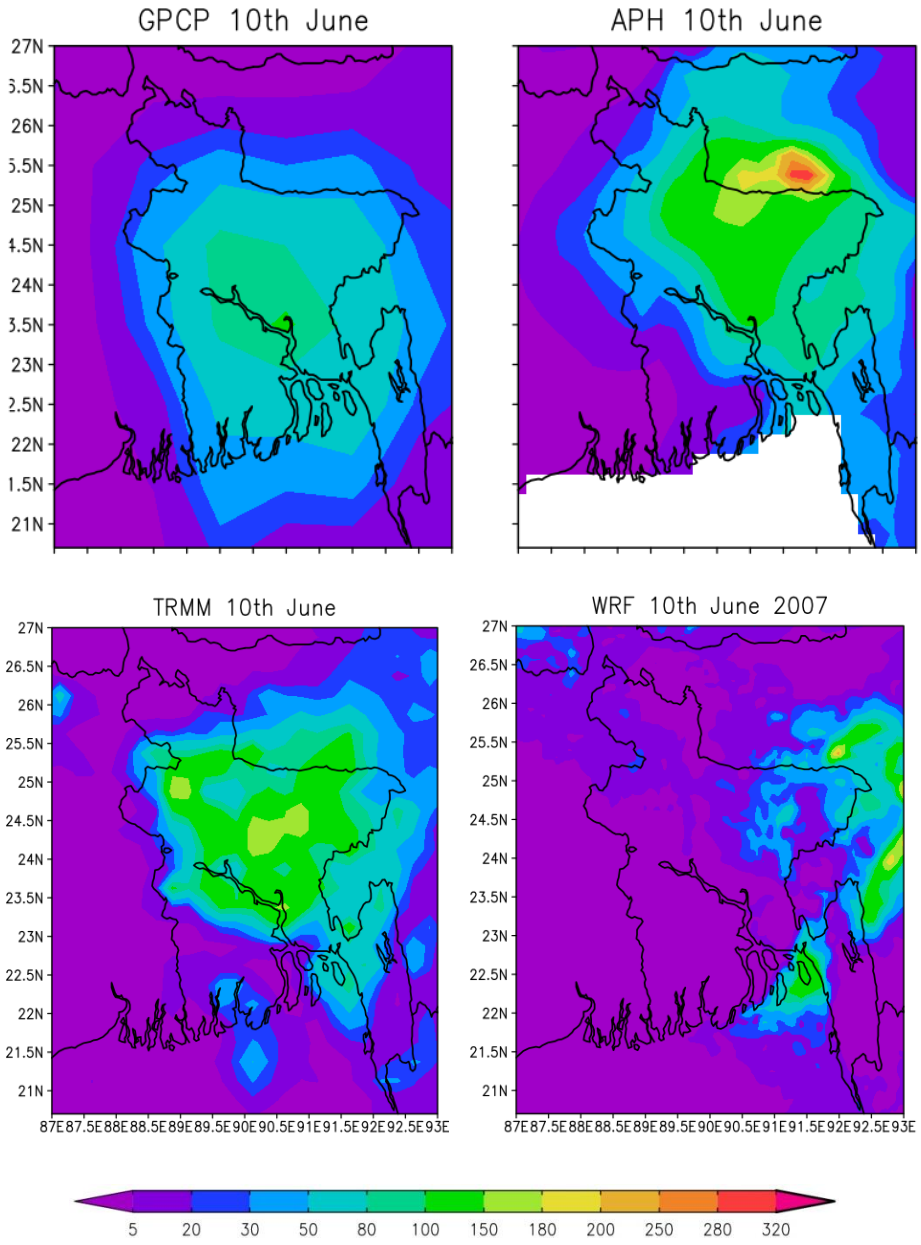

Figure 4.1: Rainfall during 10th June in TRMM, Aphrodite, GPCP and simulated WRF data over Domain 2.

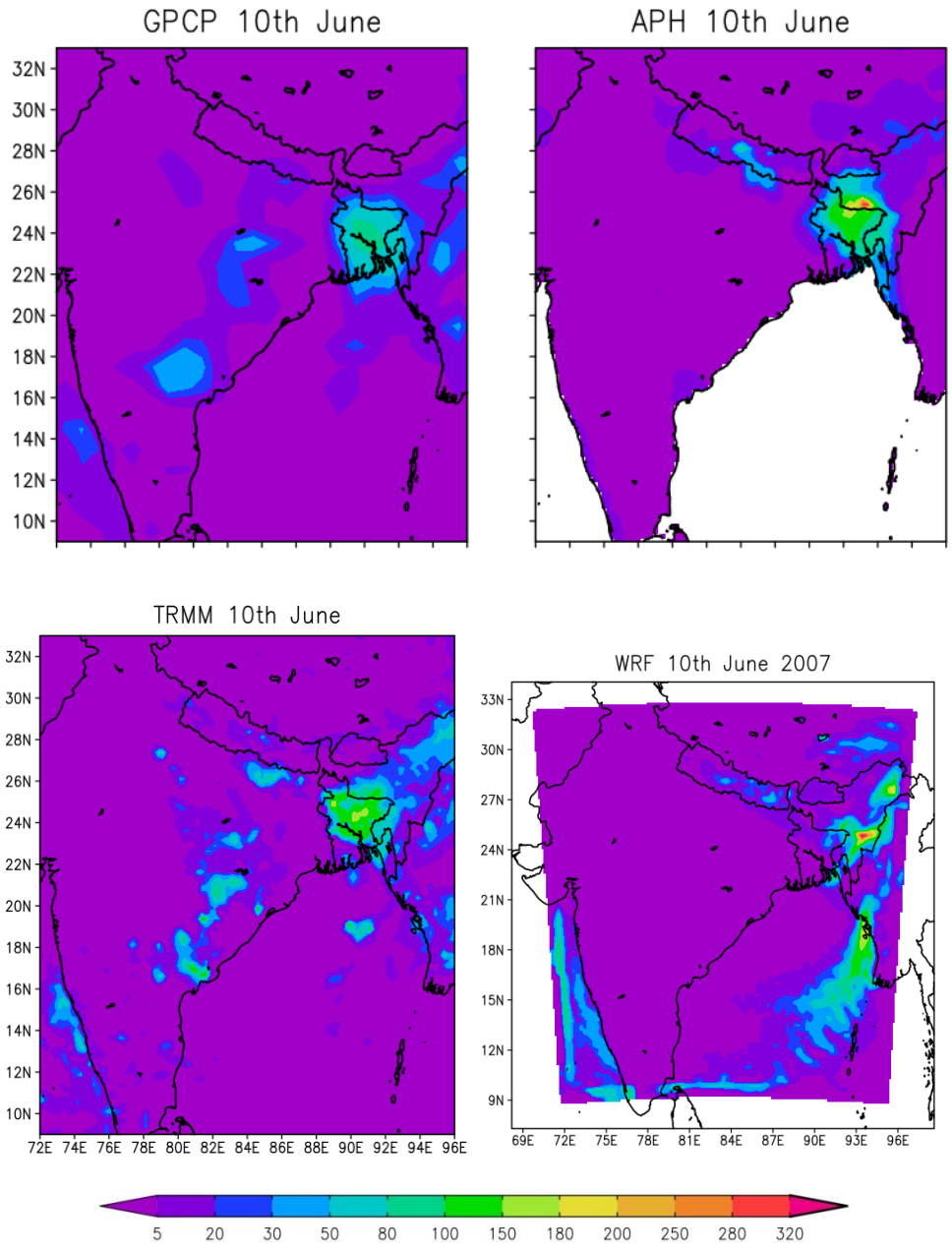

Figure 4.2: Rainfall during 10th June in TRMM, Aphrodite, GPCP and simulated WRF data over Domain 1.

List of experiments that are conducted considering different physical schemes, provided in Table 4.1.

Table 4.1: List of selected simulations with their respective micro-physics and cumulus scheme (model option is provided in the bracket)

ID	Name	Micro-physics scheme	Cumulus schemes
01	KEKF	Kessler (1)	Kain-Fritsch (new Eta) (1)
02	KEBJ	Kessler (1)	Betts-Miller-Janjic (2)
03	KEGR	Kessler (1)	New Grell (G3) (5)
04	KETD	Kessler (1)	Tiedtke (6)
05	LNKF	Lin et al. (2)	Kain-Fritsch (new Eta) (1)
06	LNBJ	Lin et al. (2)	Betts-Miller-Janjic (2)
07	LNGR	Lin et al. (2)	New Grell (G3) (5)
08	LNTD	Lin et al. (2)	Tiedtke (6)
09	WMKF	WSM6 (6)	Kain-Fritsch (new Eta) (1)
10	WMBJ	WSM6 (6)	Betts-Miller-Janjic (2)
11	WMGR	WSM6 (6)	New Grell scheme (G3) (5)
12	WMAS	WSM6 (6)	New SAS (14)
13	SUKF	SBU-YLin (13)	Kain-Fritsch (new Eta) (1)
14	SUBJ	SBU-YLin (13)	Betts-Miller-Janjic (2)
15	SUGR	SBU-YLin (13)	New Grell (G3) (5)
16	SUAS	SBU-YLin (13)	New SAS (14)
17	SUTD	SBU-YLin (13)	Tiedtke (6)
18	WMTD	WSM6 (6)	Tiedtke (6)
19	LNAS	Lin et al. (2)	New SAS (14)

The storm hit in south eastern hilly region of Bangladesh at 26th June, 2007. Therefore, it is required to investigate two days rainfall before the event which contributed in the generation of the disaster. Assessment of the four day rainfall from 24th to 27th June, 2007 needs to be done in order to evaluate physical scheme performance of WRF model. Hence, analysis has been made considering all four days of rainfall with observed TRMM and BMD data.

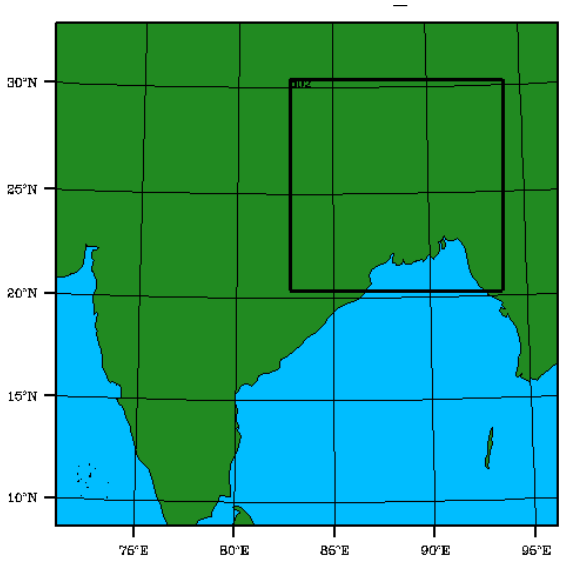

Figure 4.3: Selected Model Domain for the study.

4.3.1 Rainfall patterns in different physical schemes

The spatial pattern of TRMM rainfall data during 25th and 26th June 2012 are shown in Figure 4.4. 24th June and 27th June rainfall characteristics are also shown in the Appendix section. TRMM data used in the study as observed data because it has spatial value in each 25km over the region with 3hour interval. On the other hand, BMD station data is a point gage data without any spatial utility.

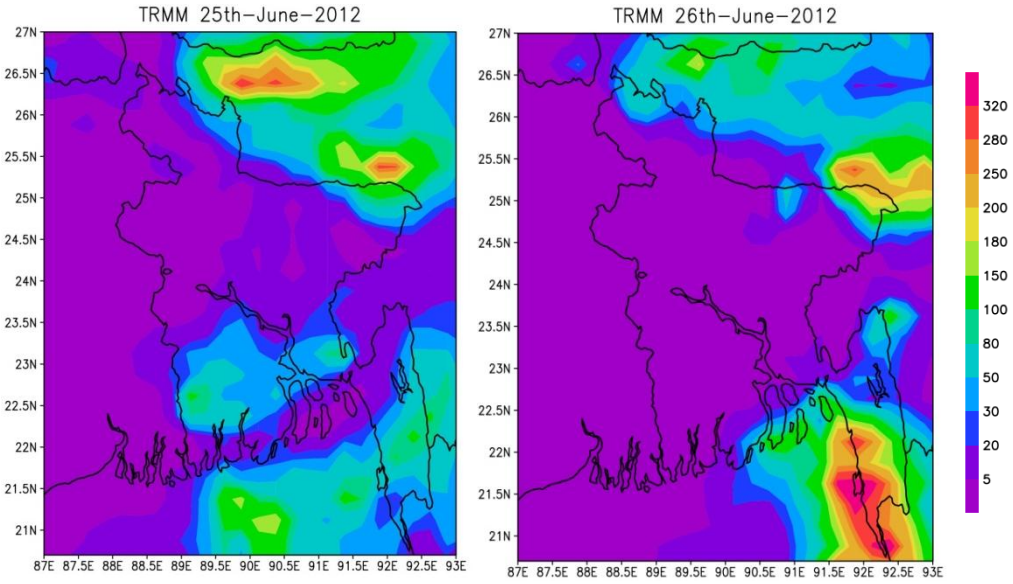

Figure 4.4: Spatial pattern of rainfall from TRMM during 25th June and 26th June, 2012.

From the figure it has found that, the heavy rainfall occurred in 25th June, 2012 over the Bay of Bangle as well as over the Meghna and Brahmaputra Basin. Sylhet area experienced some extent of rainfall depression on from the Meghalay area of India. There were also high amount of rainfall in the south-east coastal zone of the country. In consecutive day, at 26th June, Sylhet area rainfall started to shift north ward and became weak. On the hand, Chittagong, and Cox Bazar coast experienced massive rainfall from previous day rainfall depression.

To understand the performance of this rainfall event, simulations are performed and simulated pattern of rainfall in these two days are shown in Figure 4.5 and Figure 4.6.

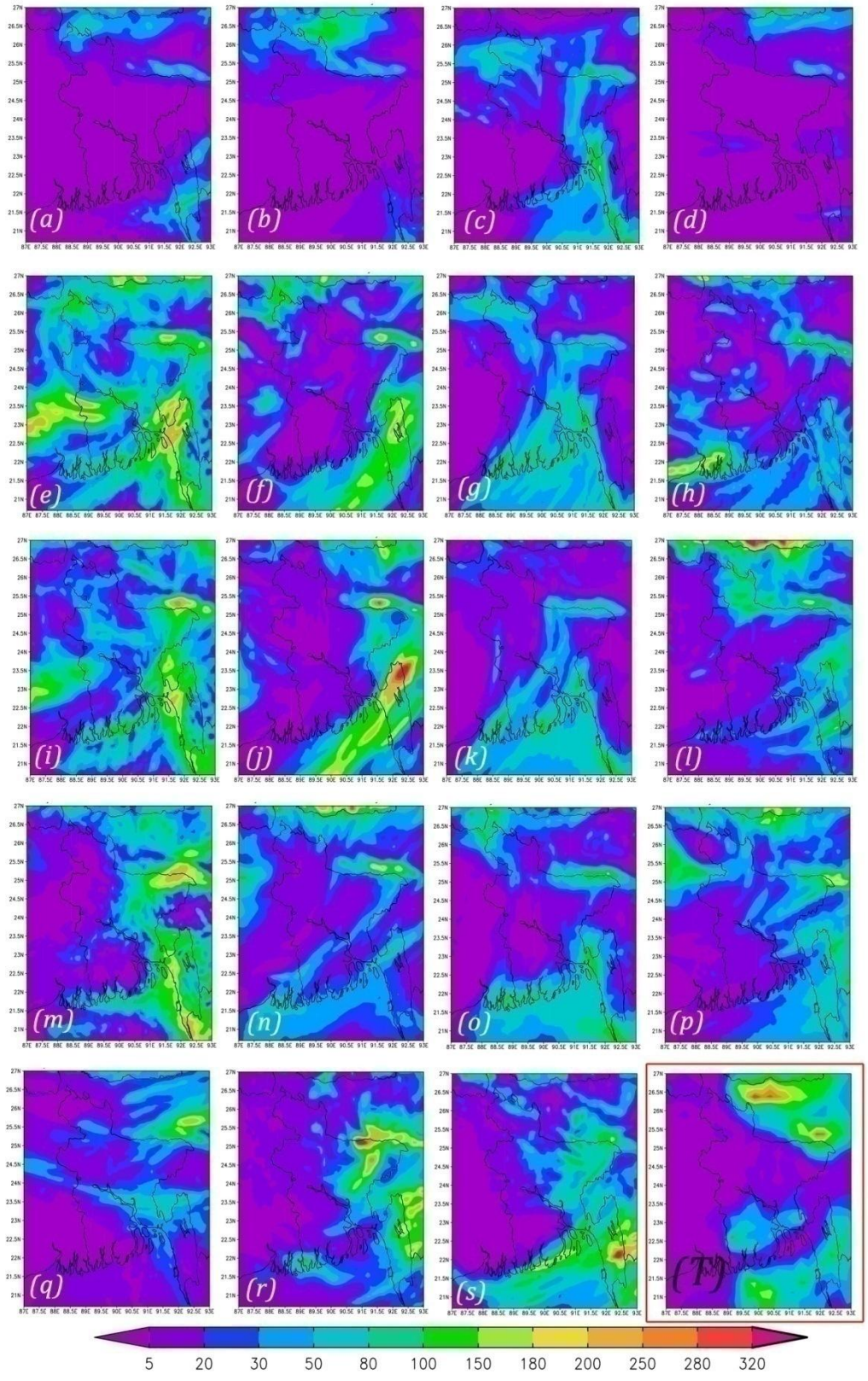

Figure 4.5: Spatial pattern of rainfall in (a)KEKF, (b)KEBJ, (c)KEGR, (d)KETD, (e)LNKF, (f)LNBJ, (g)LINGR3D, (h)LNTD (i)WMKF (j)WMBJ, (k)WMGR, (l)WMAS, (m)SUKF (n)SUBJ, (o)SUGR, (p)SUAS, (q)SUTD, (r)WMTD, (s)LNAS, scheme and (T) TRMM observed data during 25th June 2012.

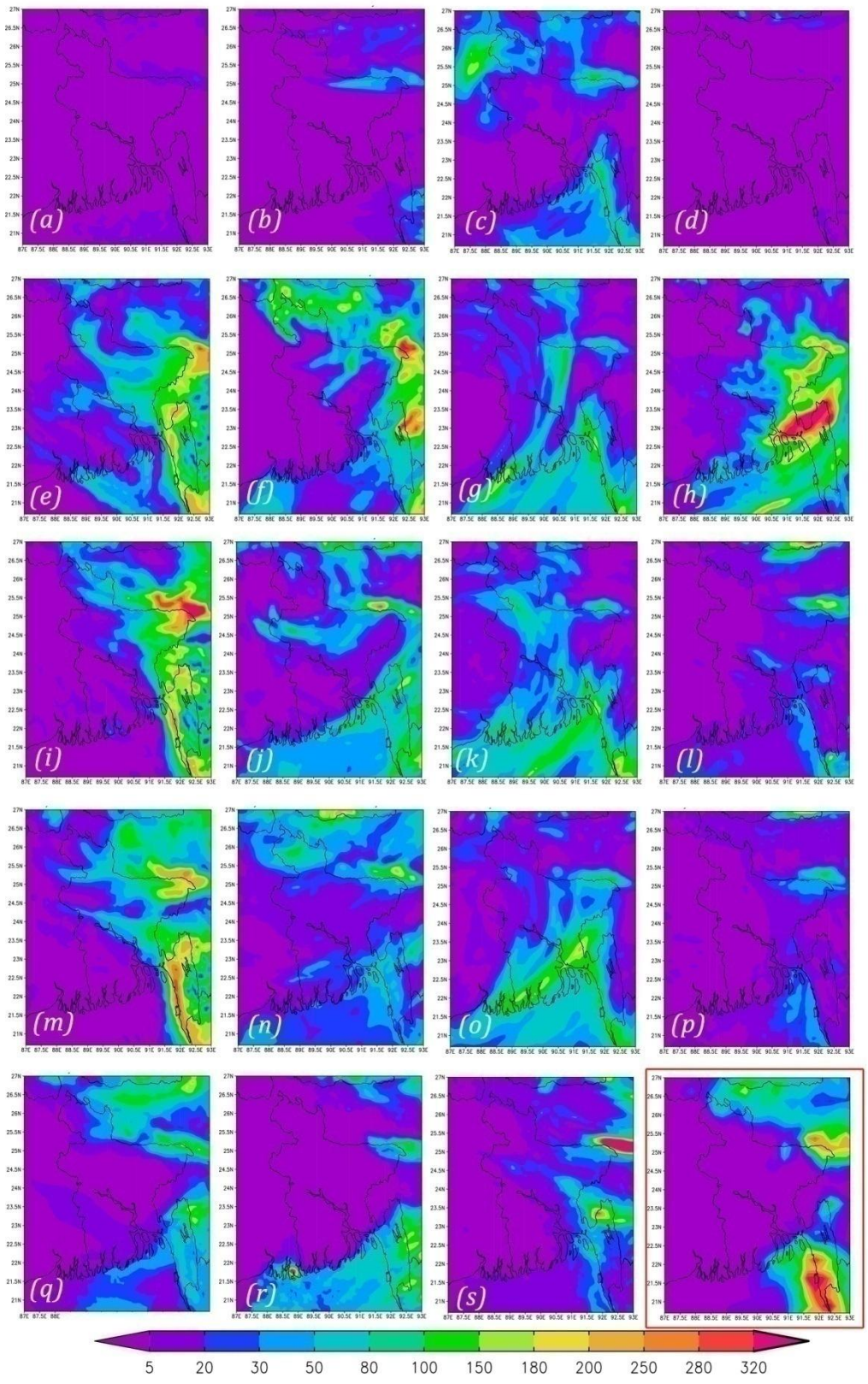

Figure 4.6: Spatial pattern of rainfall in (a)KEKF, (b)KEBJ, (c)KEGR, (d)KETD, (e)LNKF, (f)LNBJ, (g)LINGR3D, (h)LNTD (i)WMKF (j)WMBJ, (k)WMGR, (l)WMAS, (m)SUKF (n)SUBJ, (o)SUGR, (p)SUAS, (q)SUTD, (r)WMTD, (s)LNAS, scheme and (T) TRMM observed data during 26th June 2012.

From the figure several findings has been found. All of the Grell 3D cumulus schemes able to capture both north and south depression quite well. New Kain-Fritsch also showed some reasonable skill in producing the events during 25th June, though it could not captured the pattern with the Kessler scheme. Stoney Brook University scheme with New Kain-Fritsch scheme showed quite good performance in reproducing the rainfall pattern during 25th June. The worst performance has been observed for KETID simulation where none of the rainfall depression captured in that day.

During 26th June, SUKF simulation showed good result in capturing pattern of the rainfall. Experiment with Lin et. Micro-physics scheme produced considerable amount of rainfall in that day but still magnitude is quite low.

4.3.2 Rainfall magnitude in different physical schemes

Comparison of rainfall magnitude are also made using 19 simulation and observed data. TRMM and BMD data agreed each other in most of the cases. Four location of high intensive rainfall are selected in the analysis.

Figure 4.7 shows the rainfall amount in Chittagong station from 24th to 26th June. For the station, most of the model shows some time lag in producing the rainfall during first two days. In 24th, all of the model under predicts rainfall where, at 25th the majority predicts excess rainfall. For 26th June, SUKF experiment shows better result in terms of observed BMD magnitude. However, BMD and TRMM have large difference in magnitude on that day.

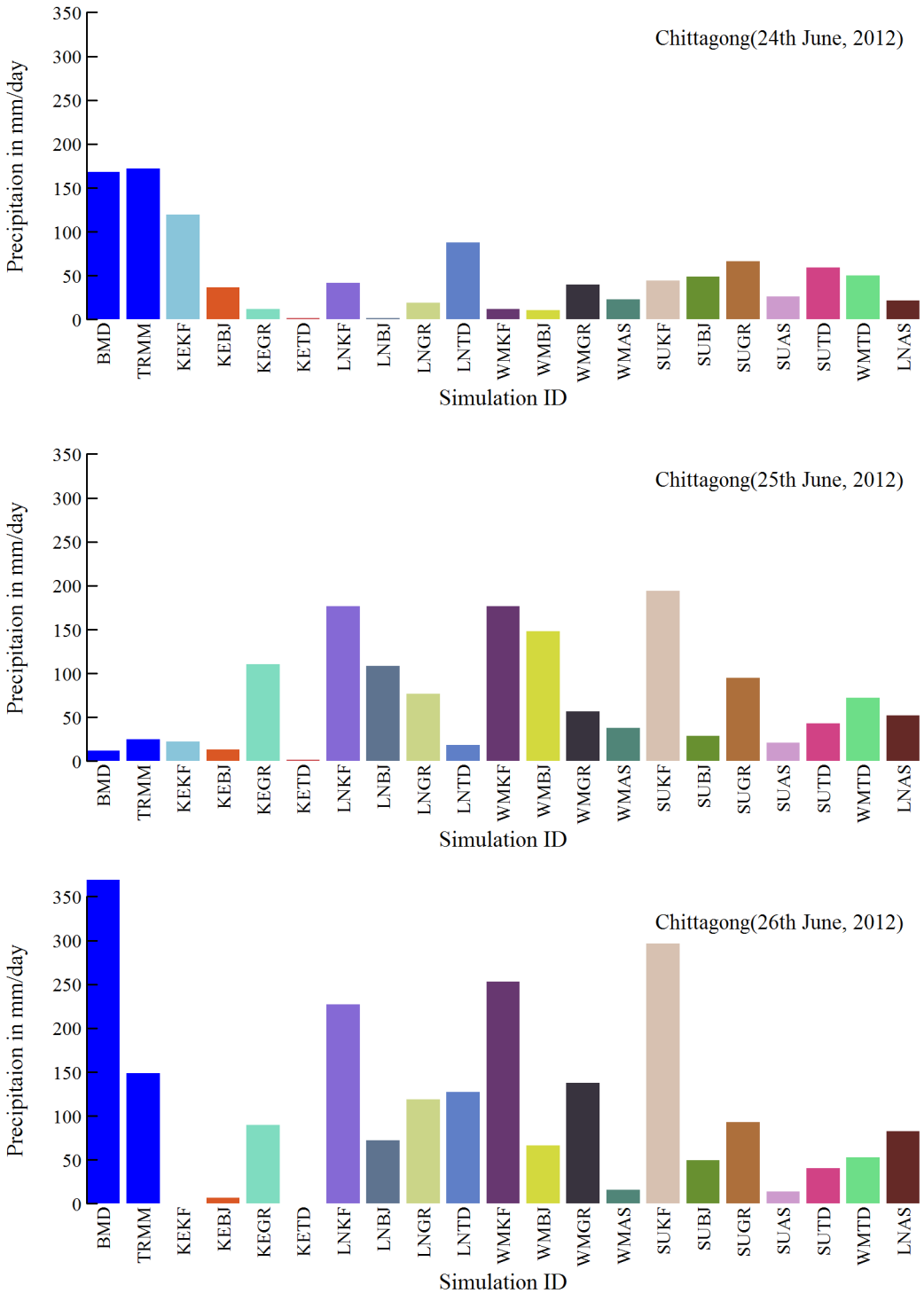

Figure 4.7: Rainfall amount of observed data and model simulation at Chittagong during 24th June, 2012 to 26th June, 2012.

Rainfall over the Teknaf station is shown in Figure 4.8. Rainfall amount has been determined with WRF model simulation during 24th June, but TRMM and BMD has some bias in magnitude. Again compare to TRMM, simulated rainfall during 25th

and 26th June show some time lag in predicting rainfall magnitude.

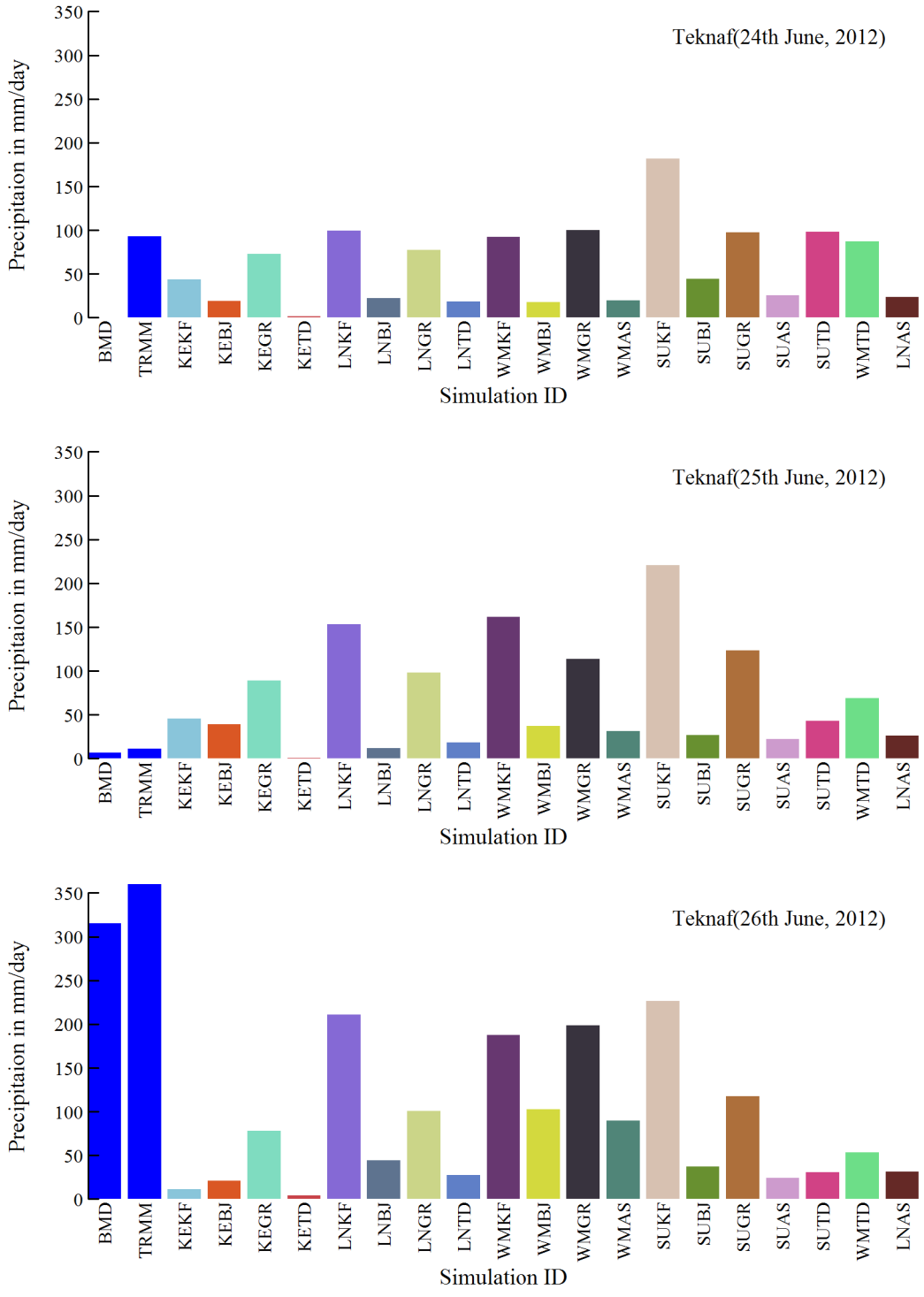

Figure 4.8: Rainfall amount of the observed data and model simulations at Teknaf during 24th-26th June, 2012

Figure 4.9 shows rainfall over Cox's Bazar station. Rainfall during 24th June is also differs from the point data source. Most of the model could not able to capture the magnitude of rainfall during 24th and 26th June. Rainfall on Khulna station, from the

south-western part of the country has also shown in Figure 4.10. For the station, TRMM data has very large bias with observed BMD data. Therefore, further analysis including this region has been avoided in the study.

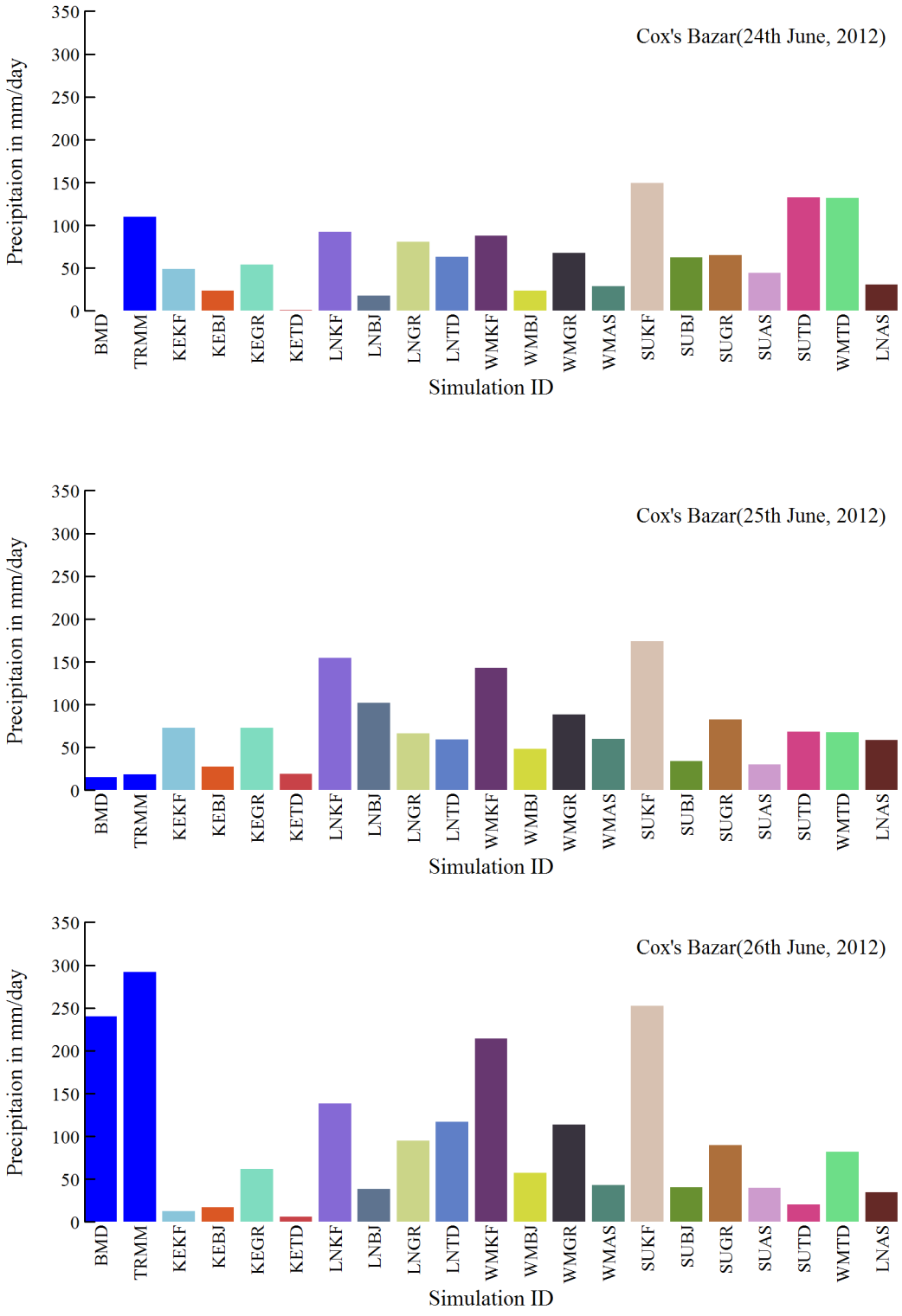

Figure 4.9: Rainfall amount of the observed data and model simulations at Cox's Bazar during 24th-26th June, 2012

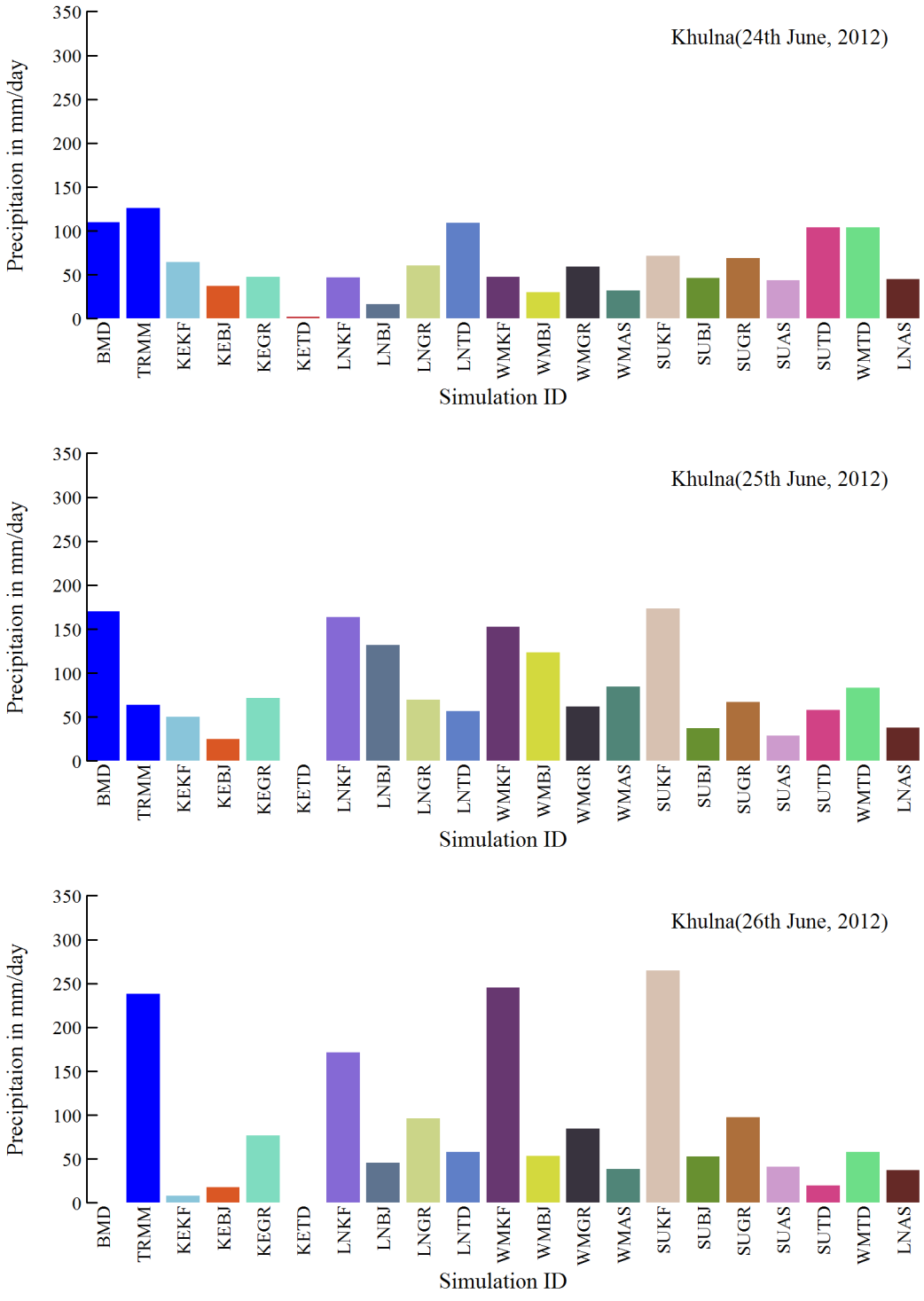

Figure 4.10: Rainfall amount of the observed data and model simulations at Khulna during 24th-26th June, 2012

4.3.3 Model evaluation:

Several indicators have been used to evaluate the performance of WRF simulations. Detail of the indicator is provided in the Methodology section.

4.3.3.1 RMSE

Root mean square error or RMSE is a widely used model evaluation parameter in hydrology study. Calculated RMSE of 19 simulations with respect to TRMM data are shown in Table 4.2. Ranking of the simulations are applied for each days of the event. Combined ranking has been made using 4 days rank value. WRF Single–moment 6–class Scheme (WM) shows good result in all four day. All three cumulus schemes with WM scheme performed well in producing the rainfall event. But for most intensive rainy day, Stony–Brook University and Tiedtke Scheme has achieved rank 1 among all simulations.

Table 4.2: Root Mean Square Error (RMSE) with respect to TRMM data during 24th to 27th June, 2012

No	Experiments	24th June	25th June	26th June	27th June	24th Rank	25th Rank	26th Rank	27th Rank	All Rank
1	**SUTD**	57	34	129	30	1	3	12	1	17
2	**WMTD**	60	67	112	36	2	14	4	6	26
3	**WMGR**	70	43	99	66	6	8	1	15	30
4	**WMAS**	83	38	124	34	14	5	9	4	32
5	**KEGR**	79	48	113	34	11	12	5	5	33
6	**SUAS**	79	41	131	32	12	7	13	2	34
7	**LNGR**	73	45	103	60	9	9	2	14	34
8	**SUBJ**	72	38	125	48	8	4	10	13	35
9	**LNTD**	72	29	177	46	7	1	19	12	39
10	**SUGR**	68	45	116	110	5	11	6	19	41
11	**LNAS**	80	59	134	33	13	13	14	3	43
12	**KEKF**	84	30	141	38	15	2	17	10	44
13	**WMBJ**	88	96	111	36	16	19	3	7	45
14	**SUKF**	67	82	121	95	3	17	7	18	45
15	**KEBJ**	102	39	137	38	19	6	15	9	49
16	**WMKF**	76	82	123	78	10	16	8	16	50
17	**LNKF**	67	94	125	87	4	18	11	17	50
18	**LNBJ**	90	69	138	37	17	15	16	8	56
19	**KETD**	91	45	144	38	18	10	18	11	57

4.3.3.2 PBIAS

To evaluate rainfall, PBIAS is widely used in weather forecasting. Table 4.3 shows calculated PBIAS for nineteen experiments considering TRMM as reference data. According to PBIAS ranking, the best scheme set that able to capture the event is Lin et al. and Tiedtke Scheme. SUTD is ranked 2nd in the order. Like RMSE, Tiedtke schemes also indicate less bias compare to other simulations. Rainfall during 26th June is well captured by SUTD run.

Table 4.3: Percent Bias (PBIAS) with respect to TRMM data during 24th to 27th June, 2012

No	Experiments	24th June	25th June	26th June	27th June	24th Rank	25th Rank	26th Rank	27th Rank	All Rank
1	**LNTD**	-28	-14	29	44	4	3	4	7	18
2	**SUTD**	-17	30	-64	67	2	7	12	9	30
3	**WMTD**	-26	126	-48	17	3	15	10	5	33
4	**KEGR**	-55	17	-66	-36	13	4	13	6	36
5	**WMKF**	-40	126	-7	151	5	16	2	14	37
6	**LNGR**	-53	11	-46	200	12	1	9	15	37
7	**WMGR**	-48	12	-40	255	10	2	8	17	37
8	**SUKF**	-15	134	3	281	1	17	1	18	37
9	**SUBJ**	-48	-26	-68	69	9	6	14	10	39
10	**SUAS**	-71	-33	-85	0	15	8	16	1	40
11	**WMBJ**	-58	138	-38	7	14	18	6	2	40
12	**LNAS**	-72	61	-61	-9	16	11	11	3	41
13	**WMAS**	-77	19	-77	-15	17	5	15	4	41
14	**SUGR**	-43	36	-39	407	7	9	7	19	42
15	**LNKF**	-41	160	-7	252	6	19	3	16	44
16	**LNBJ**	-82	111	-33	-61	18	14	5	8	45
17	**KEKF**	-48	-46	-97	-98	8	10	18	12	48
18	**KEBJ**	-51	-72	-93	-97	11	12	17	11	51
19	**KETD**	-89	-89	-99	-98	19	13	19	13	64

4.3.3.3 Threat Score (TS)

For the non probabilistic forecast, threat score (TS) is one of the indicators that shows usefulness of any forecast event. 50mm or 100mm rainfall occurred only few areas of Eastern hilly region during the event. Therefore, 20mm rainfall or 1mm rainfall events

are evaluated using this indicator. Figure 4.11 shows threat score for each experiment during chosen rainfall event.

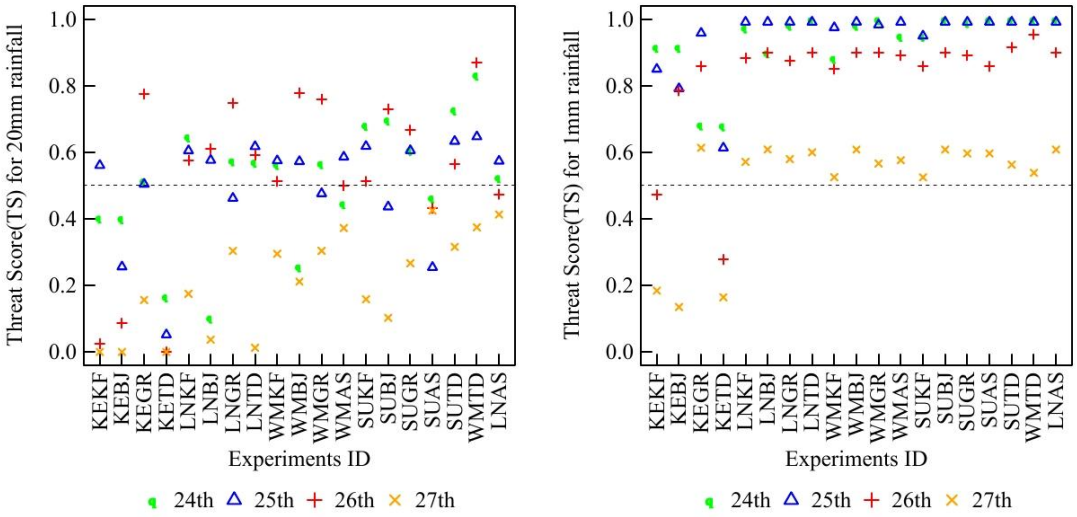

Figure 4.11: Threat score (TS) of 19 experiments for 20mm and 1mm rainfall during 24th – 27th June, 2012 rainfall event

Forecasting rainfall during 24th-26th June, all the experiments shows 50% above threat score in prediction of rainfall occurrence over the hilly region. During 27th June, performance is down for same parameter. TS of WMTD scheme with 20mm rainfall threshold indicates better performance than other schemes. Model shows comparative poor performance in prediction of 27th June rainfall for both 1mm and 20mm rainfall threshold. Actually, observed event during 27th June is quite low which leads to poor performance of TS in that day.

4.3.3.4 Proportion Correct (PC)

The proportion correct satisfies the principle of equivalence of events, since it credits correct "yes" and "no" forecasts equally. The worst possible proportion correct is zero; the best possible proportion correct is one. PC has been calculated for the selected nineteen simulations and depicted in Figure 4.12. It is found that model can predict 'yes' and 'no' forecast quite well for 1mm and 100mm irrespective of false alarm. However, some experiments show inadequate performance in 20mm and 50mm rainfall forecast. During 25th June, WRF Single–moment 6–class schemes (WM) with other cumulus schemes have showed good performance in capturing 1mm, 20mm and 100mm rainfall.

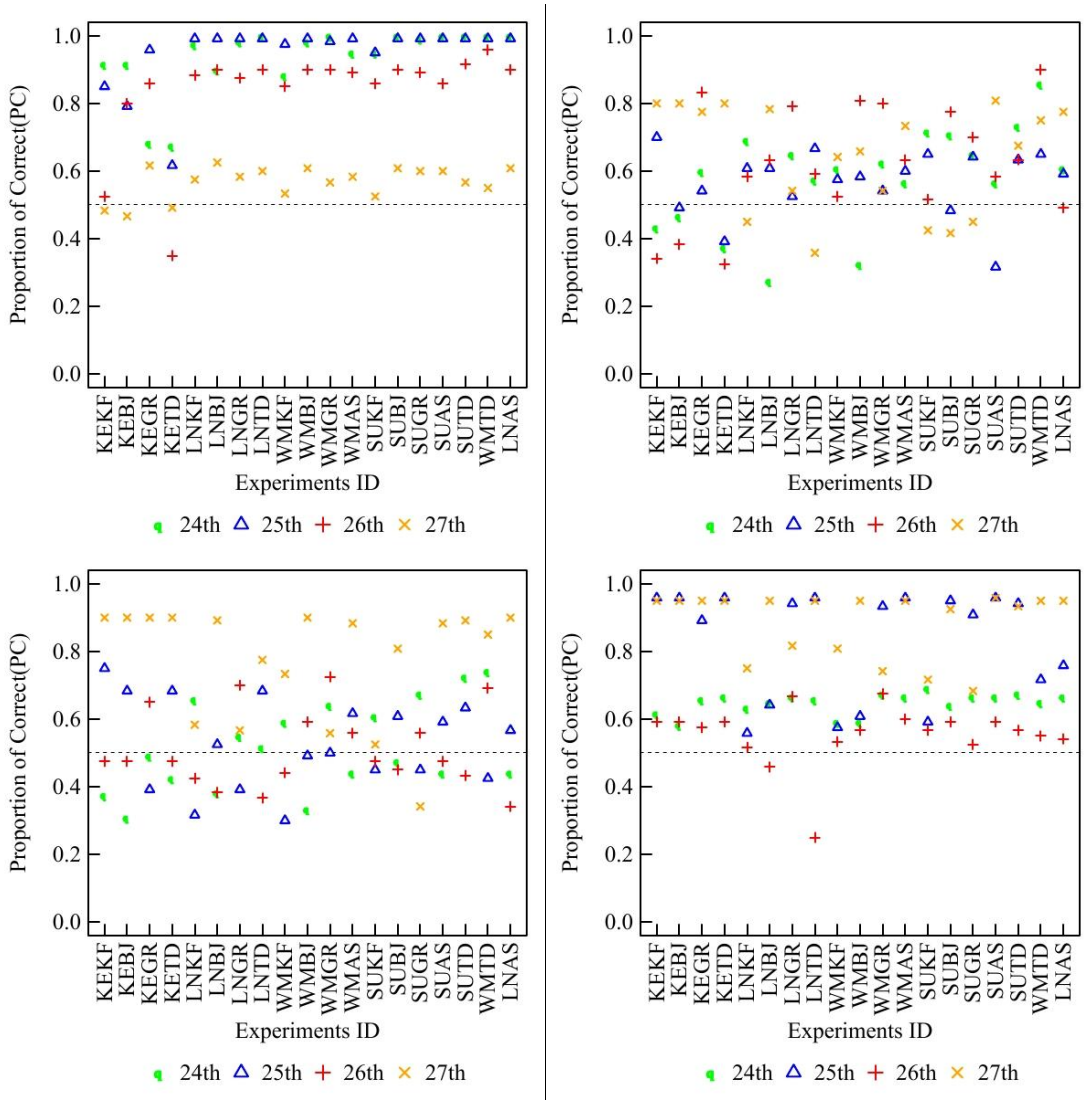

Figure 4.12: Proportion of Correct (PC) of nineteen experiments for the 1mm, 20mm, 50mm and 100mm rainfall during 24th – 27th June, 2012 rainfall event

4.3.3.5 Bias (B)

Bias of forecast means ratio of the forecast of an event with the ratio of total observed event. Table 4.4 shows the bias of 1mm, 20mm, 50mm and 100mm rainfall events during 26th June, 2012. As Bias=1 represent unbiased forecast, Stonny Brook University microphysics schemes have showed considerable good result in Bias. For 100mm rainfall prediction, SUBJ scheme has indicated slightly lower success in forecasting as observed 100m rainfall is only 14% higher that total 100mm forecast. WMKF performed well in forecasting 1mm and 50mm rainfall with only 11% and 0% under forecast respectively.

Table 4.4: Bias (B) with respect to TRMM data for 1mm, 20mm, 50mm and 100mm threshold

Names	1mm	20mm	50mm	100mm	1mm Rank	20mm Rank	50mm Rank	100mm Rank	Combined Rank
SUBJ	1.06	1.1	1.3	1.1	4	5	9	1	19
WMAS	1.06	1.2	1.0	0.5	5	10	3	5	23
KETD	1.06	1.0	0.6	0.0	3	1	10	13	27
SUAS	1.06	0.0	0.9	1.4	2	19	4	4	29
SUKF	1.09	1.2	0.5	0.4	7	7	11	7	32
WMBJ	1.11	1.1	1.3	0.5	16	3	8	6	33
LNBJ	0.99	1.0	0.3	0.0	1	2	14	18	35
SUGR	1.11	1.1	1.1	0.3	15	6	5	10	36
LNKF	1.10	1.1	0.4	0.2	10	4	12	11	37
SUTD	1.08	0.6	1.6	1.1	6	16	13	2	37
LNAS	1.09	1.2	1.3	0.0	8	11	7	14	40
WMKF	1.11	1.2	1.0	0.0	11	9	2	19	41
LNTD	1.11	0.6	1.0	0.0	13	15	1	17	46
WMGR	1.11	1.2	0.2	0.1	12	8	15	12	47
WMTD	0.28	1.4	1.1	0.3	19	14	6	8	47
LNGR	1.11	1.3	0.0	1.1	14	12	19	3	48
KEGR	1.10	1.3	0.0	0.3	9	13	18	9	49
KEBJ	0.47	0.1	0.0	0.0	18	17	16	16	67
KEKF	0.79	0.0	0.0	0.0	17	18	17	15	67

4.3.3.6 False Alarm Ratio (FAR)

False Alarm is an important aspect in weather forecasting. High number of false alarm might lead mistrust among the user of the forecast. Therefore, False Alarm Ratio (FAR) has been evaluated for the conducted simulations and an illustration of FAR is presented in Figure 4.13 for 1mm and 20mm rainfall threshold. The majority of simulations have produced significant false alarm of 1mm rainfall during 27th June. Similar phenomenon also observed for 20mm rainfall as well. KE microphysics showed less amount false alarm in both cases but the scheme is not efficient in forecasting high rainfall events.

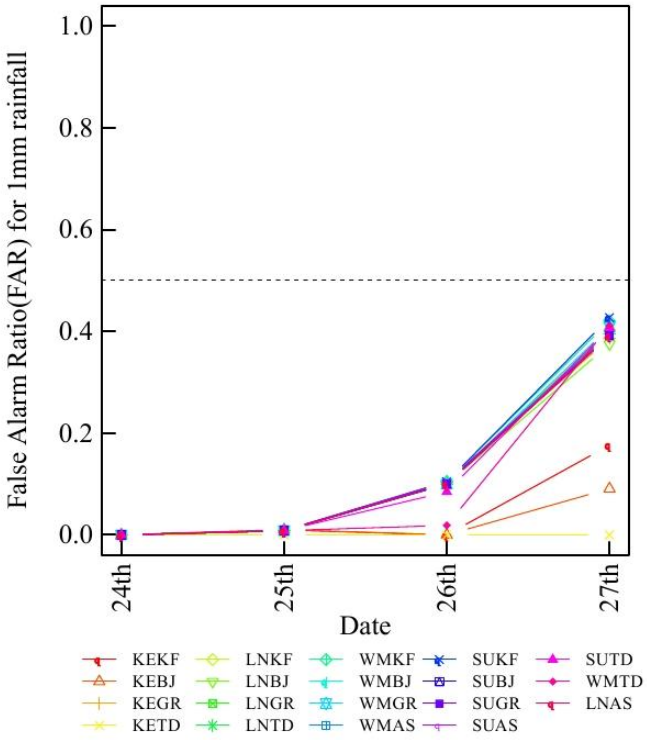

(a)

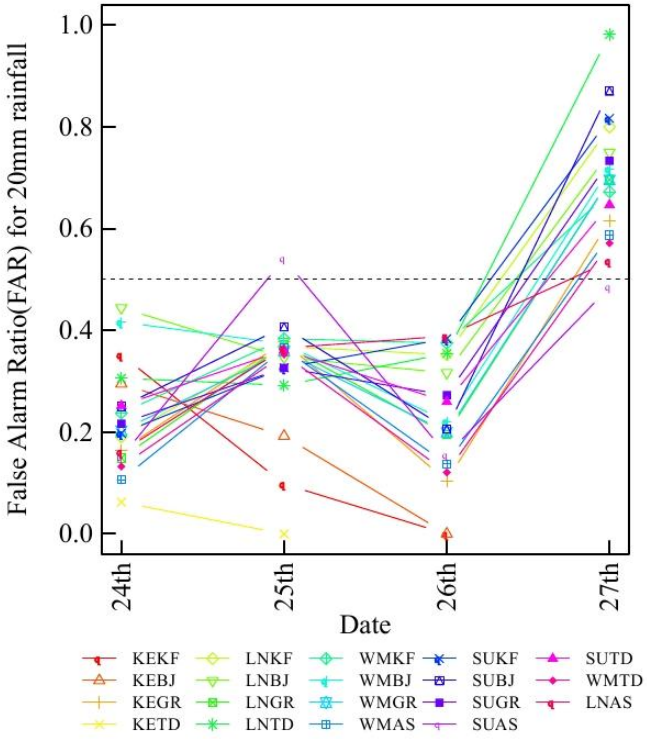

(b)

Figure 4.13: False alarm ratio (FAR) of nineteen experiments for the 1mm and 20mm rainfall during 24th – 27th June, 2012 rainfall event

4.3.3.7 False Alarm Rate (FS)

False Alarm rate is ratio of wrong forecast in respect to observed events. Table 4.5 shows the rank of 19 simulations according to FS index. WRF Single–moment 6–class (WM) performs well as WMGR, SUKF and WMKF are 1st, 2nd and 3rd rank position according to combined rank for all four days.

Table 4.5: False Alarm Rate (FS) with respect to TRMM data during the selected event

Names	24th	25th	26th	27th	Rank1	Rank2	Rank3	Rank4	Total Rank
WMGR	0.00	1.00	0.29	0.96	1	9	3	3	16
SUKF	0.43	0.96	0.53	1.00	3	5	4	5	17
WMKF	0.85	0.96	0.56	1.00	7	6	5	6	24
SUTD	0.33	1.00	0.80	0.67	2	10	11	2	25
WMTD	0.63	0.91	0.69	-	5	2	8	12	27
WMAS	-	0.50	0.00	-	16	1	1	10	28
LNKF	1.00	0.96	0.58	1	10	7	6	7	30
LNGR	-	1.00	0.15	1	15	13	2	4	34
WMBJ	1.00	0.94	0.59	-	12	4	7	11	34
LNBJ	1.00	0.93	0.81	-	11	3	12	14	40
LNTD	0.53	-	0.79	-	4	15	10	13	42
SUGR	-	1.00	0.70	1	17	14	9	8	48
SUBJ	1.00	1.00		1	13	12	15	9	49
KEGR	1.00	1.00	1.00	-	9	11	14	16	50
LNAS	-	0.96	0.88	-	19	8	13	15	55
KEKF	0.80	-	-	-	6	16	16	17	55
SUAS	-	-	-	0	18	19	19	1	57
KEBJ	1.00	-	-	-	8	17	17	18	60
KETD	-	-	-	-	14	18	18	19	69

4.3.3.8 Hit Rate (HT)

Hit rate is one of the indicators that represent true performance of a numerical model in senses of capturing a particular event with a particular threshold. The study has calculated Hit Rate index for all the run and Figure 4.10 shows the 50mm or more rainfall HT during the selected rainfall event. The result reveled that even for the 1mm rainfall forecast, some of the scheme combination like KEKF, KEBJ and KETD produce poor result in detecting the event.

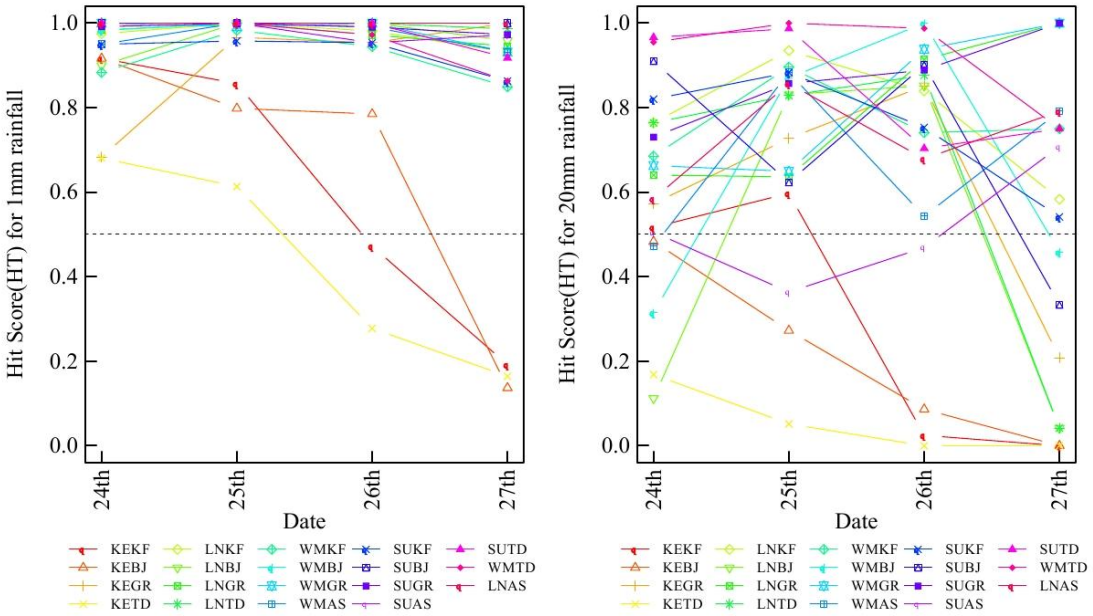

Figure 4.14: Hit Score (HT) of nineteen experiments for the 1mm and 20mm rainfall during 24th – 27th June, 2012 rainfall event

4.3.4 Model ranking

For effective forecasting, a numerical model needs to be accurate in determining a magnitude of weather event, capable of capturing large and small scale patterns, capable of capturing extreme events and also at the same needs to produce less amount of false alarm. Therefore, a set of evaluation indices has been determined in this study to understand the best set of physical scheme that can effectively forecast high rainfall events over the country.

RMSE, PBIAS and BIAS of a model simulation indicate spatial accuracy of a simulation. FS and FAR are required to understand the false alarm ratio of the mode. HT and PC indices are good for accuracy test. TS are effective to understand the model performance of high impact event. However, analysis has shown that different schemes are good in different indices. Therefore, a combined rank from the evaluated rank of each index with respect to each simulation is made to find the best possible simulation. Ranking has been done considering 1mm, 20mm, 50mm and 100mm rainfall threshold.

4.3.4.1 Model ranking for 100mm rainfall

To understand, how each model can capture 100mm rainfall, a ranking table is made with evaluated indices, presented in Table 4.6. From cumulative ranking, it is found that, SUTD scheme performed well in capturing 100mm high intensive rainfall during 24th to 27th June, 2012. It is also notable that, WM microphysics with Grell 3D, Tidtkel and AS cumulus scheme, WRF can perform well in forecasting heavy rainfall events greater than 100mm.

Table 4.6: Combined ranking of 19 sets of schemes with respect to TRMM data considering 100mm forecast performance.

Experiment ID	RMSE	PBIAS	BIAS	FS	HT	PC	TS	All
SUTD	1	2	8	4	7	7	5	34
WMGR	3	7	14	1	4	5	3	37
WMTD	2	3	11	5	6	13	6	46
WMAS	4	13	6	6	12	2	10	53
LNGR	7	6	10	8	10	4	11	56
SUKF	14	8	16	2	1	14	1	56
LNTD	9	1	19	11	3	12	4	59
WMKF	16	5	17	3	2	18	2	63
KEGR	5	4	7	14	16	9	16	71
SUAS	6	10	4	17	17	3	17	74
KEKF	12	17	1	16	11	6	12	75
WMBJ	13	11	12	9	8	15	8	76
SUBJ	8	9	5	13	19	10	19	83
KEBJ	15	18	2	18	13	8	13	87
LNAS	11	12	9	15	15	11	15	88
LNKF	17	15	18	7	5	19	7	88
SUGR	10	14	13	12	14	16	14	93
LNBJ	18	16	15	10	9	17	9	94
KETD	19	19	3	19	18	1	18	97

4.3.4.2 Model ranking for 50mm rainfall

Performance of 50mm rainfall has also been checked with combined ranking table (Table 4.7). WMTD and SUTD scheme provide good result in forecasting 50mm rainfall over the eastern hilly region of Bangladesh. For medium intensive rainfall (like 50mm or more rainfall) Grell 3D and Tiedtke cumulus scheme have showed better result compare to other schemes of WRF.

Table 4.7: Combined ranking of 19 sets of schemes with respect to TRMM data considering 50mm forecast performance.

Experiment ID	RMSE	PBIAS	BIAS	FS	HT	PC	TS	All
WMTD	2	3	6	1	1	3	1	17
SUTD	1	2	13	3	4	2	2	27
WMGR	3	7	15	2	2	7	3	39
LNTD	9	1	1	10	10	11	10	52
WMAS	4	13	3	8	13	6	13	60
LNGR	7	6	19	4	7	12	5	60
SUGR	10	14	5	6	6	13	6	60
SUKF	14	8	11	7	3	16	4	63
KEGR	5	4	18	11	12	5	11	66
WMKF	16	5	2	9	8	19	9	68
WMBJ	13	11	8	12	9	8	8	69
LNKF	17	15	12	5	5	18	7	79
SUAS	6	10	4	16	17	10	17	80
SUBJ	8	9	9	15	14	14	16	85
KEKF	12	17	17	13	16	1	14	90
LNAS	11	12	7	17	15	15	15	92
LNBJ	18	16	14	14	11	17	12	102
KETD	19	19	10	18	18	4	18	106
KEBJ	15	18	16	19	19	9	19	115

4.3.4.3 Model ranking for 20mm rainfall

Model performance in evaluating of 20mm rainfall has also been made for the selected nineteen simulations (Table 4.8). Like 50mm rainfall threshold, Tiedtke and Grell 3D shows good result in forecasting 20mm or more rainfall.

Table 4.8: Combined ranking of 19 sets of schemes with respect to TRMM data considering 20mm forecast performance.

Experiment ID	RMSE	PBIAS	BIAS	FS	HT	PC	TS	All
WMTD	2	3	14	1	1	1	1	23
SUTD	1	2	16	12	3	2	2	38
WMGR	3	7	8	6	4	6	6	40
SUGR	10	14	6	10	2	4	3	49
LNGR	7	6	12	5	6	8	7	51
KEGR	5	4	13	4	14	3	14	57
SUKF	14	8	7	13	8	7	5	62
WMAS	4	13	10	2	13	11	10	63
LNKF	17	15	4	14	5	9	4	68
LNAS	11	12	11	8	11	12	9	74
LNTD	9	1	15	16	12	14	8	75

SUBJ	8	9	5	19	9	15	12	77
WMBJ	13	11	3	18	10	13	13	81
WMKF	16	5	9	17	7	17	11	82
SUAS	6	10	19	3	16	16	15	85
LNBJ	18	16	2	15	15	10	16	92
KEKF	12	17	18	7	17	5	17	93
KETD	19	19	1	11	19	19	19	107
KEBJ	15	18	17	9	18	18	18	113

4.3.4.4 Model ranking for 1mm rainfall

Capability of different schemes in forecasting whether there would be rain in following day or not are also have analyzed with a ranking table. Table 4.9 shows the combined ranking of 1mm rainfall for each scheme sets. In this case also, Tiedtke scheme has performed quite well especially with combination of Stony–Brook University scheme.

Table 4.9: Combined ranking of 19 sets of schemes with respect to TRMM data considering 1mm forecast performance.

Experiment ID	RMSE	PBIAS	BIAS	HT	PC	TS	All
SUTD	1	2	7	4	4	4	22
LNTD	9	1	10	2	1	1	24
WMTD	2	3	4	9	5	5	28
SUBJ	8	9	13	1	2	2	35
SUAS	6	10	9	6	6	6	43
WMGR	3	7	8	8	10	9	45
LNAS	11	12	17	3	3	3	49
LNGR	7	6	11	10	11	11	56
SUGR	10	14	14	7	8	8	61
WMBJ	13	11	19	5	7	7	62
KEGR	5	4	12	14	14	14	63
WMAS	4	13	16	12	12	12	69
SUKF	14	8	5	15	15	15	72
WMKF	16	5	6	16	16	16	75
KEKF	12	17	2	17	17	17	82
LNBJ	18	16	18	11	9	10	82
LNKF	17	15	15	13	13	13	86
KEBJ	15	18	1	18	18	18	88
KETD	19	19	3	19	19	19	98

4.3.5 Impact of cumulus and microphysics schemes

Impacts of cumulus and microphysics schemes are assessed for each simulation. Percentage bar charts for each simulation during 24th to 27th June, 2012 are provided in Figure 4.14. In the figure it is found that, cumulus schemes produce higher percentage of rainfall compare to microphysics schemes over the region. Observing 25th June and 26th June rainfall, it is also found that rainfall LN microphysics plays an important role in generating high intensive rainfall. Among the cumulus schemes, GR and TD schemes are less dependent on microphysics where KF scheme has showed high variability with combination of other microphysics schemes. BJ and AS cumulus schemes have showed little rainfall in the high intensive rainfall events.

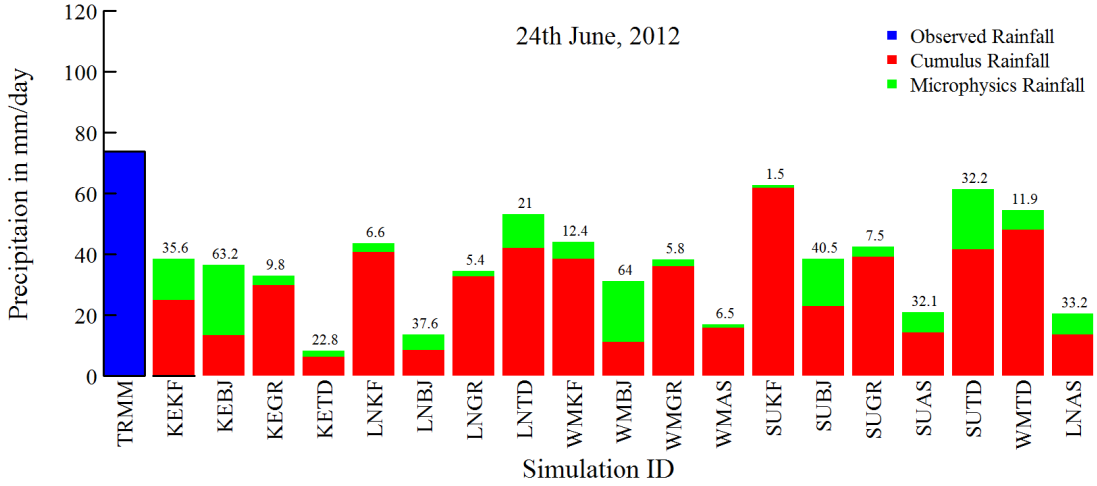

(a)

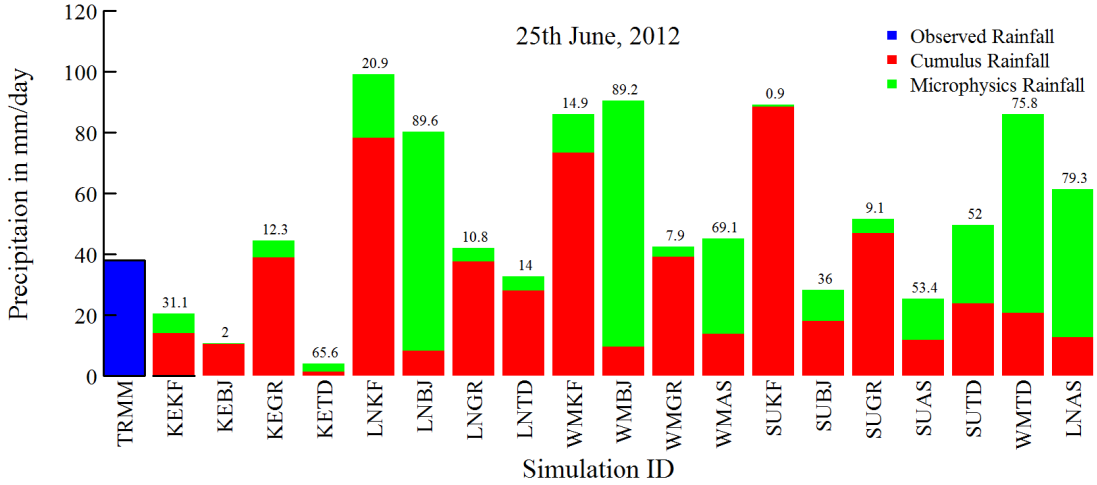

(b)

Figure 4.15: Percentage of cumulus and microphysics for the nineteen simulations during (a) 24th June and (b) 25th June, 2012 rainfall event over south-eastern region.

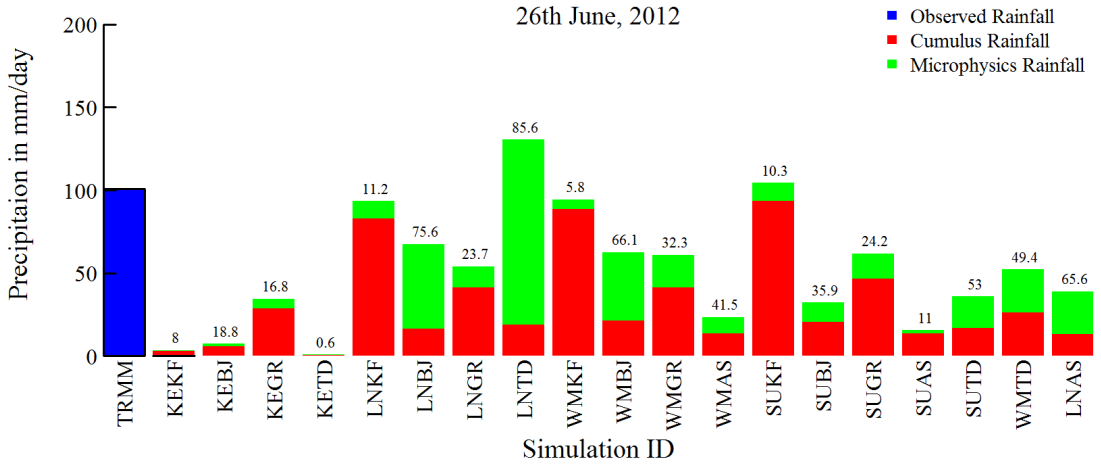

(a)

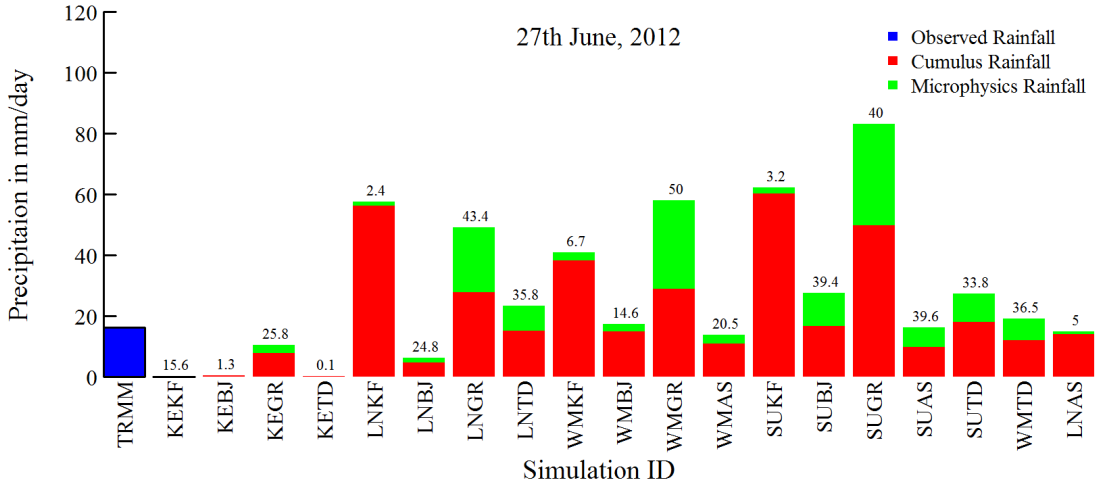

(b)

Figure 4.16: Percentage of cumulus and microphysics for the nineteen simulations during (a) 26^{h} June and (b) 27th June, 2012 rainfall event over south-eastern region.

4.3.6 Best Physical Scheme

After evaluation of all physical schemes considering different rainfall threshold, it has found that Stony–Brook University scheme microphysics scheme with Tiedtke cumulus scheme is the best available schemes to forecast heavy rainfall events over south-eastern hilly region of Bangladesh. Among cumulus scheme, Tiedtke and Grell 3D scheme can produce high intensive rainfall better than other schemes. For the

microphysics, Stony–Brook University and WRF Single–moment 6–class are the better performed physics in forecasting high intensive rainfall.

4.4 Discussions

From the obtain result several key points can be found from the study. Findings are sated in following point:

1. Observed point data from BMD and satellite based TRMM data shows similar pattern in generating heavy rainfall events. However, TRMM data could not always able to capture highest magnitude of high intensive rainfall. Such fact is also supported by Islam and Uyeda (2007). This is due to inability of distant satellite image to capture rainfall amount from cloud.
2. Monsoon rainfall may occur from the small pieces of clouds. The process becomes more complicated when it happens near high altitude areas. From the BMD rainfall, it has found that, rainfall magnitude can change in a great extent within 25km area. During 26th June, 2012 rainfall, where Chittagong station experienced 300mm exceeding rainfall, Rangamati station which is only 50km apart experienced no rainfall at all. This indicates the necessity of high resolution rainfall observation station. In TRMM data, gridded rainfall resolution is 25km by 25km.Therfore, parameterization of small cloud process is difficult to incorporate in gridded data sets as well as in the NWP models. However, from the gridded data sets an indication of heavy rainfall can be found as TRMM can capture monsoon rainfall patterns over the country.
3. BMD considered a model domain to forecast rainfall using WRF (BMD, 2014). Model domain used in the study is larger than the BMD model domain which allows capturing more global atmospheric process over the region. However, the default KE and KF schemes did not showed good performance in capturing high intensive rainfall events. The simulation even failed to project the rainfall in observed location. Ahasan et al. (2013a) and Mannan et al. (2013)also indicated similar result for KF scheme. In the domain size experiment, KEKF simulation has been considered as it is BMD standard scheme. Therefore, though it able to capture large scale precipitation over the country, there were biases for the scheme set in simulating 11 June, 2007 rainfall events.

4. SUKF and LNTD run have showed most similar spatial patterns in producing rainfall compare to TRMM observed data during 25th and 26th June, 2012. All the SU microphysics scheme and TD scheme have showed good performance in capturing core weather processes over Bangladesh. Mannan et al. (2013) conducted sensitivity test with only KF scheme with other microphysics schemes where they found LN schemes performed better that other microphysics. In our case, similar result has been obtained with addition to accurate cumulus scheme.
5. WM scheme give high performance in 100mm forecast as heavy rainfall pattern is quite well captured in this scheme which have agreement with previous studies over Bangladesh(Ahasan et al., 2014; Ahasan et al., 2013b; Ahasan et al., 2012) .

CHAPTER V
CONCLUSIONS AND RECOMENDATION

5.1 Conclusion

Heavy rainfall events become significant over Bangladesh as they caused catastrophic damage on the live and properties in recent decades. Forecasting such events, especially in the Indian monsoon region is quite challenging to the scientific community as well as weather forecaster. Therefore, this study has made an attempt to improve heavy rainfall forecasting using a Numerical weather prediction model called WRF. Different physical schemes that are responsible for rainfall generation of WRF model have been tested with observed BMD and TRMM data. The specific conclusions drawn from this study are summarized below.

BMD and TRMM observed data are compared with Model data. Though both are observed data set, BMD data are more accurate in sense that it is observed gage data where TRMM is satellite generated precipitation data. For the selected two events, BMD and TRMM data shows almost same result. However, in Chittagong district, peak of heavy rainfall event could not be captured by TRMM data sets. A possible cause of such error might be difference between collection times of two data sets.

After simulating, 11th June of 2007 event, It has found that, model data could not capture high intensive rainfall event with the default WRF physical scheme (default is Kessler and Kain-Fritsch scheme). Even with the proper adjust of the domain; model fails to capture the rainfall pattern using the scheme. Note that this scheme is currently used by Bangladesh Meteorological Department (BMD) to simulate WRF model forecast.

Among the nineteen sets of physical schemes of WRF, SUKF scheme shows high amount of rainfall in compare to rainfall data of TRMM. However, all the physical schemes of WRF have failed to capture the pick of 400mm rainfall event during 26th June, 2012. Conventional numerical models are still unable to capture the highest pick of monsoon rainfall over the Indian hilly region.

LNTD scheme shows reasonable good spatial pattern as observed TRMM data. However, the point of intensive rainfall varies largely in model from observed data.

Area averaged root mean square error (RMSE) shows quite high value during 26th June, compare to other days. This indicates that model fails to capture the pick of extreme events over the region.

According to RMSE, SUTD scheme performed best among the other schemes sets. WRF 6-class moment scheme also performed well with Tidetkel and Grell 3D cumulus schemes. Microphysics schemes are more dominant it respects to RMSE indicator rather than cumulus schemes. For 24th and 27th June, SUTD scheme shows only 30mm bias from the observed data.

As PBIS is not unit dependent and have positive and negative value, it provides overestimation and underestimation of model results with respect to observe. LNTD scheme best result in respect to PBIAS for all four days. During 24th and 25th June, the scheme underestimates only 10% and 12% of rainfall respectively, and in contrary, during 26th and 27th June; it overestimates the rainfall about 12% and 44% respectively. Therefore, it could be a great option to judge the magnitude of heavy rainfall over this region.

In forecasting occurrence of rainfall in following day, Tiedtke scheme performed best result among the cumulus schemes. It produces best result with incorporation Stoony Brook University microphysics scheme.

For medium range rainfall forecast (50mm or more), Tiedtke and Grell 3d scheme are quite good both in sense of higher accuracy with lower false alarm. WMTD, SUTD and WMGR has ranked 1st, 2nd and 3rd respectively in forecasting medium range rainfall forecast.

For forecasting 100mm rainfall, SUTD, WMTD and WMGR are found to be the top three efficient physical schemes in forecasting the events.

Considering 50mm threshold, TD scheme has showed satisfactory result in capturing medium range rainfall events. However, this scheme also has showed great performance in whether there will be rainfall on next day or not.

As cumulus schemes are more dominant than microphysics schemes, heavy rainfall in weather models is generated due to strong convective process during monsoon season. However, KF scheme shows diversity in terms of magnitude in combination of other microphysics schemes. Due to greater variability, analysis considering KF scheme needs be done in future. LN and WM microphysics schemes have also contributed in generation of heavy rainfall as in some cases they can produce up to 60% of total during the intensity rainfall events.

BJ and KF along with KE scheme show very low performance in prediction of all kind of rainfall events including 1mm rainfall events. Therefore, such scheme can be avoided in future study especially for the hilly region of Bangladesh.

In summary, it has found that Stoony Brook University microphysics scheme with Tiedtke cumulus can produce best rainfall forecast for the high intensive rainfall events over the eastern hilly region of Bangladesh.

From the analysis it is also found that, KEKF scheme did not perfumed well in forecasting 1mm, 20mm, 50mm and 100mm rainfall threshold. It is a default scheme of WRF and currently used by Bangladesh Meteorological Department (BMD) for 24H and 72H rainfall forecast. Therefore, it can be an option for BMD to use a set of ensemble mean generated from the SU and WM schemes with combination of TD and GR cumulus schemes to effective forecast high intensive rainfall events during monsoon season.

5.2 Recommendations

In this study, all available cumulus schemes with suitable microphysics schemes are evaluated considering an optimized domain size. As study shows that SUTD scheme is the best scheme for forecasting heavy rainfall event, more accurate domain size experiment can be done using the scheme over the Indian region.

REFERENCES

Adler, R.F. et al., 2003. The version-2 global precipitation climatology project (GPCP) monthly precipitation analysis (1979-present). Journal of Hydrometeorology, 4(6): 1147-1167.

Ahasan, M., Chowdhury, M., Quadir, D., 2013a. Simulation of High Impact Rainfall Events Over Southeastern Hilly Region of Bangladesh Using MM5 Model. International Journal of Atmospheric Sciences, 2013.

Ahasan, M., Chowdhury, M., Quadir, D., 2014. Sensitivity test of parameterization schemes of mm5 model for prediction of the high impact rainfall events over bangladesh. Journal of Mechanical Engineering, 44(1): 33-42.

Ahasan, M., Debsarma, S., 2014. Impact of data assimilation in simulation of thunderstorm (squall line) event over Bangladesh using WRF model, during SAARC–STORM Pilot Field Experiment 2011. Natural Hazards: 1-14.

Ahasan, M., Rayhun, K., Mannan, M., Debsarma, S., 2013b. Synoptic Analysis of a Heavy Rainfall Event over Southeast Region of Bangladesh Using WRF Model. Journal of Scientific Research, 5(3).

Ahasan, M.N., Chowdhury, M.M., Quadir, D., 2012. Prediction of high impact rainfall events over Bangladesh using high resolution MM5 model. Sri Lankan Journal of Physics, 12: 43-58.

Ali, A., 1999. Climate change impacts and adaptation assessment in Bangladesh. Climate Research, 12(2-3): 109-116.

AMS, 2014. Glossary of Meteorology. http://glossary.ametsoc.org/wiki/rainfall [date accessed: 02/08/2014]

Arakawa, A., Lamb, V.R., 1977. Computational design of the basic dynamical processes of the UCLA general circulation model. Methods in computational physics, 17: 173-265.

Banglapedia, 2014. Banglapedia: national encyclopedia of Bangladesh. Asiatic society of Bangladesh.

BBC, 2012. Heavy rains and landslides in Bangladesh kill 90.http://www.bbc.co.uk/news/world-asia-18605765 [date accessed: 06-02-2014]

BMD, 2014. Bangladesh Meterological Department : WRF 24h rainfall forecast http://www.bmd.gov.bd/NWPP.php?NWPID=WRF24HR [date accessed: 12th August 2014]

Brammer, H., 1990. Floods in Bangladesh: geographical background to the 1987 and 1988 floods. Geographical journal: 12-22.

Bukovsky, M.S., Karoly, D.J., 2009. Precipitation simulations using WRF as a nested regional climate model. Journal of Applied Meteorology and Climatology, 48(10): 2152-2159.

Cannon, T., 2002. Gender and climate hazards in Bangladesh. Gender & Development, 10(2): 45-50.

Chang, C.-P., Krishnamurti, T.N., 1987. Monsoon meteorology. Oxford University Press.

Choudhury, N.Y., Paul, A., Paul, B.K., 2004. Impact of costal embankment on the flash flood in Bangladesh: a case study. Applied Geography, 24(3): 241-258.

Das, M.K., Debsarma, S.K., Das, S., Chowdhury, M., 2011. Tornadic storms of 2008 over Bangladesh: observed by radar and simulated by using WRF-ARW model 6th European Conference on Severe Storms (ECSS 2011), Balearic Islands, Spain.

Das, P.K., 1988. The monsoons. National Book Trust, India.
Das, S. et al., 2008. Skills of different mesoscale models over Indian region during monsoon season: Forecast errors. Journal of earth system science, 117(5): 603-620.
De Silva, G., Herath, S., Weerakoon, S., Rathnayake, U., 2010. Application of WRF with different cumulus parameterization schemes for precipitation forecasting in a tropical river basin.
Deb, S., Srivastava, T., Kishtawal, C., 2008. The WRF model performance for the simulation of heavy precipitating events over Ahmedabad during August 2006. Journal of earth system science, 117(5): 589-602.
Desai, D., Thade, N., Huprikar, M., 1996. Very heavy rainfall over Punjab, Himachal Pradesh and Haryana during 24-27 September 1988-case study. Mausam, 47: 269-274.
Dhar, O., Nandargi, S., 1995. Zones of severe rainstorm activity over India—some refinements. International journal of climatology, 15(7): 811-819.
Doswell III, C.A., 2004. Weather forecasting by humans-Heuristics and decision making. Weather and Forecasting, 19(6): 1115-1126.
Dudhia, J., 1989. Numerical study of convection observed during the winter monsoon experiment using a mesoscale two-dimensional model. Journal of the Atmospheric Sciences, 46(20): 3077-3107.
Ebert, E., McBride, J., 2000. Verification of precipitation in weather systems: Determination of systematic errors. Journal of Hydrology, 239(1): 179-202.
Finley, J.P., 1884. Tornado prediction. Amer Meteor J.
Ganesan, G., Muthuchami, A., Ponnuswamy, A., 2001. Various classes of rainfall in the coastal stations of Tamil Nadu. Mausam, 52(2): 433-436.
Gilbert, G.K., 1884. Finley's tornado predictions. Burr.
Grell, G.A., Dévényi, D., 2002. A generalized approach to parameterizing convection combining ensemble and data assimilation techniques. Geophysical Research Letters, 29(14): 38-1-38-4.
Grell, G.A., Freitas, S.R., 2013. A scale and aerosol aware stochastic convective parameterization for weather and air quality modeling. Atmospheric Chemistry and Physics Discussions, 13(9): 23845-23893.
Gruber, A., Levizzani, V., 2008. Assessment of global precipitation products. WCRP-128, WMO Technical Document, 1430: 57.
Gupta, H.V., Sorooshian, S., Yapo, P.O., 1999. Status of automatic calibration for hydrologic models: Comparison with multilevel expert calibration. Journal of Hydrologic Engineering, 4(2): 135-143.
Haines, A., Kovats, R.S., Campbell-Lendrum, D., Corvalán, C., 2006. Climate change and human health: impacts, vulnerability and public health. Public health, 120(7): 585-596.
Haltiner, G.J., Williams, R.T., 1980. Numerical prediction and dynamic meteorology, 2. Wiley New York.
Han, J., Pan, H.-L., 2011. Revision of convection and vertical diffusion schemes in the NCEP global forecast system. Weather and Forecasting, 26(4): 520-533.
Hasan, M.A., Islam, A.S., Bhaskaran, B., 2013. Predicting future precipitation and temperature over Bangladesh using high resolution regional scenarios generated by multi-member ensemble climate simulations.
Hong, S.-Y., Dudhia, J., Chen, S.-H., 2004. A revised approach to ice microphysical processes for the bulk parameterization of clouds and precipitation. Monthly Weather Review, 132(1): 103-120.

Hong, S.-Y., Lim, J.-O.J., 2006. The WRF single-moment 6-class microphysics scheme (WSM6). J. Korean Meteor. Soc, 42(2): 129-151.
Huffman, G.J., Adler, R.F., Bolvin, D.T., Nelkin, E.J., 2010. The TRMM multi-satellite precipitation analysis (TMPA), Satellite rainfall applications for surface hydrology. Springer, pp. 3-22.
Im, E.-S., In, S.-R., Han, S.-O., 2013. Numerical simulation of the heavy rainfall caused by a convection band over Korea: a case study on the comparison of WRF and CReSS. Natural Hazards, 69(3): 1681-1695.
Islam, M.N., Uyeda, H., 2007. Use of TRMM in determining the climatic characteristics of rainfall over Bangladesh. Remote Sensing of Environment, 108(3): 264-276.
Jacobson, M.Z., 2005. Fundamentals of atmospheric modeling. Cambridge University Press.
Janjic, Z., Gall, R., Pyle, M.E., Testbed, J.N., 2010. National center for atmospheric research PO BOX 3000 boulder, colorado 80307-3000.
Janjic, Z.I., 1994. The step-mountain eta coordinate model: Further developments of the convection, viscous sublayer, and turbulence closure schemes. Monthly Weather Review, 122(5): 927-945.
Kain, J.S., 2004. The Kain-Fritsch convective parameterization: an update. Journal of Applied Meteorology, 43(1): 170-181.
Kain, J.S., Fritsch, J.M., 1990. A one-dimensional entraining/detraining plume model and its application in convective parameterization. Journal of the Atmospheric Sciences, 47(23): 2784-2802.
Kessler, E., 1969. On the distribution and continuity of water substance in atmospheric circulation.
Klemp, J.B., Skamarock, W.C., Dudhia, J., 2007. Conservative split-explicit time integration methods for the compressible nonhydrostatic equations. Monthly Weather Review, 135(8): 2897-2913.
Krishnamurthy, V., Kinter III, J.L., 2003. The Indian monsoon and its relation to global climate variability, Global Climate. Springer, pp. 186-236.
Kumar, A., Dudhia, J., Bhowmik, S., 2010. Evaluation of Physics options of the Weather Research and Forecasting (WRF) Model to simulate high impact heavy rainfall events over Indian Monsoon region. Geofizika, 27(2): 101-125.
Kumar, A., Dudhia, J., Rotunno, R., Niyogi, D., Mohanty, U., 2008. Analysis of the 26 July 2005 heavy rain event over Mumbai, India using the Weather Research and Forecasting (WRF) model. Quarterly Journal of the Royal Meteorological Society, 134(636): 1897-1910.
Kumar, R. et al., 2012. Simulations over South Asia using the Weather Research and Forecasting model with Chemistry (WRF-Chem): chemistry evaluation and initial results. Geoscientific Model Development Discussions, 5(1): 1-66.
Laprise, R., 1992. The Euler equations of motion with hydrostatic pressure as an independent variable. Monthly weather review, 120(1): 197-207.
Lim, K.-S.S., Hong, S.-Y., 2010. Development of an effective double-moment cloud microphysics scheme with prognostic cloud condensation nuclei (CCN) for weather and climate models. Monthly Weather Review, 138(5): 1587-1612.
Lin, Y.-L., Farley, R.D., Orville, H.D., 1983. Bulk parameterization of the snow field in a cloud model. Journal of Climate and Applied Meteorology, 22(6): 1065-1092.

Lin, Y., Colle, B.A., 2011. A new bulk microphysical scheme that includes riming intensity and temperature-dependent ice characteristics. Monthly Weather Review, 139(3): 1013-1035.

Litta, A., Mohanty, U., 2008. Simulation of a severe thunderstorm event during the field experiment of STORM programme 2006, using WRF-NMM model. Current Science, 95(2): 204-215.

Mannan, M.A., Chowdhury, M.A.M., Karmakar, S., 2013. Application of NWP model in prediction of heavy rainfall in Bangladesh. Procedia Engineering, 56: 667-675.

Maussion, F. et al., 2011. WRF simulation of a precipitation event over the Tibetan Plateau, China-an assessment using remote sensing and ground observations. Hydrology and Earth System Sciences, 15: 1795-1817.

Milbrandt, J., Yau, M., 2005. A multimoment bulk microphysics parameterization. Part II: A proposed three-moment closure and scheme description. Journal of the atmospheric sciences, 62(9): 3065-3081.

Mirza, M.M.Q., 2002. Global warming and changes in the probability of occurrence of floods in Bangladesh and implications. Global Environmental Change, 12(2): 127-138.

Mlawer, E.J., Taubman, S.J., Brown, P.D., Iacono, M.J., Clough, S.A., 1997. Radiative transfer for inhomogeneous atmospheres: RRTM, a validated correlated-k model for the longwave. Journal of Geophysical Research: Atmospheres (1984–2012), 102(D14): 16663-16682.

Mooney, P., Mulligan, F., Fealy, R., 2013. Evaluation of the sensitivity of the weather research and forecasting model to parameterization schemes for regional climates of Europe over the period 1990–95. Journal of Climate, 26(3): 1002-1017.

Morrison, H., Thompson, G., Tatarskii, V., 2009. Impact of cloud microphysics on the development of trailing stratiform precipitation in a simulated squall line: Comparison of one-and two-moment schemes. Monthly Weather Review, 137(3): 991-1007.

Ooyama, K.V., 1990. A thermodynamic foundation for modeling the moist atmosphere. Journal of the Atmospheric Sciences, 47(21): 2580-2593.

Pan, H., Wu, W.-S., 1995. Implementing a mass flux convection parameterization package for the NMC medium-range forecast model. NMC office note, 409(40): 20,233-9910.

Pattanaik, D., Rao, Y.R., 2009. Track prediction of very severe cyclone 'Nargis' using high resolution weather research forecasting (WRF) model. Journal of earth system science, 118(4): 309-329.

Pattanayak, S., Mohanty, U., 2008. A comparative study on performance of MM5 and WRF models in simulation of tropical cyclones over Indian seas. Current Science, 95(7): 923-936.

Pielke Sr, R.A., 2013. Mesoscale meteorological modeling, 98. Academic press.

Rafiuddin, M., Uyeda, H., Islam, M.N., 2010. Characteristics of monsoon precipitation systems in and around Bangladesh. International Journal of Climatology, 30(7): 1042-1055.

Raghavan, K., 1973. Break-monsoon over India. Monthly Weather Review, 101(1): 33-43.

Rahman, M.M., Rafiuddin, M., Alam, M.M., 2013. Seasonal forecasting of Bangladesh summer monsoon rainfall using simple multiple regression model. Journal of Earth System Science, 122(2): 551-558.

Rajeevan, M. et al., 2010. Sensitivity of WRF cloud microphysics to simulations of a severe thunderstorm event over Southeast India, Annales Geophysicae. Copernicus GmbH, pp. 603-619.

Rakhecha, P., Pisharoty, P., 1996. Heavy rainfall during monsoon season: Point and spatial distribution. Current Science, 71(3): 179-186.

Ratnam, J.V., Cox, E., 2006. Simulation of monsoon depressions using MM5: sensitivity to cumulus parameterization schemes. Meteorology and Atmospheric Physics, 93(1-2): 53-78.

Routray, A., Mohanty, U., Niyogi, D., Rizvi, S., Osuri, K.K., 2010. Simulation of heavy rainfall events over Indian monsoon region using WRF-3DVAR data assimilation system. Meteorology and atmospheric physics, 106(1-2): 107-125.

Rutledge, S.A., Hobbs, P., 1983. The mesoscale and microscale structure and organization of clouds and precipitation in midlatitude cyclones. VIII: A model for the "seeder-feeder" process in warm-frontal rainbands. Journal of the Atmospheric Sciences, 40(5): 1185-1206.

Sarker, A.A., Rashid, A.M., 2013. Landslide and Flashflood in Bangladesh, Disaster Risk Reduction Approaches in Bangladesh. Springer, pp. 165-189.

Saucier, W.J., 1989. Principles of meteorological analysis. Courier Dover Publications.

Schneider, U., Fuchs, T., Meyer-Christoffer, A., Rudolf, B., 2008. Global precipitation analysis products of the GPCC. Global Precipitation Climatology Centre (GPCC), DWD, Internet Publikation: 1-12.

Shah, S., Rao, B., Kumar, P., Pal, P., 2010. Verification of cloud cover forecast with INSAT observation over western India. Journal of earth system science, 119(6): 775-781.

Shahid, S., 2010. Rainfall variability and the trends of wet and dry periods in Bangladesh. International Journal of Climatology, 30(15): 2299-2313.

Shahid, S., 2011. Trends in extreme rainfall events of Bangladesh. Theoretical and applied climatology, 104(3-4): 489-499.

Shamarock, W. et al., 2008. A description of the advanced research WRF version 3.

Shelter, Cluster, 2012. Flooding in South East Bangladesh phase 3 joint needs assessment report, August 2012 (Chittagong, Bandarban and Cox's Bazar Districts).

Skamarock, W.C. et al., 2008. A description of the advanced research WRF version 3. NCAR Technical note, 113.

Sohrabinia, M., Rack, W., Zawar-Reza, P., 2012. Analysis of MODIS LST compared with WRF model and in situ data over the Waimakariri River basin, Canterbury, New Zealand. Remote Sensing, 4(11): 3501-3527.

Tao, W.-K., Simpson, J., McCumber, M., 1989. An ice-water saturation adjustment. Monthly weather review, 117(1): 231-235.

Thapliyal, V., 1997. Preliminary and final long range forecast for seasonal monsoon rainfall over India. Journal of arid environments, 36(3): 385-403.

Thompson, G., Field, P.R., Rasmussen, R.M., Hall, W.D., 2008. Explicit forecasts of winter precipitation using an improved bulk microphysics scheme. Part II: Implementation of a new snow parameterization. Monthly Weather Review, 136(12): 5095-5115.

Thompson, G., Rasmussen, R.M., Manning, K., 2004. Explicit forecasts of winter precipitation using an improved bulk microphysics scheme. Part I: Description and sensitivity analysis. Monthly Weather Review, 132(2): 519-542.

Unit, U.o.E.A.C.R., Regions, t., Project, C.I.L., 1997. Climate impacts LINK Project: applying results from the Hadley Centre's climate change experiments for climate change impacts assessments. University of East Anglia, Climatic Research Unit.

Wang, W. et al., 2009. ARW Version 3 Modelling System User's Guide.

Wardah, T., Kamil, A., Sahol Hamid, A., Maisarah, W., 2009. Quantitative Precipitation Forecast using MM5 and WRF models for Kelantan River Basin.

Warner, T.T., 2011. Numerical weather and climate prediction, 526. Cambridge University Press Cambridge.

Webster, P.J. et al., 1998. Monsoons: Processes, predictability, and the prospects for prediction. Journal of Geophysical Research: Oceans (1978–2012), 103(C7): 14451-14510.

Wicker, L.J., Skamarock, W.C., 2002. Time-splitting methods for elastic models using forward time schemes. Monthly Weather Review, 130(8): 2088-2097.

Wicker, L.J., Wilhelmson, R.B., 1995. Simulation and analysis of tornado development and decay within a three-dimensional supercell thunderstorm. Journal of the atmospheric sciences, 52(15): 2675-2703.

Yatagai, A. et al., 2012. APHRODITE: Constructing a long-term daily gridded precipitation dataset for Asia based on a dense network of rain gauges. Bulletin of the American Meteorological Society, 93(9): 1401-1415.

Yeh, H.-C., Chen, G.T.-J., 2004. Case study of an unusually heavy rain event over eastern Taiwan during the Mei-yu season. Monthly weather review, 132(1): 320-337.

Zhang, C., Wang, Y., Hamilton, K., 2011. Improved Representation of Boundary Layer Clouds over the Southeast Pacific in ARW-WRF Using a Modified Tiedtke Cumulus Parameterization Scheme*. Monthly Weather Review, 139(11): 3489-3513.

APPENDIX A: Description of namelist.wps file

A.1 Sample "namelist.wps" which has used domain selection experiment

```
&share
 wrf_core = 'ARW',
 max_dom = 2,
 start_date = '2014-08-04_06:00:00','2014-08-04_06:00:00',
 end_date   = '2014-08-08_06:00:00','2014-08-08_06:00:00',
 interval_seconds = 10800
 io_form_geogrid = 2,
/

&geogrid
 parent_id         =   1,   1,
 parent_grid_ratio =   1,   3,
 i_parent_start    =   1,  43,
 j_parent_start    =   1,  43,
 e_we              =  91, 115,
 e_sn              =  91,  115,
 geog_data_res     = '30s','30s',
 dx = 30000,
 dy = 30000,
 map_proj = 'lambert',
 ref_lat   =  21.0,
 ref_lon   =  83.50,
 truelat1  =  21.0,
 stand_lon =  83.50,
 geog_data_path = '/home/iwfm/WRF/geog'
/


&ungrib
 out_format = 'WPS',
```

```
 prefix = 'GFS2',
/


&metgrid
 fg_name = 'GFS2'
 io_form_metgrid = 2,
/
```

A.2 Description of 'namelist.input' file

Namelist.input file contain four section, share section, geogrib section, ungrib section, and metgrib section.

Share Section of namelist.input file

This section contains some common information for WPS simulation.

- WRF_CORE : A character string set to either `'ARW'` or `'NMM'` that tells the WPS which dynamical core the input data are being prepared for. Default value is `'ARW'`.
- MAX_DOM : An integer specifying the total number of domains/nests, including the parent domain, in the simulation. Default value is 1.
- START_YEAR : A list of MAX_DOM 4-digit integers specifying the starting UTC year of the simulation for each nest. No default value.
- START_MONTH : A list of MAX_DOM 2-digit integers specifying the starting UTC month of the simulation for each nest. No default value.
- START_DAY : A list of MAX_DOM 2-digit integers specifying the starting UTC day of the simulation for each nest. No default value.
- START_HOUR : A list of MAX_DOM 2-digit integers specifying the starting UTC hour of the simulation for each nest. No default value.
- END_YEAR : A list of MAX_DOM 4-digit integers specifying the ending UTC year of the simulation for each nest. No default value.
- END_MONTH : A list of MAX_DOM 2-digit integers specifying the ending UTC month of the simulation for each nest. No default value.
- END_DAY : A list of MAX_DOM 2-digit integers specifying the ending UTC day of the simulation for each nest. No default value.

- END_HOUR : A list of MAX_DOM 2-digit integers specifying the ending UTC hour of the simulation for each nest. No default value.
- START_DATE : A list of MAX_DOM character strings of the form 'YYYY-MM-DD_HH:mm:ss' specifying the starting UTC date of the simulation for each nest. The start_date variable is an alternate to specifying start_year, start_month, start_day, and start_hour, and if both methods are used for specifying the starting time, the start_date variable will take precedence. No default value.
- END_DATE : A list of MAX_DOM character strings of the form 'YYYY-MM-DD_HH:mm:ss' specifying the ending UTC date of the simulation for each nest. The end_date variable is an alternate to specifying end_year, end_month, end_day, and end_hour, and if both methods are used for specifying the ending time, the end_date variable will take precedence. No default value.
- INTERVAL_SECONDS : The integer number of seconds between time-varying meteorological input files. No default value.
- ACTIVE_GRID : A list of MAX_DOM logical values specifying, for each grid, whether that grid should be processed by geogrid and metgrid. Default value is .TRUE..
- IO_FORM_GEOGRID : The WRF I/O API format that the domain files created by the geogrid program will be written in. Possible options are: 1 for binary; 2 for NetCDF; 3 for GRIB1. When option 1 is given, domain files will have a suffix of .int; when option 2 is given, domain files will have a suffix of .nc; when option 3 is given, domain files will have a suffix of .gr1. Default value is 2 (NetCDF).
- OPT_OUTPUT_FROM_GEOGRID_PATH : A character string giving the path, either relative or absolute, to the location where output files from geogrid should be written to and read from. Default value is './'.

Geogrib Section of namelist.input file

This section contains information to run ‘geogrib.exe’:

- PARENT_ID: A list of MAX_DOM integers specifying, for each nest, the domain number of the nest's parent; for the coarsest domain, this variable should be set to 1. Default value is 1.
- PARENT_GRID_RATIO: A list of MAX_DOM integers specifying, for each nest, the nesting ratio relative to the domain's parent. No default value.
- I_PARENT_START: A list of MAX_DOM integers specifying, for each nest, the x-coordinate of the lower-left corner of the nest in the parent *unstaggered* grid. For the coarsest domain, a value of 1 should be specified. No default value.
- J_PARENT_START: A list of MAX_DOM integers specifying, for each nest, the y-coordinate of the lower-left corner of the nest in the parent *unstaggered* grid. For the coarsest domain, a value of 1 should be specified. No default value.
- S_WE: A list of MAX_DOM integers which should all be set to 1. Default value is 1.
- E_WE: A list of MAX_DOM integers specifying, for each nest, the nest's full west-east dimension. For nested domains, e_we must be one greater than an integer multiple of the nest's parent_grid_ratio (i.e., e_we = *n**parent_grid_ratio+1 for some positive integer *n*). No default value.
- S_SN: A list of MAX_DOM integers which should all be set to 1. Default value is 1.
- E_SN: A list of MAX_DOM integers specifying, for each nest, the nest's full south-north dimension. For nested domains, e_sn must be one greater than an integer multiple of the nest's parent_grid_ratio (i.e., e_sn = *n**parent_grid_ratio+1 for some positive integer *n*). No default value.
- GEOG_DATA_RES: A list of MAX_DOM character strings specifying, for each nest, a corresponding resolution or list of resolutions separated by + symbols of source data to be used when interpolating static terrestrial data to the nest's grid.
- DX: A real value specifying the grid distance in the x-direction where the map scale factor is 1. For ARW, the grid distance is in meters for the 'polar', 'lambert', and 'mercator' projection, and in degrees longitude for the 'lat-lon'

projection; Grid distances for nests are determined recursively based on values specified for parent_grid_ratio and parent_id. No default value.

- DY: A real value specifying the nominal grid distance in the y-direction where the map scale factor is 1. For ARW, the grid distance is in meters for the 'polar', 'lambert', and 'mercator' projection, and in degrees latitude for the 'lat-lon' projection; Grid distances for nests are determined recursively based on values specified for parent_grid_ratio and parent_id. No default value.
- MAP_PROJ: A character string specifying the projection of the simulation domain. For ARW, accepted projections are 'lambert', 'polar', 'mercator', and 'lat-lon'. Default value is 'lambert'.
- REF_LAT: A real value specifying the latitude part of a (latitude, longitude) location whose (i,j) location in the simulation domain is known. For ARW, ref_lat gives the latitude of the center-point of the coarse domain by default (i.e., when ref_x and ref_y are not specified). No default value.
- REF_LON: A real value specifying the longitude part of a (latitude, longitude) location whose (i, j) location in the simulation domain is known. For ARW, ref_lon gives the longitude of the center-point of the coarse domain by default (i.e., when ref_x and ref_y are not specified). No default value.
- REF_X: A real value specifying the i part of an (i, j) location whose (latitude, longitude) location in the simulation domain is known. The (i, j) location is always given with respect to the mass-staggered grid, whose dimensions are one less than the dimensions of the unstaggered grid. Default value is (((E_WE-1.)+1.)/2.) = (E_WE/2.).
- REF_Y: A real value specifying the j part of an (i, j) location whose (latitude, longitude) location in the simulation domain is known. The (i, j) location is always given with respect to the mass-staggered grid, whose dimensions are one less than the dimensions of the unstaggered grid. Default value is (((E_SN-1.)+1.)/2.) = (E_SN/2.).
- TRUELAT1: A real value specifying, for ARW, the first true latitude for the Lambert conformal projection, or the only true latitude for the Mercator and polar stereographic projections. No default value.

- TRUELAT2: A real value specifying, for ARW, the second true latitude for the Lambert conformal conic projection. For all other projections, truelat2 is ignored. No default value.
- STAND_LON: A real value specifying, for ARW, the longitude that is parallel with the y-axis in the Lambert conformal and polar stereographic projections. For the regular latitude-longitude projection, this value gives the rotation about the earth's geographic poles. No default value.
- POLE_LAT: For the latitude-longitude projection for ARW, the latitude of the North Pole with respect to the computational latitude-longitude grid in which -90.0° latitude is at the bottom of a global domain, 90.0° latitude is at the top, and 180.0° longitude is at the center. Default value is 90.0.
- POLE_LON : For the latitude-longitude projection for ARW, the longitude of the North Pole with respect to the computational lat/lon grid in which -90.0° latitude is at the bottom of a global domain, 90.0° latitude is at the top, and 180.0° longitude is at the center. Default value is 0.0.
- GEOG_DATA_PATH: A character string giving the path, either relative or absolute, to the directory where the geographical data directories may be found. This path is the one to which rel_path specifications in the GEOGRID.TBL file are given in relation to. No default value.
- OPT_GEOGRID_TBL_PATH: A character string giving the path, either relative or absolute, to the GEOGRID.TBL file. The path should not contain the actual file name, as GEOGRID.TBL is assumed, but should only give the path where this file is located. Default value is './geogrid/'.

Ungrib Section of namelist.input file

This section contains information to run 'ungrib.exe':

- OUT_FORMAT: A character string set either to `'WPS'`, `'SI'`, or `'MM5'`. If set to `'MM5'`, ungrib will write output in the format of the MM5 pregrid program; if set to `'SI'`, ungrib will write output in the format of grib_prep.exe; if set to `'WPS'`, ungrib will write data in the WPS intermediate format. Default value is `'WPS'`.
- PREFIX: A character string that will be used as the prefix for intermediate-format files created by ungrib; here, prefix refers to the string *PREFIX* in the filename *PREFIX*:*YYYY-MM-DD_HH* of an intermediate file. The prefix may

contain path information, either relative or absolute, in which case the intermediate files will be written in the directory specified. This option may be useful to avoid renaming intermediate files if ungrib is to be run on multiple sources of GRIB data. Default value is `'FILE'`.

metgrib Section of namelist.input file

This section contains information to run 'metgrib.exe':

- FG_NAME: A list of character strings specifying the path and prefix of ungribbed data files. The path may be relative or absolute, and the prefix should contain all characters of the filenames up to, but not including, the colon preceding the date. When more than one `fg_name` is specified, and the same field is found in two or more input sources, the data in the last encountered source will take priority over all preceding sources for that field. Default value is an empty list (i.e., no meteorological fields).
- CONSTANTS_NAME: A list of character strings specifying the path and full filename of ungribbed data files which are time-invariant. The path may be relative or absolute, and the filename should be the complete filename; since the data are assumed to be time-invariant, no date will be appended to the specified filename. Default value is an empty list (i.e., no constant fields).

- IO_FORM_METGRID: The WRF I/O API format that the output created by the metgrid program will be written in. Possible options are: 1 for binary; 2 for NetCDF; 3 for GRIB1. When option 1 is given, output files will have a suffix of .int; when option 2 is given, output files will have a suffix of .nc; when option 3 is given, output files will have a suffix of .gr1. Default value is 2 (NetCDF).
- OPT_OUTPUT_FROM_METGRID_PATH: A character string giving the path, either relative or absolute, to the location where output files from metgrid should be written to. The default value is the current working directory (i.e., the default value is './').
- OPT_METGRID_TBL_PATH: A character string giving the path, either relative or absolute, to the METGRID.TBL file; the path should not contain the actual file name, as METGRID.TBL is assumed, but should only give the path where this file is located. Default value is './metgrid/'.

- PROCESS_ONLY_BDY: An integer specifying the number of boundary rows and columns to be processed by metgrid for time periods after the initial time; for the initial time, metgrid will always interpolate to every grid point. Setting this option to the intended value of spec_bdy_width in the WRF namelist.input will speed up processing in metgrid, but it should not be set if interpolated data are needed in the domain interior. If this option is set to zero, metgrid will horizontally interpolate meteorological data to every grid point in the model domains.

APPENDIX B: Description of 'namelist.input' file

B.1 Sample "namelist.input" which has used sensitivity experiment

```
&time_control
 run_days                  = 0,
 run_hours                 = 12,
 run_minutes               = 0,
 run_seconds               = 0,
 start_year                = 2000, 2000, 2000,
 start_month               = 01,   01,   01,
 start_day                 = 24,   24,   24,
 start_hour                = 12,   12,   12,
 start_minute              = 00,   00,   00,
 start_second              = 00,   00,   00,
 end_year                  = 2000, 2000, 2000,
 end_month                 = 01,   01,   01,
 end_day                   = 25,   25,   25,
 end_hour                  = 12,   12,   12,
 end_minute                = 00,   00,   00,
 end_second                = 00,   00,   00,
 interval_seconds          = 21600
 input_from_file           = .true.,.true.,.true.,
 history_interval          = 180,  60,   60,
 frames_per_outfile        = 1000, 1000, 1000,
 restart                   = .false.,
 restart_interval          = 5000,
 io_form_history           = 2
 io_form_restart           = 2
 io_form_input             = 2
 io_form_boundary          = 2
 debug_level               = 0
/
```

```
&domains
time_step                  = 180,
time_step_fract_num        = 0,
time_step_fract_den        = 1,
max_dom                    = 1,
e_we                       = 74,    112,   94,
e_sn                       = 61,    97,    91,
e_vert                     = 28,    28,    28,
p_top_requested            = 5000,
num_metgrid_levels         = 27,
num_metgrid_soil_levels    = 4,
dx                         = 30000, 10000,  3333.33,
dy                         = 30000, 10000,  3333.33,
grid_id                    = 1,     2,     3,
parent_id                  = 0,     1,     2,
i_parent_start             = 1,     31,    30,
j_parent_start             = 1,     17,    30,
parent_grid_ratio          = 1,     3,     3,
parent_time_step_ratio     = 1,     3,     3,
feedback                   = 1,
smooth_option              = 0
/

&physics
mp_physics                 = 3,     3,     3,
ra_lw_physics              = 1,     1,     1,
ra_sw_physics              = 1,     1,     1,
radt                       = 30,    30,    30,
sf_sfclay_physics          = 1,     1,     1,
sf_surface_physics         = 2,     2,     2,
bl_pbl_physics             = 1,     1,     1,
bldt                       = 0,     0,     0,
cu_physics                 = 1,     1,     0,
```

```
cudt                 = 5,     5,     5,
isfflx               = 1,
ifsnow               = 1,
icloud               = 1,
surface_input_source = 1,
num_soil_layers      = 4,
sf_urban_physics     = 0,     0,     0,
/

&fdda
/

&dynamics
w_damping            = 0,
diff_opt             = 1,
km_opt               = 4,
diff_6th_opt         = 0,      0,      0,
diff_6th_factor      = 0.12,   0.12,   0.12,
base_temp            = 290.
damp_opt             = 0,
zdamp                = 5000.,  5000.,  5000.,
dampcoef             = 0.2,    0.2,    0.2
khdif                = 0,      0,      0,
kvdif                = 0,      0,      0,
non_hydrostatic      = .true., .true., .true.,
moist_adv_opt        = 1,      1,      1,
scalar_adv_opt       = 1,      1,      1,
/

&bdy_control
spec_bdy_width       = 5,
spec_zone            = 1,
relax_zone           = 4,
```

```
specified                    = .true., .false.,.false.,
nested                       = .false., .true., .true.,
/

&grib2
/

&namelist_quilt
nio_tasks_per_group = 0,
nio_groups = 1,
/
```

B.2 Description of 'namelist.input' file

Variable Names	Value	Description
&time_control		**Time control**
run_days	1	run time in days
run_hours	0	run time in hours
run_minutes	0	run time in minutes
run_seconds	0	run time in seconds
start_year (max_dom)	2001	four digit year of starting time
start_month (max_dom)	06	two digit month of starting time
start_day (max_dom)	11	two digit day of starting time
start_hour (max_dom)	12	two digit hour of starting time
start_minute (max_dom)	00	two digit minute of starting time
start_second (max_dom)	00	two digit second of starting time
end_year (max_dom)	2001	four digit year of ending time
end_month (max_dom)	06	two digit month of ending time
end_day (max_dom)	12	two digit day of ending time
end_hour (max_dom)	12	two digit hour of ending time
end_minute (max_dom)	00	two digit minute of ending time
end_second (max_dom)	00	two digit second of ending time
interval_seconds	10800	time interval between incoming real data, which will be the interval between the lateral

Variable Names	Value	Description
		boundary condition file (for real only)
input_from_file (max_dom)	T (logical)	logical; whether nested run will have input files for domains other than 1
fine_input_stream		selected fields from nest input
history_interval (max_dom)	60	history output file interval in minutes (integer only)
history_interval_mo (max_dom)	1	history output file interval in months
frames_per_outfile (max_dom)	1	output times per history output file, used to split output files into smaller pieces
restart	F (logical)	whether this run is a restart run
restart_interval	1440	restart output file interval in minutes
reset_simulation_start	F	whether to overwrite simulation_start_date with forecast start time
cycling	F	whether this run is a cycling run (initialized from wrfout file)
io_form_history	2	2 = netCDF; 102 = split netCDF files one per processor (no supported post-processing software for split files)
io_form_restart	2	2 = netCDF; 102 = split netCDF files one per processor (must restart with the same number of processors)
io_form_input	2	2 = netCDF
	102	Allows program real.exe to read in split met_em* files, and write split wrfinput files. No split file for wrfbdy.
io_form_boundary	2	netCDF format
cycling	.false.	Indicating if the run is using wrfout file as input file. In this case, Thompson initialization routine will not be called again (performance issue)
debug_level	0	50,100,200,300 values give increasing prints
write_input	t	write input-formatted data as output for 3DVAR application
inputout_interval	180	interval in minutes when writing input-

Variable Names	Value	Description
		formatted data
input_outname		Output file name from 3DVAR
&domains		domain definition: dimensions, nesting parameters
time_step	60	time step for integration in integer seconds (recommended 6*dx in km for a typical case)
time_step_fract_num	0	numerator for fractional time step
time_step_fract_den	1	denominator for fractional time step Example, if you want to use 60.3 sec as your time step, set time_step = 60, time_step_fract_num = 3, and time_step_fract_den = 10
max_dom	1	number of domains - set it to > 1 if it is a nested run
s_we (max_dom)	1	start index in x (west-east) direction (leave as is)
e_we (max_dom)	91	end index in x (west-east) direction (staggered dimension)
s_sn (max_dom)	1	start index in y (south-north) direction (leave as is)
e_sn (max_dom)	82	end index in y (south-north) direction (staggered dimension)
s_vert (max_dom)	1	start index in z (vertical) direction (leave as is)
e_vert (max_dom)	28	end index in z (vertical) direction (staggered dimension - this refers to full levels). Most variables are on unstaggered levels. Vertical dimensions need to be the same for all nests.
dx (max_dom)	10000	grid length in x direction, unit in meters
dy (max_dom)	10000	grid length in y direction, unit in meters
ztop (max_dom)	19000.	height in meters; used to define model top for idealized cases
grid_id (max_dom)	1	domain identifier
parent_id (max_dom)	0	id of the parent domain

Variable Names	Value	Description
i_parent_start (max_dom)	1	starting LLC I-indices from the parent domain
j_parent_start (max_dom)	1	starting LLC J-indices from the parent domain
parent_grid_ratio (max_dom)	1	parent-to-nest domain grid size ratio: for real-data cases the ratio has to be odd; for idealized cases, the ratio can be even if feedback is set to 0.
parent_time_step_ratio (max_dom)	1	parent-to-nest time step ratio; it can be different from the parent_grid_ratio
feedback	1	feedback from nest to its parent domain; 0 = no feedback
smooth_option	0	smoothing option for parent domain, used only with feedback option on. 0: no smoothing; 1: 1-2-1 smoothing; 2: smoothing-desmoothing
&physics		Physics options
mp_physics (max_dom)		*microphysics option*
	0	no microphysics
	1	Kessler scheme
	2	Lin et al. scheme
	3	WSM 3-class simple ice scheme
	4	WSM 5-class scheme
	5	Ferrier (new Eta) microphysics
	6	WSM 6-class graupel scheme
	7	Goddard GCE scheme (also use gsfcgce_hail and gsfcgce_2ice)
	8	Thompson graupel scheme (2-moment scheme in V3.1)
	10	Morrison 2-moment scheme
	14	double moment, 5-class scheme
	16	double moment, 6-class scheme
	98	Thompson scheme in V3.0
ra_lw_physics (max_dom)		longwave radiation option
	0	no longwave radiation

Variable Names	Value	Description
	1	rrtm scheme
	3	CAM scheme
	4	rrtmg scheme
	99	GFDL (Eta) longwave (semi-supported)
ra_sw_physics (max_dom)		shortwave radiation option
	0	no shortwave radiation
	1	Dudhia scheme
	2	Goddard short wave
	3	CAM scheme
	4	rrtmg scheme
	99	GFDL (Eta) longwave (semi-supported)
radt (max_dom)	30	minutes between radiation physics calls. Recommend 1 minute per km of dx (e.g. 10 for 10 km grid); use the same value for all nests
co2tf	1	CO2 transmission function flag for GFDL radiation only. Set it to 1 for ARW, which allows generation of CO2 function internally
cam_abs_freq_s	21600	CAM clear sky longwave absorption calculation frequency (recommended minimum value to speed scheme up)
levsiz	59	for CAM radiation input ozone levels
paerlev	29	for CAM radiation input aerosol levels
cam_abs_dim1	4	for CAM absorption save array
cam_abs_dim2	same as e_vert	for CAM 2nd absorption save array
sf_sfclay_physics (max_dom)		surface-layer option
	0	no surface-layer
	1	Monin-Obukhov scheme
	2	Monin-Obukhov (Janjic Eta) scheme
	3	NCEP GFS scheme (NMM only)
	4	QNSE
	5	MYNN
	7	Pleim-Xu (ARW only), only tested with Pleim-Xu surface and ACM2 PBL

Variable Names	Value	Description
sf_surface_physics (max_dom)		land-surface option (set before running *real*; also set correct num_soil_layers)
	0	no surface temp prediction
	1	thermal diffusion scheme
	2	unified Noah land-surface model
	3	RUC land-surface model
	7	Pleim-Xu scheme (ARW only)
sf_urban_physics (max_dom)		urban physics option (replacing ucmcall option in previous versions); works with Noah LSM
	0	no urban physics
	1	single-layer UCM (Kusaka, ucmcall=1)
	2	multi-layer, BEP (Martilli); works with BouLac and MYJ PBL only.
bl_pbl_physics (max_dom)		boundary-layer option
	0	no boundary-layer
	1	YSU scheme
	2	Mellor-Yamada-Janjic (Eta) TKE scheme
	3	NCEP GFS scheme (NMM only)
	4	QNSE
	5	MYNN 2.5 level TKE, works with sf_sfclay_physics=1,2, and 5
	6	MYNN 3rd level TKE, works with sf_sfclay_physics=5 only
	7	ACM2 (Pleim) scheme
	8	Bougeault and Lacarrere (BouLac) TKE
	99	MRF scheme (to be removed)
bldt (max_dom)	0	minutes between boundary-layer physics calls. 0 = call every time step
grav_settling	0	Gravitational settling of fog/cloud droplet, MYNN PBL only
cu_physics (max_dom)		cumulus option
	0	no cumulus
	1	Kain-Fritsch (new Eta) scheme
	2	Betts-Miller-Janjic scheme

Variable Names	Value	Description
	3	Grell-Devenyi ensemble scheme
	4	Simplied Arakawa-Schubert (NMM only)
	5	New Grell scheme (G3)
	99	previous Kain-Fritsch scheme
cudt	0	minutes between cumulus physics calls. 0 = call every time step
maxiens	1	Grell-Devenyi and G3 only
maxens	3	G-D only
maxens2	3	G-D only
maxens3	16	G-D only
ensdim	144	G-D only. These are recommended numbers. If you would like to use any other number, consult the code, know what you are doing.
cugd_avedx	1	number of grid boxes over which subsidence is spread. 1= default, for large grid sizes; 3=, for small grid sizes (<5km)
isfflx	1	heat and moisture fluxes from the surface 1 = with fluxes from the surface 0 = no flux from the surface (not for sf_surface_sfclay = 2). If diff_opt=2, km_opt=2 or 3 then 0 = constant fluxes defind by tke_drag_coefficient, tke_heat_flux; 1 = use model computed u*, and heat and moisture fluxes; 2 = use model computed u*, and specified heat flux by tke_heat_flux
ifsnow	0	snow-cover effects (only works for sf_surface_physics = 1) 1 = with snow-cover effect 0 = without snow-cover effect
icloud	1	cloud effect to the optical depth in radiation (only works for ra_sw_physics = 1 and ra_lw_physics = 1) 1 = with cloud effect

Variable Names	Value	Description
		0 = without cloud effect
swrad_scat	1.	Scattering tuning parameter (default 1 is 1.e-5 m^2/kg)
surface_input_source	1,2	where landuse and soil category data come from: 1 = WPS/geogrid; 2 = GRIB data from another model (only if arrays VEGCAT/SOILCAT exist)
num_soil_layers		number of soil layers in land surface model (set in *real*)
	5	thermal diffusion scheme for temp only
	4	Noah land-surface model
	6	RUC land-surface model
	2	Pleim-Xu land-surface model
pxlsm_smois_init (max_dom)	1	PX LSM soil moisture initialization option 0: from analysis 1: from LANDUSE.TBL (SLMO)
num_land_cat	24	number of landuse categories in input data
num_soil_cat	16	number of soil categories in input data
usemonalb	.false.	whether to use monthly albedo map instead of table values. Recommended for sst_update = 1
rdmaxalb	.true.	use snow albedo from geogrid; false means use snow albedo from table
rdlai2d	.false.	use LAI from input data; false means using values from table
seaice_threshold	271.	tsk < seaice_threshold, if water point and 5-layer slab scheme, set to land point and permanent ice; if water point and Noah scheme, set to land point, permanent ice, set temps from 3 m to surface, and set smois and sh2o
sst_update		option to use time-varying SST, seaice, vegetation fraction, and albedo during a model simulation (set before running *real*)

Variable Names	Value	Description
	0	no SST update
	1	*real.exe* will create wrflowinp_d01 file at the same time interval as the available input data. To use it in wrf.exe, add auxinput4_inname = "wrflowinp_d<domain>", auxinput4_interval in namelist section *&time_control*
tmn_update	1	update deep layer soil temperature, useful for long simulations
lagday	150	days over which tmn is computed using skin temperature
skin_sst	1	calculate skin SST, useful for long simulations
bucket_mm	-1.	bucket reset values for water accumulation (unit in mm), useful for long simulations; -1 = inactive
bucket_j	-1.	bucket reset value for energy accumulations (unit in Joules) useful for long simulations; -1 = inactive
slope_rad	0	slope effects for ra_sw_physics=1 (1=on, 0=off)
topo_shading	0	neighboring-point shadow effects for ra_sw_physics=1 (1=on, 0=off)
shadlen	25000.	max shadow length in meters for topo_shading = 1
omlcall	0	simple ocean mixed layer model (1=on, 0=off), only works with sf_surface_physics = 1
oml_hml0	50.	initial ocean mixed layer depth (m), constant everywhere
oml_gamma	0.14	lapse rate in deep water for oml (K m-1)
isftcflx	0	alternative Ck, Cd for tropical storm application. (1=on, 0=off)
fractional_seaice	0.	treat seaice as fractional field (1) or ice/no ice flag (0)
gwd_opt	0	gravity wave drag option (1= on)